THE CHARACTERIZATION OF MACRO- AND MICROERRORS OF JOURNAL BEARING ROUNDNESS USING THE THEORY OF STOCHASTIC EXCURSIONS

by

Benne Velsher

A THESIS
IN THE
FACULTY OF ENGINEERING

Presented in partial fulfilment of
the requirements for the degree of

MASTER OF ENGINEERING

at

Concordia University
Montreal, Canada
July, 1975

ABSTRACT

by

Benne Velsher

THE CHARACTERIZATION OF MACRO-AND MICROERRORS OF JOURNAL BEARING ROUNDNESS USING THE THEORY OF STOCHASTIC EXCURSIONS

A new approach for the characterization of form error and surface roughness of round bearings is presented. The method employs the theory of random function excursions to describe the macro - and microerrors of the round surface in both radial and circumferential directions.

The mathematical principle of the measuring technique is given and it is shown that an accurate description of the roundness can be obtained from the knowledge of the intercept probabilities of the crest and valley excursions of the surface trace about a given reference circle. Based on the mathematical model, new indices for the characterization of journal bearing roundness are proposed. These indices are computed directly from data obtained from commercially available roundness measuring devices. A number of experiments were performed to justify the validity of the proposed roundness indices. Roundness measurements were carried out on a number of differently machined cylinders using a specially equipped measuring device (Talyrond 51) with a link to a hybrid computer EAI-690. The theoretically computed indices compared favorably with the measurements made on the actual round surfaces.

Based on the theoretical and experimental results, it is concluded

that:

a) Five indices are required for full characterization of roundness error:

1. O.O.R. value - out-of-roundness
2. M.V.E. - mean valley excursion
3. N.P. value - number of peaks (=½ ANC at M line)
4. T.V.E. value - total valley excursion (=MVE x NP)
5. C.L.A. value - center line average.

b) For accurate characterization of roundness errors a full circumference is required as a sampling length. A portion of the circumference will result in a much unreliable description of the roundness error.

c) For measuring the microerror (circumferential surface roughness) of the round surface, a part of the circumference as a sampling is sufficient. Sampling length and "cut-off" values of high-pass filters required for this measurement are similar to those used in conventional surface texture measurements.

d) Results obtained from measuring amplitude distribution of several journal bearings with the aid of amplitude distribution analyzer show that the amplitude distribution of roundness error is generally non Gaussian.

ACKNOWLEDGEMENTS

The author wishes to express his gratitude to his supervisors, Dr. M.O.M. Osman and Dr. T.S. Sankar, under whose guidance this investigation was carried out.

The support of the National Research Council of Canada, Grants Nos. A5181 and A7104 and the Formation de Chercheurs et d'Action Concertée of the Government of Quebec, Grant No. 242-110 are gratefully acknowledged.

Thanks are also due to Mr. G. Boast for his assistance with the EAI-690 Hybrid computer and to Mr. Ter-Mors for his help in building a certain electronic device used in this investigation.

TABLE OF CONTENTS

LIST OF TABLES

LIST OF FIGURES

NOMENCLATURE

a	sample point spacing
a_n, b_n	coefficients
AMS or η'	absolute mean slope of surface texture
CLA	center line average height of $y(x)$
D_{ij}	algebraic co-factor of determinant D
$E[\ ]$	ensemble average
E-system	envelope reference profile
K_{ij}	correlation coefficient for the random function $y(x)$ at x_i and x_j
L	sampling length
M-system	mean-line reference profile
MCE	mean crest excursion
MVE	mean valley excursion
n	number of data points
n_a	number of distinct values of λ or A
N_c	average number of crossings per unit length
$p_c(\lambda)$	probability density of crest excursions
$P_c(\lambda)$	probability distribution of crest excursions
$p_v(\lambda)$	probability density of valley excursions
$P_v(\lambda)$	probability distribution of valley excursions
RMS or σ	root mean square value of $y(x)$
RMSCE	root mean square crest excursion
RMS or σ'	root mean square value of the slope $y'(x)$
RMSVE	root mean square valley excursion

x	lengthwise directional coordinate
$\bar{y}$	average of y_i, $i=1 \ldots n$
y_s	pre-selected crossing level measured from the mean line equal to c (CLA)
$y(x)$	function of the signal reproduced by a measurement of a surface
$y'(x)$	slope of the function $y(x)$
$\Delta\lambda$	increment of λ
c	multiplication factor to determine crest calculation level in terms of CLA value
Λ	valley intercept (interval between excursions
λ	crest intercept (duration of excursions)
λ_c	cut-off value of high-pass filter
λ_{lu}	range of lower and upper crest intercepts
λ_w	wave length
K	co-variance function
μ	variable difference between the abscissae of two cross-sections of the profilogram
C	coefficient dependent on the shape of the irregularities and on the law governing their height distribution
r	index of the frequency composition of the random irregularities
γ	coefficient for the height of random asperities
β and ν	coefficient for the height of the irregularities with periods of T_β and T_ν
h_m	mean variation of the surface irregularities
λ_{mm}	average wavelength

OOR	out-of-roundness value
NP	number of peaks value
TVE	total valley excursion value
p	unit load on projected area
s	viscosity of fluid
N	journal speed
h_m	minimum film thickness at point of closest approach
D	diameter of bearing
V	bearing length
t	eccentricity ratio
F	friction force
M	mass of rotating parts
W	bearing load

CHAPTER 1

LITERATURE SURVEY ON THE METHODS FOR THE CHARACTERIZATION OF MACRO - AND MICROERRORS OF ROUND SURFACES

CHAPTER 1

LITERATURE SURVEY ON THE METHODS FOR THE CHARACTERIZATION OF MACRO - AND MICROERRORS OF ROUND SURFACES

The surface geometry of the machined part plays a very important role in its performance characteristics. It influences such parameters as the load bearing capacity, lubricability, fatigue strength, friction properties, corrosion resistance, bearing noise and stability, etc.

In order to fully characterize a round surface of a journal bearing two types of deviations must be described:

1) the macro-error which specifies the deviation between a reference ideal circle and a so called out-of-roundness error. This out-of-roundness error is basically made of the low frequency component of the roundness error.
2) the micro-error which specifies the surface roughness characteristics of the round surface. This error is basically made of the high frequency component of the roundness error (see Figure 1.1)

There are numerous investigations which deal with characterization of micro-errors of machined round surfaces, yet limited work has been reported on characterization of macroerrors of journal bearings. In the rest of this chapter, existing methods standardized or proposed in the literature to specify micro- and macroerrors on round surfaces will be critically reviewed and suggested methods will be evaluated against each other.

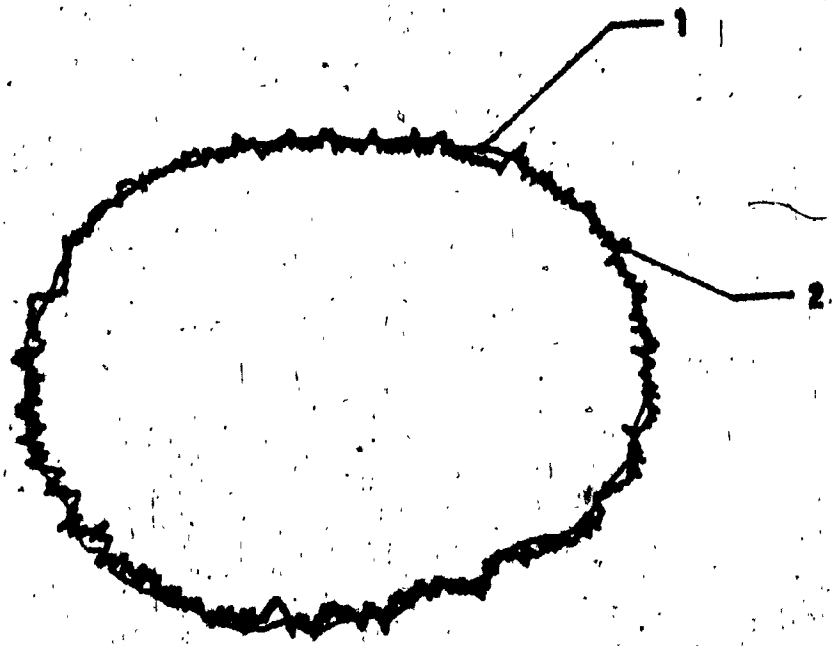

FIG. 1.1 - ROUNDNESS ERROR ILLUSTRATION

1) Low frequency component
2) High frequency component

1.1 Description of Macro-Errors of Round Surfaces

The peak-to-valley height of the measured profile expressed as the difference between the maximum and minimum radii of the profile measured from a chosen center is commonly used as an assessment of the departure of a work piece from perfect roundness. In [1]* the author shows that this chosen center can be determined in at least four different ways. These four ways lead to slightly different positions of the center in the general case. All four have their limitations and sources of error.

The four ways are referred to and described as follows:

a) Ring Gauge Center.

If the graph represents a shaft, it is possible to imagine shaft to be surrounded with the smallest possible ring gauge that would go without interference. See Figure 1.2.

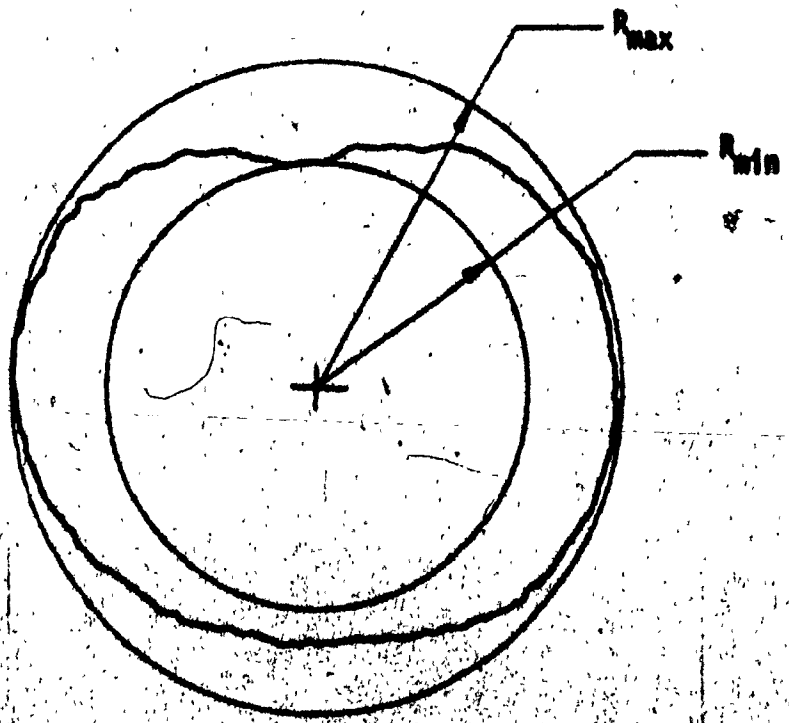

FIG. 1.2 - RING GAUGE CENTER

$R_{max} - R_{min} = 2.0$

*Numbers in brackets designate references at the end of the thesis.

b) Plug Gauge Center.

If the graph represents a hole, the procedure is reversed, and the circle first drawn is the largest possible inscribing circle, representing the largest plug gauge that will pass through. See Figure 1.3.

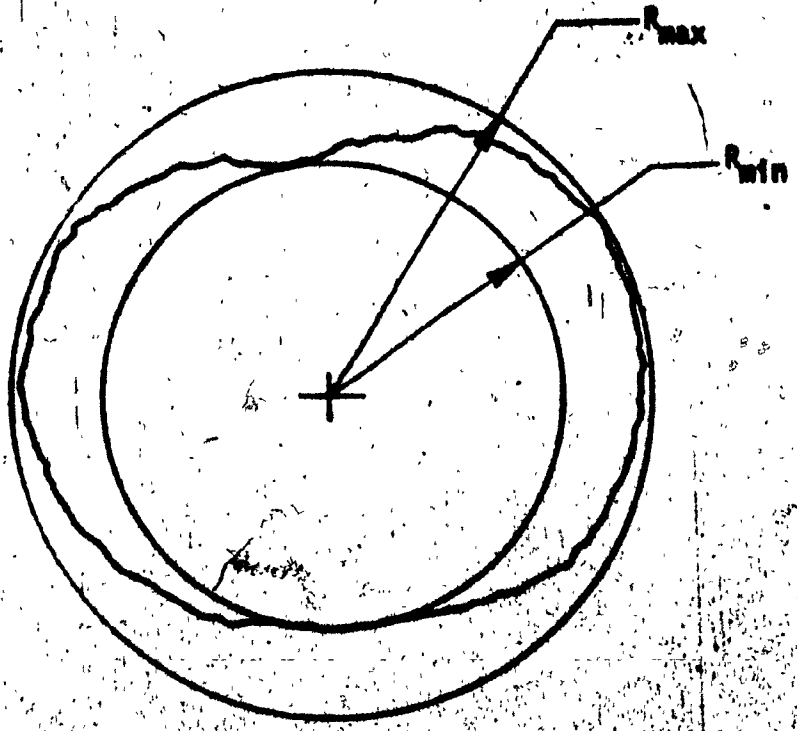

FIG. 1.3 - PLUG GAUGE CENTER

$R_{max} - R_{min} = 3.0u$

c) Minimum Zone Center.

Another approach is to find a center from which can be drawn two concentric circles that will enclose the graph and have a minimum radial separation. See Figure 1.4.

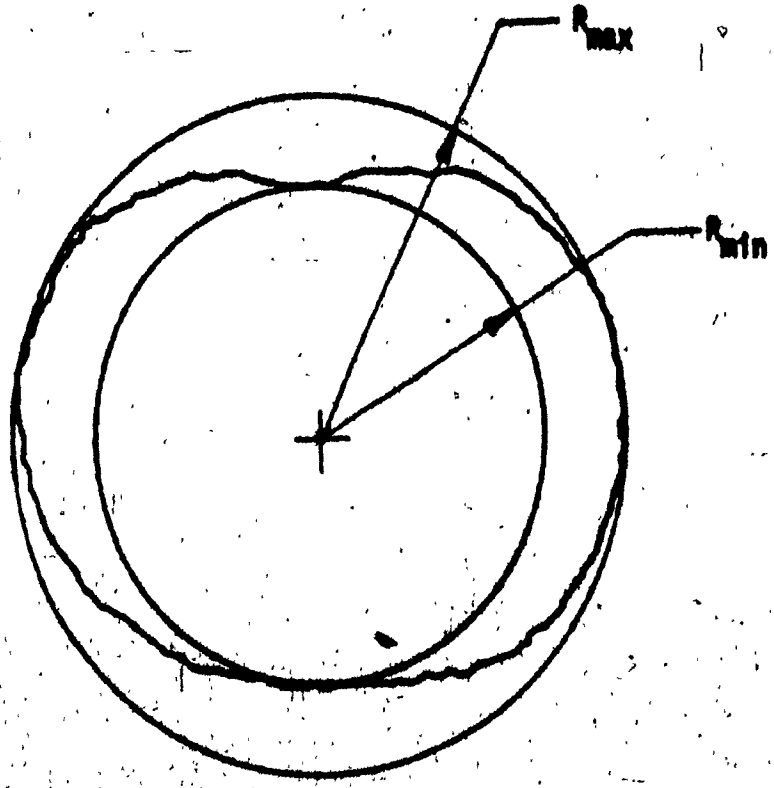

FIG. 1.4 - MINIMUM ZONE CENTER

$R_{max} - R_{min} = 2.75\mu$

d) Least Squares Center.

The center of the least squares circle can be defined as a point from which the sum of the squares of a sufficient number of equally spaced radial ordinates has a minimum value. See Figure 1.5.

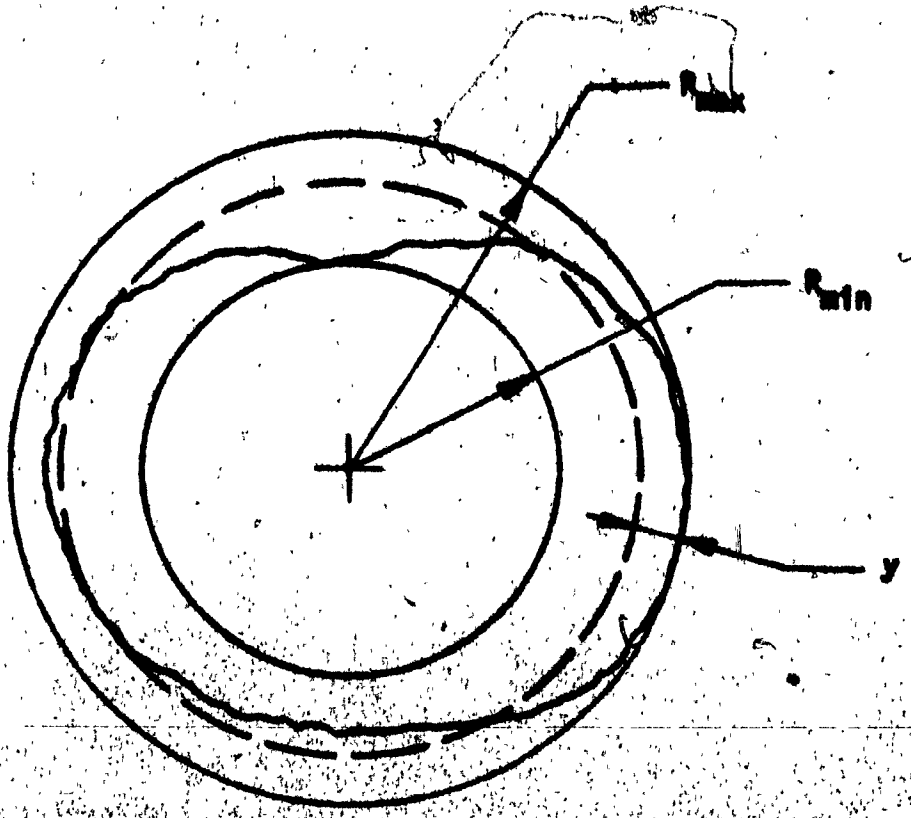

FIG. 1.5 - LEAST SQUARES CENTER

$R_{max} - R_{min} = 4.2\mu$

The least squares mean line is very attractive because of a number of important advantages it presents. This line is unique, can be easily found by calculation, and many electrical instruments work from it naturally. Meter indications of peak-to-valley heights, average values, bearing areas, etc. become a practical proposition.

The graphical procedure for determining the least squares center and circle is seen from Figure 1.6.

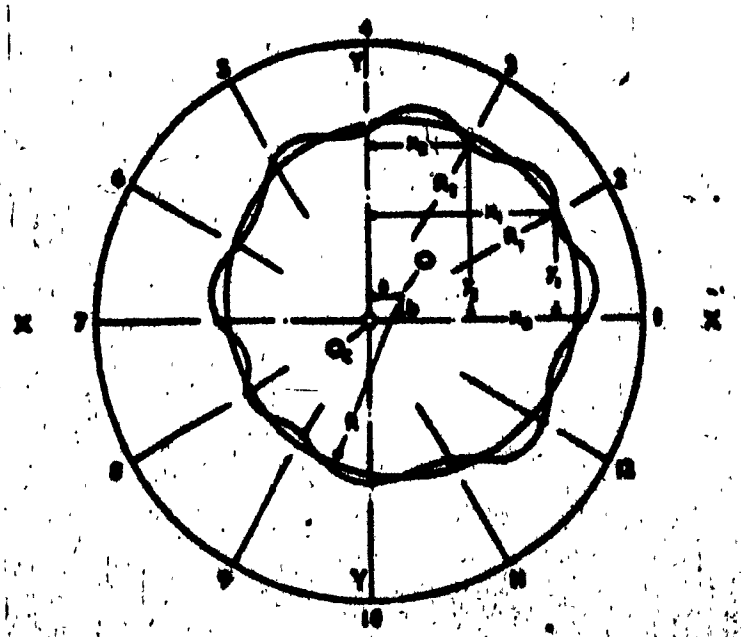

FIG. 1.6 - GRAPHICAL PROCEDURE FOR DETERMINING THE LEAST SQUARES CENTER AND CIRCLE

Here O is the least squares center, and O_c is the center of rotation of the chart. Then it could be shown that to a first order of approximation:

$$a = 2\left\{\frac{X_1 + X_2 + X_3 + \ldots + X_n}{n}\right\} \tag{1.1}$$

$$b = 2\left\{\frac{y_1 + y_2 + y_3 + \ldots + y_n}{n}\right\} \tag{1.2}$$

$$R = \frac{r_1 + r_2 + r_3 + \ldots + r_n}{n} \tag{1.3}$$

The extent to which the out-of-roundness of the same-sample may vary while using different reference circles is of practical interest.

In [1] and [2] the authors report the results of investigations on this subject. In [2] the digital computer was used for this purpose.

The entire investigation consisted of three stages:

1) Plotting the charts of groups of workpieces machined on various types of machine-tools, and determining the harmonic components, statistical frequency, and amplitude spectra of the charts obtained.
2) Working out algorithms for making up various types of basic circles using coordinates of a plurality of points on the graph.
3) Statistical modelling of the chart and comparison of the results obtained by various assessments of departures from roundness by means of digital computer. The results of this investigation show that in most cases the separation of centers is less then 0.25 of the out-of-roundness value.

Therefore, it seems feasible to use the least-squares center as the reference center for numerical assessment of the workpiece roundness.

1.2 Description of Micro-Errors of Round Surfaces

Although useful, the existing standards [3-7] take little or no account of the openness or closeness of the surface irregularities which affect to a great extent surface lubricability and bearing capacity. Consequently, there exist no means to define the given surface texture uniquely. The observation of profilograms shows that the circumferential characteristics may differ considerably while the radial characteristics remain very close.

Recently, new approaches to the definition of the surface texture have been developed. They employ statistical features and/or parametrical descriptions of the profile.

1.2.1 Proposals of Additional Parameters

Some researchers tried to elaborate on the existing standards in order to work out several additional parameters and achieve a correlation between the surface performance and these additional parameters.

One suggestion, [8] is to specify the different sampling length out of the standard row of sampling lengths. A similar approach is seen in [9]. The obvious draw-back here is:

a) the limited choice of sampling lengths,

b) the necessity to provide instructions to the designer which sampling length corresponds to the particular

characteristic of the part,

c) only a qualitative characterization of the surface is achieved,

d) an intensive investigation is required before the correlation between performance of the surface and the sampling length could possibly be established.

In another approach, [10] it is suggested that in addition to the CLA value of the surface roughness following parameters should be specified:

a) method of surface machining,

b) directional lay,

c) form of asperities,

d) maximum depth of valleys,

e) bearing area in percents.

Some of the suggested parameters are strictly qualitative and there is no indication how the suggested parameters should be established.

Since many investigations in the area of journal bearing performance showed the importance of having the maximum peak height, different methods to calculate that parameter were developed. One of the earliest investigations, [11] is based on the extensive number of experiments and it establishes the "predominant peak" roughness for different machining processes (see Table 1.1). The "predominant peak" roughness is a coefficient by which the profilometer reading should be multiplied in order to obtain the actual peak-to-valley distances. Unfortunately, the given coefficients are inherently approximate and vary considerably within the given class of surface finish.

Type of finish	$y_{max/RMS}$ for							
	Cylindrical surfaces				Flat surfaces			
	"Predominant peak" roughness		"Deepest maximum" roughness		"Predominant peak" roughness		"Deepest maximum" roughness	
	Average value	Range of values	Average value	Range of values	Average value	Range of values	Average value	Range of values
Ground	4½	3½ - 5	8½	6½ - 10	7	5 - 8	11	7 - 15
Hyprelapped	6½	5½ - 7½	13	13 - 14	6	5½ - 6½	15	9½ - 21
Sandpapered	7	5½ - 9	12	10 - 13	7	6½ - 7½	17	14 - 19
Superfinished	7	5 - 9½	13	11 - 16	5½	3½ - 7½	10	9 - 12
Loose-abrasive-lapped	10	7½ - 13	19	15 - 23	10	5½ - 13	17	12 - 22

TABLE 1.1 - AVERAGE VALUE AND RANGE OF VALUES OF $y_{max/RMS}$ FOR VARIOUS TYPES OF FINISH (after Tarasov, [11])

A theoretical relationship is established in [12] which gives the expected value of the maximum peak height from the mean line. The theoretical results correlate well with the experimental ones (Figure 1.7). This relationship is established though, under the assumption that the trace of the surface profile has the correlation function and all its derivatives.

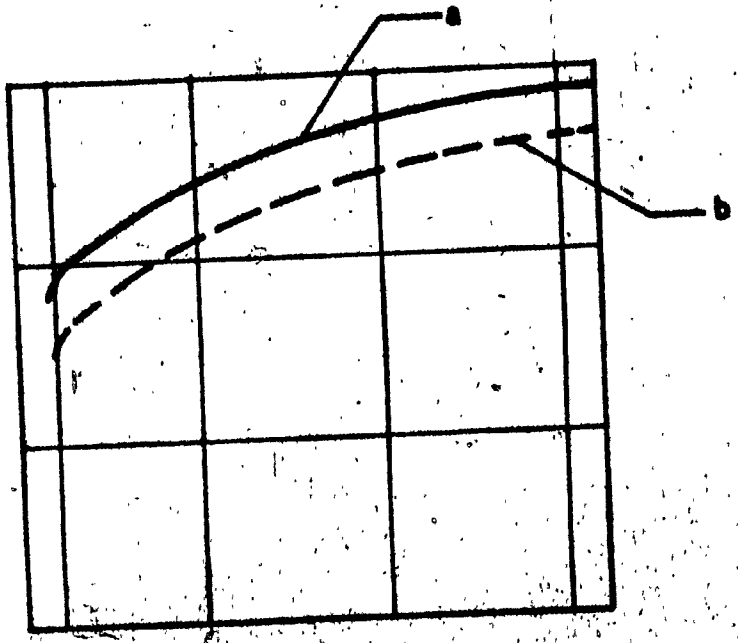

FIG. 1.7 - THE CHANGE IN AVERAGE VALUE OF y_{max} VERSUS THE SAMPLING LENGTH

a) theoretical

b) experimental

In [13], the author analyzes different aspects of surface performance and suggests that five distinct parameters be used for surface texture characterization. These parameters are:

1) Size
2) Spacing — Factors for typical average asperity (macro-roughness)
3) Shape
4) Micro-roughness at asperity peaks
5) Height distribution of asperities

The suggested parameters might characterize the surface texture well enough, but the author does not suggest any way of obtaining these parameters. Also, the author arrives at the above set of parameters by reviewing all the main areas of utilization of surface texture effects. Because of this, the suggested set of parameters is very general and does not take into account the particularities of each area.

1.2.2 Proposals Based on Pictorial Representation

Yet another approach to obtain a more complete characterization of the surface geometry is presented in [14],[15]. The author proposes a new parameter - GST - "General Surface Texture" (see Figure 1.8). It establishes the upper and lower reference lines to be individually placed so that 10 percent of the peaks and 10 percent of the valleys are truncated. Mathematically, this is expressed:

$$P_1 + P_2 + P_3 + \ldots = 0.1L$$

$$V_1 + V_2 + V_3 + \ldots = 0.1L$$

The idea behind that is that the placement of the reference lines is intended to duplicate surface wear-in conditions. The surface between

the upper and lower reference lines is by definition, considered to be the effective boundaries of the workable surface for the service life of the component. This area between the upper and lower reference lines is called the general surface texture.

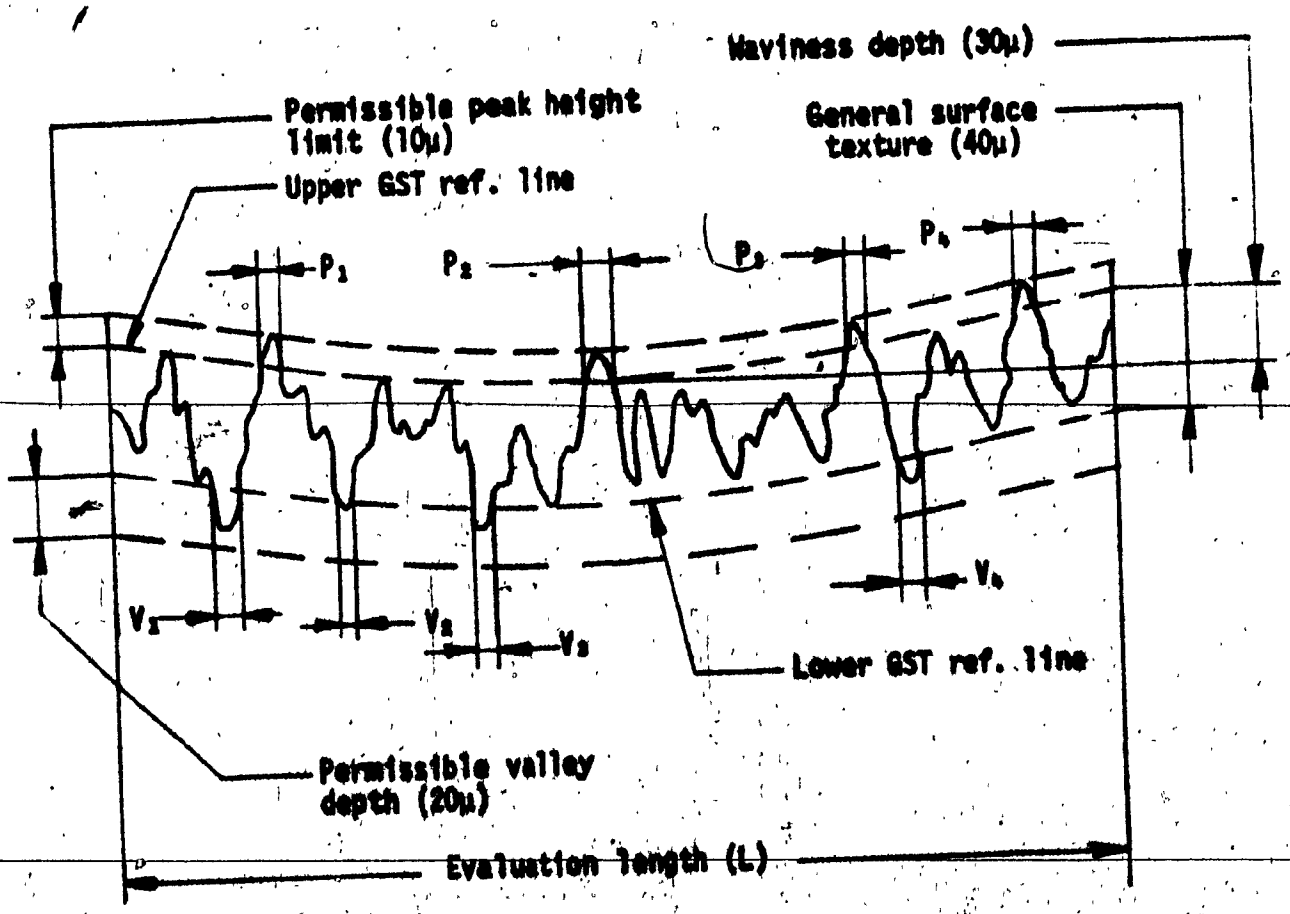

FIG. 1.8 - GRAPHICAL REPRESENTATION OF THE "GST" PROPOSAL

(after Hydell, [15])

In actual practice, the upper and lower reference lines are drawn on the chart, estimating by eye the truncation of the crests and valleys at 10:1 ratio. The biggest drawback in that proposal is, of course, the fact that there is no characterization at all of the lengthwise parameters of the surface. Secondly, we have to rely on pictorial presentations of the surface.

In [16] the authors also suggest the use of pictorial classification in addition to the C.L.A. value. They classify the surface profiles into six categories (Figure 1.9).

Again, the characterization of this kind is only qualitative and a large number of experiments is required to establish the functional behaviour of surfaces of each type. In [16] the drawbacks of the suggested approach are realized and it is agreed that a quantitative value for the characterization of the openness of closeness of the surface texture is necessary.

The influence of sampling length on the common surface texture parameters was investigated in [17]. A number of surfaces were investigated and the following conclusions were drawn from the results:

a) in the ground surfaces, the amplitude distribution approaches to the normal distribution,

b) increase of sampling length reduces the scatter between the values recorded at different positions on the surface,

c) increase of sample size has little influence on the mean C.L.A. and R.M.S. values.

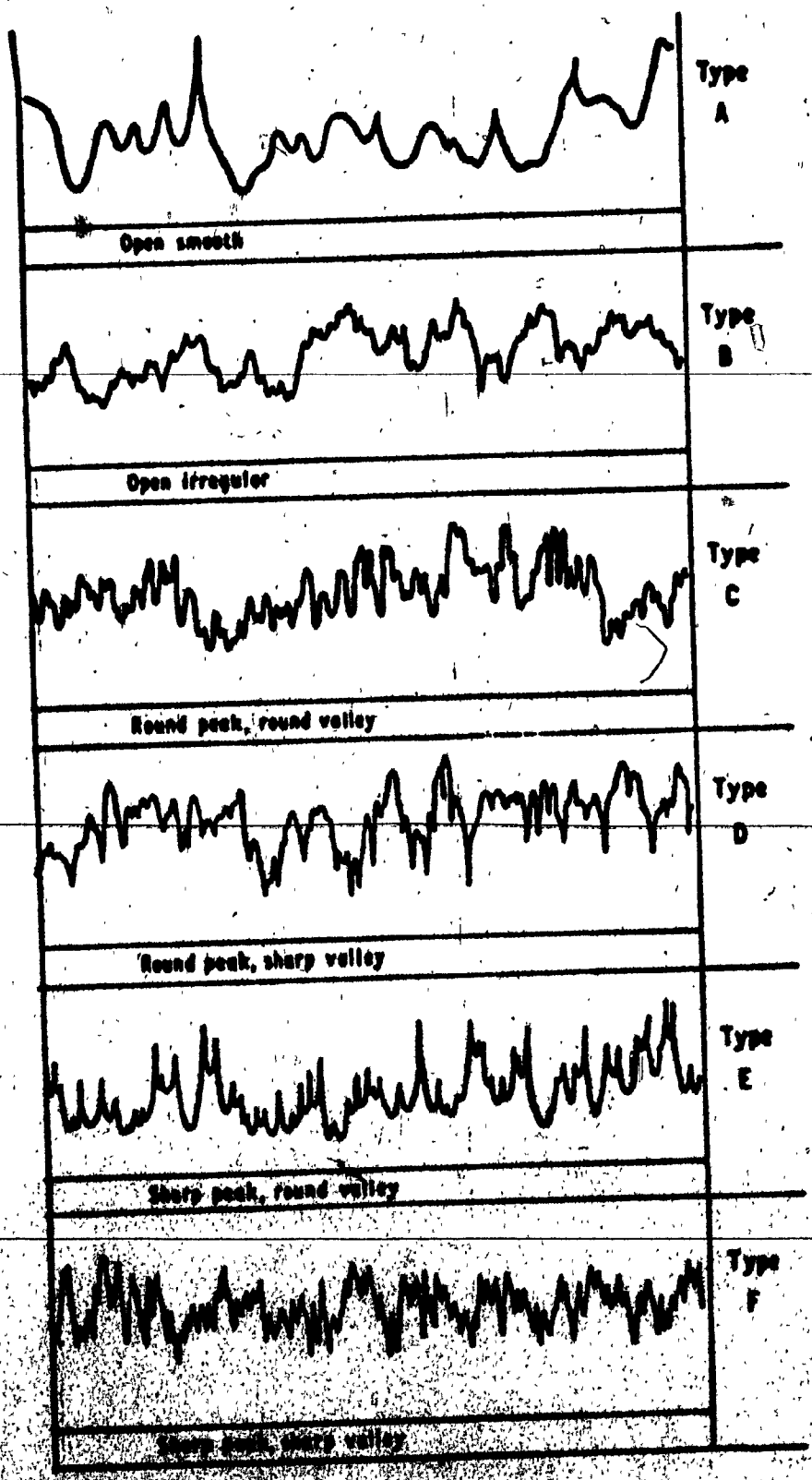

FIG. 1.9 - CLASSIFICATION OF SHEET METAL SURFACE TEXTURE TYPES (Verar Outer, [16])

1.2.3 Proposals Based on the Use of Statistical Features of the Profile

The evaluation of surface geometry by means of co-variance function is proposed in [18]. The author considers the surface profile to be a periodic curve on which random fluctuations are superimposed. The equation for the co-variance function was derived in the form:

$$k(\mu) = C^2 R_a^2 \left[\gamma e^{-\eta\mu} + \beta \cos \frac{2\pi}{\tau_\beta} \mu + \gamma \cos \frac{2\pi}{\tau_\nu} \mu\right];$$

The coefficients γ, β, ν define the proportion of roughness attributable to each component; here $\gamma + \beta + \nu = 1$. The type of surface can be seen from the relationship of these coefficients. One apparent advantage of the described method is its simplicity. On the other hand, a large number of experiments is required to establish the above coefficents for typical surfaces. Also, it is assumed that at most, two periodic components are present. In the case when that number is greater the evaluation of co-variance functions becomes very cumbersome from the numerical point of view.

Finally, high-cost instrumentation like frequency analyzer is required. In [19], [20] and [21] the use of autocorrelation functions is proposed for the characterization of surface geometry. Since the knowledge of autocorrelation function of the surface profile is not possible without complex and costly instrumentation, the investigation [20] shows theoretically and experimentally that the standard deviation of the slope and the mean thickness of the surface profile correlate well with the autocorrelation function. It shows further that these two numbers may be easily computed

for any surface in terms of the average number of crossings per unit length between the profile and a certain level.

In the investigation [21] the work was continued and the two basic elements here are the correlation length and the wavelength correlation. They serve as parameters for the proposed surface typology and define the fundamental surface element. The use of correlation functions is advantageous because of their ability to separate the random and periodic components in a profile. The above method is based on the concept that every surface profile may be described by basic autocorrelation function or a combination of these functions. Based on profile shapes the surfaces are classified in five groups. Analysis of surfaces within each group shows that surfaces manufactured by different methods and consequently having different CLA or RMS values are classified as the same type. Similarly, surfaces with identical CLA or RMS values belong to different groups. The disadvantages of the described method are:

a) complex and costly instrumentation,

b) system of classification is too complex and cumbersome to be practical at the shop level.

In [22] a single parameter for characterization of surface texture is proposed - the spectral density. Though such a parameter does take account to some extent of the circumferential characteristics of the surface texture its determination is difficult. Also, this parameter provides qualitative rather than quantitative characterization of the surface texture.

In [23] the characterization of surface texture is proposed through the amplitude density curves. Again, that approach is inferior to

parametrical characterization, since it requires costly instrumentation and extensive experimental research without giving the designer a definite set of numerical parameters.

1.2.4 Proposal Based on the Use of Angular Frequency

In [24] the authors propose the use of an additional parameter - average wavelength - plus to the C.L.A. value. This parameter is derived by the following formula:

$$\lambda_{RMS} = 2\pi \frac{a}{\sigma'};$$

and should give the characterization of the surface in the lengthwise direction.

The average wavelength λ_{RMS} is calculated through the angular frequency rather than through the wavelength directly. In this investigation, the authors made a computation of the spectrum and correlation functions of a large number of practical machined surfaces which has shown that most surfaces fall roughly into two categories: first order random and second order random. The way in which these surfaces differ from the periodic is in the shape of the amplitude distribution. The authors show that for first and second order random waveform, the amplitude distributions tend to be Gaussian whereas for the periodic waves they are not. Single point machined surfaces can usually be classified some where in between the second order random and the periodic. It should be noted that the average wavelength is a useful indication of wear as compared to bearing area parameters used presently.

1.2.5. Proposal Based on the Use of Random Excursion Theory

In [25] and [26] the authors employ the theory of stochastic excursions to characterize the surface texture in the amplitude and and lengthwise directions. The investigation shows that an accurate characterization of the roughness can be obtained from the knowledge of the intercept probabilities of the crest and valley excursions of the surface about any given level, specified with respect to the mean line. Based on these probability densities the authors propose new surface texture parameters. These are:

- CLA - center line average height of the profile
- RMS - root mean square value of the profile
- AMS - absolute mean slope of surface texture
- RMSS - root mean square value of the slope
- MCE - mean crest excursion
- RMSCE - root mean square crest excursion
- MVE - mean valley excursion
- RMSVE - root mean square valley excursion.

One of the advantages of these proposed parameters is that they correspond well to the mechanical properties of the surface and can therefore be used in specifications. On the other hand, it is relatively complicated to work with a large number of parameters (eight) and an extensive experimental research has to be conducted to establish precise correlation of the proposed parameters with surface texture performance.

1.2.6 Proposals Based on the Use of Friction Theory

The use of friction theory for characterization of surface micro-

topography is shown in [27]. The author gives experimental constants which characterize the "overall measure or roughness". Once again, it should be remembered that no single parameter can be used to satisfactorily characterize the functional behaviour of the surface. Also, even for characterization of only friction properties this parameter can be used only after a large number of experiments were conducted.

Another work [28] is also devoted to the investigation of friction properties of the surface. For this purpose the authors suggest the use of "topographic index" to characterize the surface micro-geometry. This index is given as a function of the size of an individual asperity and the number of those asperities per unit area. Such a parameter may be useful for characterization of friction properties of the surface but in other aspects of surface performance not much can be derived from it.

1.3 Concluding Remarks

As a conclusion it appears that there is a need for more accurate description of round surface to specify besides the O.O.R. value the size of valleys, number of peaks, the size of total valley area on the round surface and the CLA value of surface texture.

Some of these parameters could be determined through amplitude density curves [23], correlation functions [19,20,21], spectral density [22]. Yet these approaches proved to be more qualitative than quantitative.

In this investigation the mathematical theory of stochastic excursions is employed to obtain unique values describing valley width and number of peaks with respect to a mean line describing a reference circle. It is proposed that such an approach will give sufficient

number of key roundness parameters in both radial and circumferential directions. The method is easily computerized for practical applications and lends itself to automated quality control as well as "on-line" roundness evaluation in production.

CHAPTER 2

MATHEMATICAL MODELLING OF MACRO - AND MICROGEOMETRY OF ROUND SURFACE THROUGH THE THEORY OF STOCHASTIC EXCURSIONS

CHAPTER 2

MATHEMATICAL MODELLING OF MACRO - AND MICROGEOMETRY OF ROUND SURFACE THROUGH THE THEORY OF STOCHASTIC EXCURSIONS

Figure 2.1 represents a typical curve of profile as it is drawn by the measuring device, in our case - "Talyrond 51". As it is seen, the graph shown is the polar representation of the signal. The reference circle which is in this case the reference line is taken as the least-mean square circle and in the previous chapter it is explained why this particular reference circle is chosen.

The characteristics of the surface geometry are calculated by including the probability densities of the number of excursions of the random signal about a given reference curve and also the intercepts of this excursion about this level. In the present case, this level is chosen with respect to the CLA-value, which is in itself an accepted statistical value representing the average height of surface irregularities.

The information required for the proposed x-directional characteristics of a surface are then the following probabilistic quantities:

1. the average number of crossings N_c per unit length of the surface undulations about a preselected level $y = y_1$ along the x-axis,
2. the probability density $p_c(\lambda)$ of the crest excursions of the surface signal equal to or less than a λ-value that is specified,

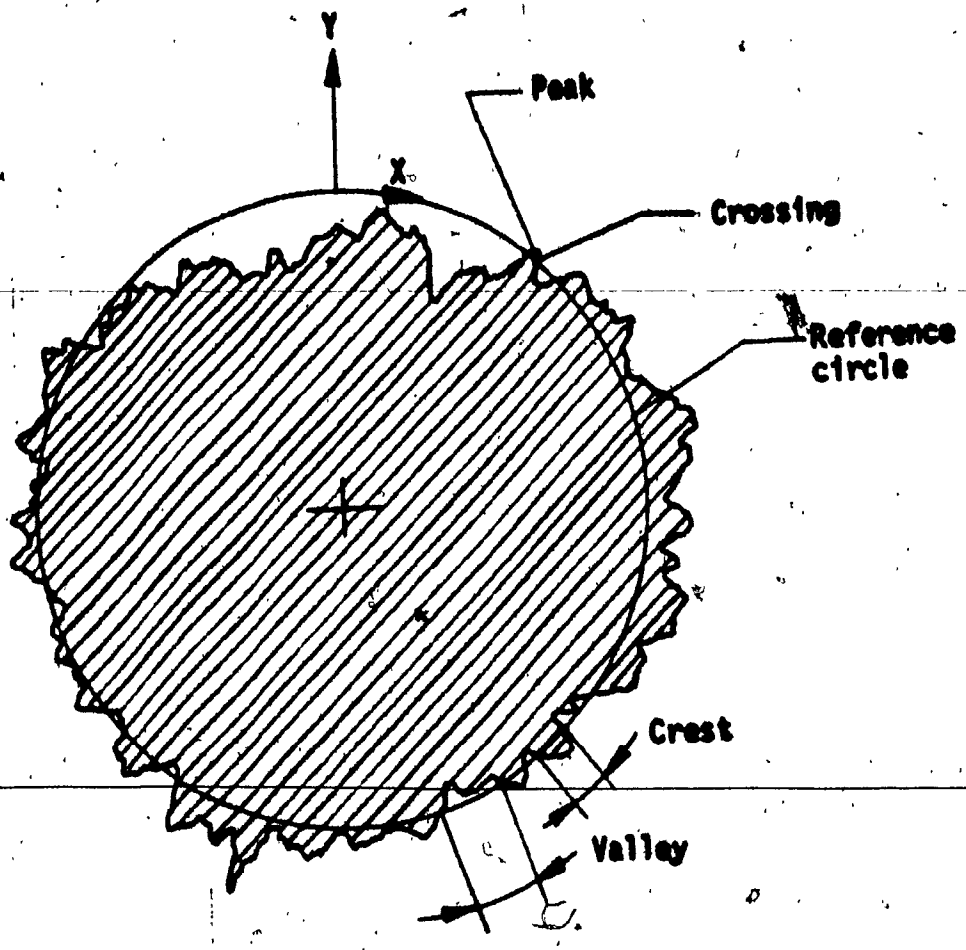

FIG. 2.1 - TYPICAL SURFACE PROFILE

3. the probability density $p_v(\Lambda)$ of valley excursions of the surface signal equal to or less than a Λ-value that is specified.

The probabilities $p_c(\lambda)$ and $p_v(\Lambda)$ mentioned in 2 and 3 above are computed about the preselected level $y = y_1$. The level y_1 is defined with respect to the CLA-value according to the explanation presented earlier in this paper. y_1 can then be defined as

$$y_1 = \varepsilon[\text{CLA-value}]. \tag{2.1}$$

where ε is a multiplication factor to determine crest calculation level in terms of CLA. ε is taken as unity in this paper.

2.1 Determination of OOR Value

The out-of-roundness value can then be defined as:

$$OOR = y_{max} - y_{min} \tag{2.2}$$

2.2 Determination of CLA Value

The center line average height of the surface profile can be calculated by the following equation:

$$CLA = \sum_{i=1}^{n} \frac{|y_i|}{n} \tag{2.3}$$

2.3 Determination of RC Value

Let the signal reproduced by a measurement of a surface be represented by a function $y = y(x)$. Further, let the random signal so obtained

be stationary and Gaussian in nature. Such an assumption is quite valid for most real processes and especially true in the case of surface undulations. The probability density distribution of a Gaussian signal can be written as

$$p(y) = \frac{1}{\sigma\sqrt{2\pi}} \exp(-y^2/2\sigma^2), \tag{2.4}$$

where $$\sigma^2 = E[y^2(x)] \ , \tag{2.5}$$

if $$E[y(x)] = 0.$$

Here, σ is the standard deviation of $y(x)$, i.e. the RMS value of the signal, and E denotes the ensemble average. If $E[y(x)]$ is not equal to zero, the value of σ is then given by

$$\begin{aligned} \sigma^2 &= E[\{y(x) - E[y(x)]\}^2] \\ &= E[y^2(x)] - E[y(x)]^2 \end{aligned} \tag{2.6}$$

Generally it is preferable, for the sake of simplicity, to choose the x-axis such that $E[y(x)] = 0$. This may be achieved by a shift of the abscissa to a desired level in the y-direction.

The mean slope η' (AMS) and the standard deviation σ' (RMSS) of the slope of the surface texture are defined respectively as

$$\begin{aligned} \eta' &= E[|y'(x)|], \text{ and} \\ (\sigma')^2 &= E[\{y'(x)\}^2] \end{aligned} \tag{2.7}$$

where $y'(x)$ is the slope (dy/dx) of the function $y(x)$. The values of σ and σ' may be easily computed for any given random signal and are required in the calculation of N_c, $P_c(\lambda)$ and $P_y(A)$.

N_c about a level $y = y_1$ is given by the equation

$$N_c = \frac{1}{2\pi\sigma}\sigma' \exp(-y_1^2/2\sigma^2). \qquad (2.8)$$

As it is seen from Figure 2.1, the NP value is calculated as

$$NP = \frac{N_c}{2} \qquad (2.9)$$

2.4 Determination of MVE value

Now the probability density of the duration of the surface excursions $p_c(\lambda)$ and the density of the interval between the excursions $p_v(\Lambda)$ about any specified level y_1 can be evaluated using the following procedure. A part of this procedure is due to Tikhonov [29], and is presented here in the context of the present problem. Let the crest excursion over the level y_1 be started at the length coordinate $x = x_0$ and continue till $x = x_1$. Then

$$y_0 = y(x)\Big|_{x = x_0} = y(x_0) = y_1$$

and (2.10)

$$y_0' = \frac{d}{dx}y(x)\Big|_{x = x_0} = y'(x_0) > 0$$

Similarly,

$$y_1 = y(x_1) \text{ and } y_1' < 0 \text{ at } x = x_1$$

Under these conditions, an approximate expression for the probability density $p_c(\lambda)$ may be written in terms of the random variables (y_0, y_1, y_0', y_1') as [29].

$$p_c(\lambda) = \frac{1}{N_c(y_2)} \int_0^{\infty} \int_0^{-\infty} y'_0 y'_1 p_2(y_0, y_1, y'_0, y'_1) dy'_0 dy'_1 \qquad (2.11)$$

Here the probability densities p_n for the signal y(x) are given by the general form

$$P_n(y_1, y_2, \ldots y_n) = (2\pi)^{-\frac{n}{2}} D^{-\frac{1}{2}} \sigma^{-n} \exp\left[-\frac{1}{2D} \sum_{i,j=1}^{n} D_{ij} \frac{Y_i Y_j}{\sigma^2}\right] \qquad (2.12)$$

where D is the n-the order determinant

$$D = \begin{vmatrix} K_{11} & K_{12} & \cdots & K_{1n} \\ \vdots & & & \\ K_{n1} & K_{n2} & \cdots & K_{nn} \end{vmatrix} \qquad (2.13)$$

and D_{ij} is the algebraic cofactor of the K_{ij} element of this determinant. Further, $K_{ij} = K(x_i - x_j)$ is the value of the correlation coefficient for the random function y(x) at values x_i and x_j. Using the general form (2.12), the probability density $p_2(y_0, y_1, y'_0, y'_1)$ in equation (2.11) can be written for the values of the function y(x) and its derivatives at positions x_0 and x_1 that are apart by an interval λ, equal to the crest width.

The correlation coefficients in the determinant (2.13) for the four random variables (y_0, y_1, y'_0, y'_1) may be expressed in terms of the following coefficients:

$$K = \frac{E[y(x_0)y(x_1)]}{\sigma^2}$$

$$K_1 = \frac{E[y(x_0)y'(x_1)]}{\sigma\sigma'} \qquad (2.14)$$

and $$K_2 = \frac{E[y'(x_0)y'(x_2)]}{\sigma'^2} \qquad (2.14)$$

It may be noted here that the correlation coefficient corresponding to the correlation between the same random function will be equal to unity and that corresponding to the correlation between random function and its derivative, say, for example, $E[y(x_0)y'(x_0)]$, will be zero.

The determinant D for the variables then takes the symmetric form

$$D = \begin{vmatrix} 1 & K & 0 & K_1 \\ K & 1 & -K_1 & 0 \\ 0 & -K_1 & 1 & K_2 \\ K_1 & 0 & K_2 & 1 \end{vmatrix} \qquad (2.15)$$

It may be possible to consider the correlation coefficient $K(\tau)$ to be of the Gaussian form (valid for surface textures)

$$K(\tau) = \exp(-\alpha\tau^2) , \qquad (2.16)$$

where α is defined for the type of process $y(x)$ under consideration. The selection of such a $K(\tau)$ is quite valid in problems involving real and non-Markovian processes. It follows then from equation (2.16) that

$$\begin{aligned} \sigma_1' &= \sigma(2\alpha)^{\frac{1}{2}} \\ K_1 &= -\sqrt{2\alpha}\,\tau\,K(\tau) \\ K_2 &= (1 - 2\alpha\tau^2)\,K(\tau) \end{aligned} \qquad (2.17)$$

The D_{ij}'s in equation (2.15) may now be written in terms of K, K_1 and K_2. For example,

$$D_{11} = \begin{vmatrix} 1 & -K_1 & 0 \\ -K_1 & 1 & K_2 \\ 0 & K_2 & 1 \end{vmatrix} = 1-K_1^2-K_2^2$$

and

$$D_{12} = -\begin{vmatrix} K & 0 & K_1 \\ -K_1 & 1 & K_2 \\ 0 & K_2 & 1 \end{vmatrix} = K_1K_2^2 - K(1-K_2^2); \text{ etc.}$$

Using the above results in equation (2.12), an expression for $p_2(y_0,y_1,\dot{y}_0,\dot{y}_1)$ may be obtained. Substituting this result in equation (2.11) and carrying out the integration, the probability density for the crest intercepts having a crest width less than or equal to λ about the level y_1 may be otained as in [27]

$$p_c(\lambda) = M(\bar{y}_1,\lambda)\left[a_0^2 + \sum_0^\infty \frac{a_n^2}{n!}\zeta^n\right], \qquad (2.18)$$

where $\bar{y}_1 = \frac{y_1}{\sigma}$, and the function

$$M(\bar{y}_1,\lambda) = \frac{(2\alpha)^{\frac{1}{2}}}{(1-K^2)^{1.5}} D_{33} \exp\left[\bar{y}_1^2\left(\frac{1}{2} - \frac{D_{11}}{D}\right)\right]$$

with

$$\zeta = \frac{D_{34}}{D_{33}}.$$

The coefficients a_n are given by Tikhonov [27] as

$$
\begin{aligned}
a_0 &= (2\pi)^{-\frac{1}{2}} - \gamma f(-\gamma), \\
a_1 &= \gamma(2\pi)^{-\frac{1}{2}} - (\gamma^2+1)f(-\gamma), \\
a_2 &= (\gamma^2+1)\,(2\pi)^{-\frac{1}{2}} - (\gamma^3+2\gamma)f(-\gamma), \\
a_3 &= (\gamma^3+2\gamma)\,(2\pi)^{-\frac{1}{2}} - (\gamma^4+3\gamma^2)f(-\gamma), \\
a_4 &= (\gamma^4+3\gamma^2-1)\,(2\pi)^{-\frac{1}{2}} - (\gamma^5+4\gamma^3)f(-\gamma), \\
a_5 &= (\gamma^5+4\gamma^3-2\gamma)\,(2\pi)^{-\frac{1}{2}} - (\gamma^6+5\gamma^4)f(-\gamma),
\end{aligned}
\tag{2.19}
$$

where

$$\gamma = \bar{y}_1 D_2 \,(D_{33}^2 - D_{34}^2)^{-\frac{1}{2}}\,[(1-K^2)D_{33}]^{\frac{1}{2}},$$

$$f(-\gamma) = \psi(-\gamma)\exp\left|\frac{\gamma^2}{2}\right|,$$

and

$$\psi(-\gamma) = (2\pi)^{-\frac{1}{2}} \int_{-\infty}^{-\gamma} \exp(-\tfrac{u^2}{2})\,du.$$

It may be observed that in the quation (2.18) for $p_c(\lambda)$, the summation need be taken only over the first six terms, say n=5, as an approximation. Such an approximation is quite valid if the range of the coefficient γ is between -1.4 and 0 with the value of $\bar{y}_1 < 4$ (or $y_1 < 4\sigma$) for all positive values of x. This is admissible for the problem under consideration.

The quantity $p_c(\lambda)$ represents the probability density of the surface signal excursion having an intercept or crest width less than or equal to a specified value λ about the level y_1. The probability distribution $p_c(\lambda)$, which may be required sometimes in many surface specifications, may be obtained from the relation

$$P_c(\lambda) = \int_0^{\lambda} p_c(\lambda)d\lambda = \Sigma p_c(\Delta\lambda)\Delta\lambda \tag{2.20}$$

where the specified crest width λ is considered to be made up of a number of smaller intercepts $\Delta\lambda$ and the individual probability densities are summed.

The shape of $p_c(\lambda)$ vs λ curve provides valuable information on the surface roughness. Two new surface roughness parameters can now be defined from the knowledge of $p_c(\lambda)$. These can be termed as the mean crest excursion (MCE) and root-mean-square crest excursion (RMSCE) which are similar in character to the mean line CLA- and RMS-values of the surface amplitudes. As the mean and RMS-values give the amplitude fluctuation information in the height direction, the MCE and RMSCE-values define surface characteristics in the lengthwise direction. Then, by definition,

$$\text{MCE} = E[\lambda] = \int_{-\infty}^{\infty} \lambda p_c(\lambda) d\lambda = \sum_{i=1}^{n_a} \lambda_i P_c(\lambda_i) \tag{2.21}$$

and

$$\begin{aligned} \text{RMSCE} = \{E[(\lambda-\text{MCE})]\}^{\frac{1}{2}} &= \left[\int_{-\infty}^{\infty} (\lambda-\text{MCE})^2 P_c(\lambda) d\lambda\right]^{\frac{1}{2}} \\ &= \left[\sum_{i=1}^{n_a} (\lambda_i-\text{MCE})^2 P_c(\lambda_i)\right]^{\frac{1}{2}} \end{aligned} \tag{2.22}$$

where n_a is the number of distinct values of λ.

Once the $p_c(\lambda)$ vs λ curve is available for different values of possible excursion intercepts, the parameters MCE and RMSCE can be computed using the moment formulae (2.21), (2.22). MCE gives the mean crest intercepts at the level y_i for the surface sample and RMSCE gives the standard deviation of the crest excursions from the mean spacing of the surface texture.

For an estimate of the probability of valley excursions, $p_v(\Lambda)$, a similar procedure can be adopted. The mathematical formulation can be easily derived similar to equation (2.18); the probability is then given by

$$p_v(\Lambda) = M(\overline{y}_1, \Lambda) \left[b_0^2 + \sum_0^\infty \frac{b_n}{n!} \zeta^n \right] \tag{2.23}$$

with the same nomenclature, except that the valley interval Λ is used in the computations. The coefficients b_n may be obtained from the coefficients a_n that are previously given in (2.19) using the relations

$$\begin{aligned}
b_0 &= a_0 + \exp[\tfrac{\gamma^2}{2}] \\
b_1 &= -a_1 - (\gamma^2 + 1) \exp[\tfrac{\gamma^2}{2}] \\
b_2 &= a_2 + (\gamma^2 + 2) \exp[\tfrac{\gamma^2}{2}] \\
b_3 &= -a_3 - \gamma^2(\gamma^2 + 3) \exp[\tfrac{\gamma^2}{2}] \\
b_4 &= a_4 + \gamma^3(\gamma^2 + 4) \exp[\tfrac{\gamma^2}{2}] \\
b_5 &= -a_5 - \gamma^5(\gamma^2 + 5) \exp[\tfrac{\gamma^2}{2}]
\end{aligned} \tag{2.24}$$

Based on $p_v(\lambda)$, two more surface parameters can be generated that give information on mean and root mean square value of valley excursions, namely, MVE and RMSVE. Again, by definition,

$$\text{MVE} = E[\Lambda] = \int_{-\infty}^{\infty} \Lambda p_v(\Lambda) d\Lambda = \sum_{i=1}^{n_a} \Lambda_i \, P_v(\Lambda_i) \tag{2.25}$$

and

$$\begin{aligned}
\text{RMSVE} = \{E[(\Lambda - \text{MVE})^2]\}^{\frac{1}{2}} &= \left[\int_{-\infty}^{\infty} (\Lambda - \text{MVE})^2 \, p_v(\Lambda) d\Lambda \right]^{\frac{1}{2}} \\
&= \left[\sum_{i=1}^{n_a} (\Lambda_i - \text{MVE})^2 \, p_v(\Lambda_i) \right]^{\frac{1}{2}}
\end{aligned} \tag{2.26}$$

and can be computed from the $p_v(\Lambda)$ vs Λ curve. These parameters give additional lengthwise descriptions but it may be only necessary to generate MCE and RMSCE values since the valley excursions are directly related to these former parameters in equations (2.21) and (2.22).

2.5 Determination of TVE Value

The total valley excursion value (TVE) is obtained from equation:

$$TVE = NP - MVE \tag{2.27}$$

2.6 Computational Sequence of Roundness Parameters

A computer program is compiled based on the theory described in this chapter to calculate the five roundness parameters. These are: OOR, CLA, NP, MVE and TVE.

Suppose n discrete surface measurements are made on the specimen. This data is stored in magnetic tapes after analog to digital conversion. The computer program processes the data and calculates the required roundness parameters in the following manner:

a) Compute the OOR value as in (2.2).

b) Compute the CLA value as in (2.3).

c) Compute the average $\bar{y}$ of the amplitudes.

d) Normalize the n data points with respect to $\bar{y}$ (by shifting the x-axis to $\bar{y}$-level), and read the new normalized n points, with $\bar{y} = 0$.

e) Compute y', η' and σ' using equation (2.7) and standard subroutines for entire signal in the discretized form.

f) Evaluate the average number of crossings N_c, about level y_1, using equation (2.8).

g) Compute the NP value, according to equation (2.9).

h) Using equations (2.18) and (2.19), compute $p_c(\lambda)$ for different values of λ starting from a small value and increasing in steps of $\Delta\lambda$.

i) Calculate MCE and RMSCE from the $P_c(\lambda)$ vs λ plot, using equations (2.21) and (2.22).

j) Calculate $P_v(\lambda)$ using equations (2.23) and (2.24) and obtain MVE and RMSVE from (2.25) and (2.26).

k) Compute TVE value using equation (2.27).

A flow chart for computation of these parameters is given in Figure 2.2.

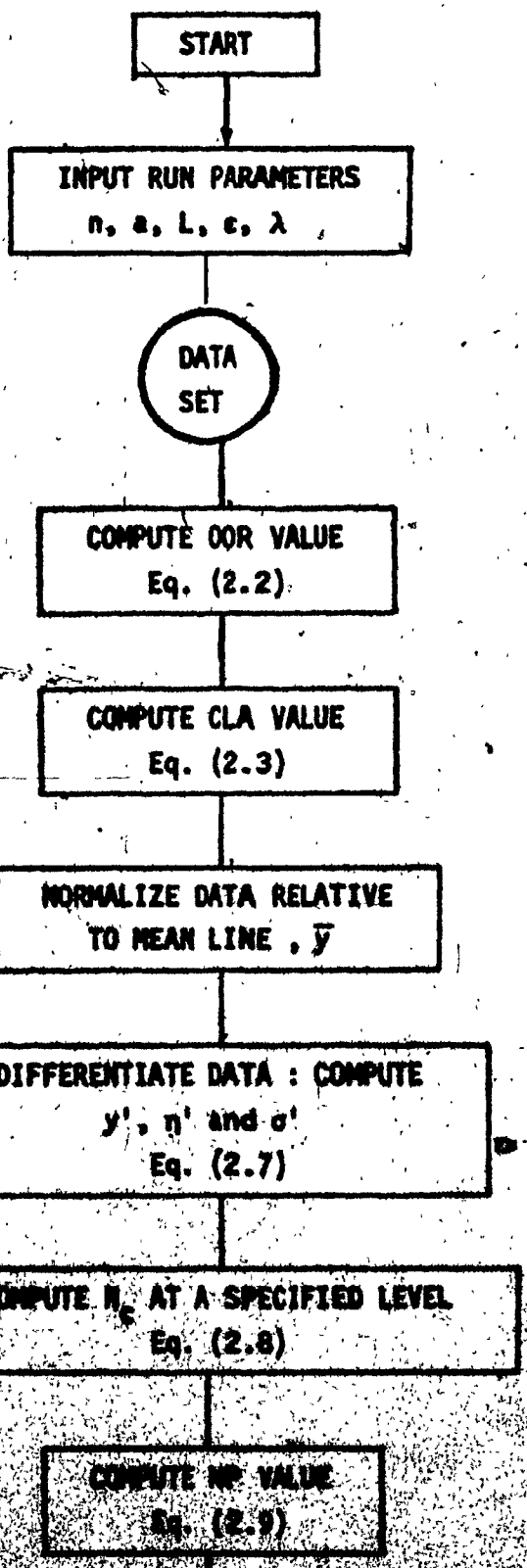

(Continued on page 37)

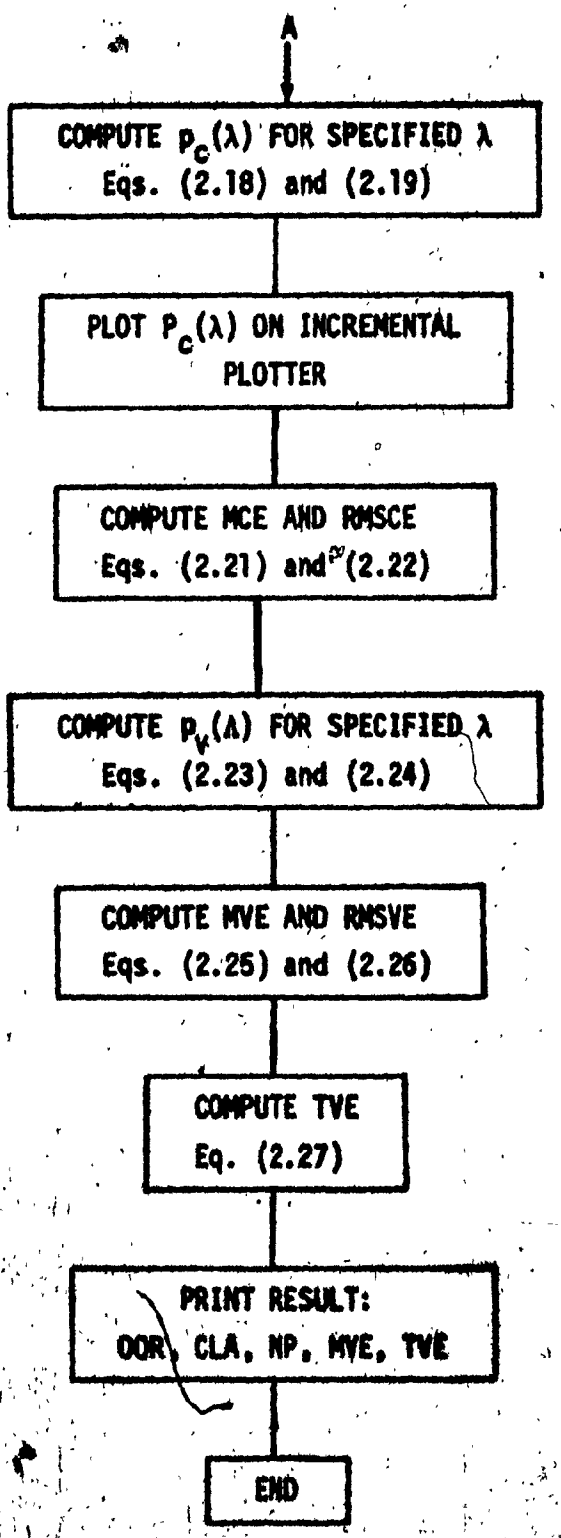

FIG. 2.2 - FLOW CHART FOR COMPUTATION OF ROUNDNESS PARAMETERS

CHAPTER 3

EXPERIMENTAL SET-UP AND DATA SAMPLING OF OBTAINED ROUNDNESS SIGNAL

CHAPTER 3

EXPERIMENTAL SET-UP AND DATA SAMPLING OF OBTAINED ROUNDNESS SIGNAL

3.1 Experimental Set-up

The device used for recording the sample roundness was "Talyrond 51" by Taylor Hobson Inc. The characteristics of the machine are given in Appendix I.

The signal of surface roundness appears on the polar chart drawn by the recording head of "Talyrond 51". This curve represents, in the magnified form, the displacement of the stylus which is converted into the voltage driving the pen of the recorder. The hybrid computer works from an analog signal such as electric voltage. This signal was recorded and stored on the magnetic tape. The block diagram of the above arrangement is shown in the Figure 3.1. The pictures of the actual experimental set-up are shown in Figures 3.2 and 3.3. This arrangement allowed us to observe the signal on the screen of the oscilloscope and to store it on the magnetic tape as an electrical signal which could be put through a computer for further processing.

3.2 Data Transmission

The difference in the capacitances of the "Talyrond 51" and the magnetic tape recorder required the use of the special amplifier (Figure 3.4). At the same time, this amplifier allowed the use of different gains in the network which was essential when samples with different surface roughness were used.

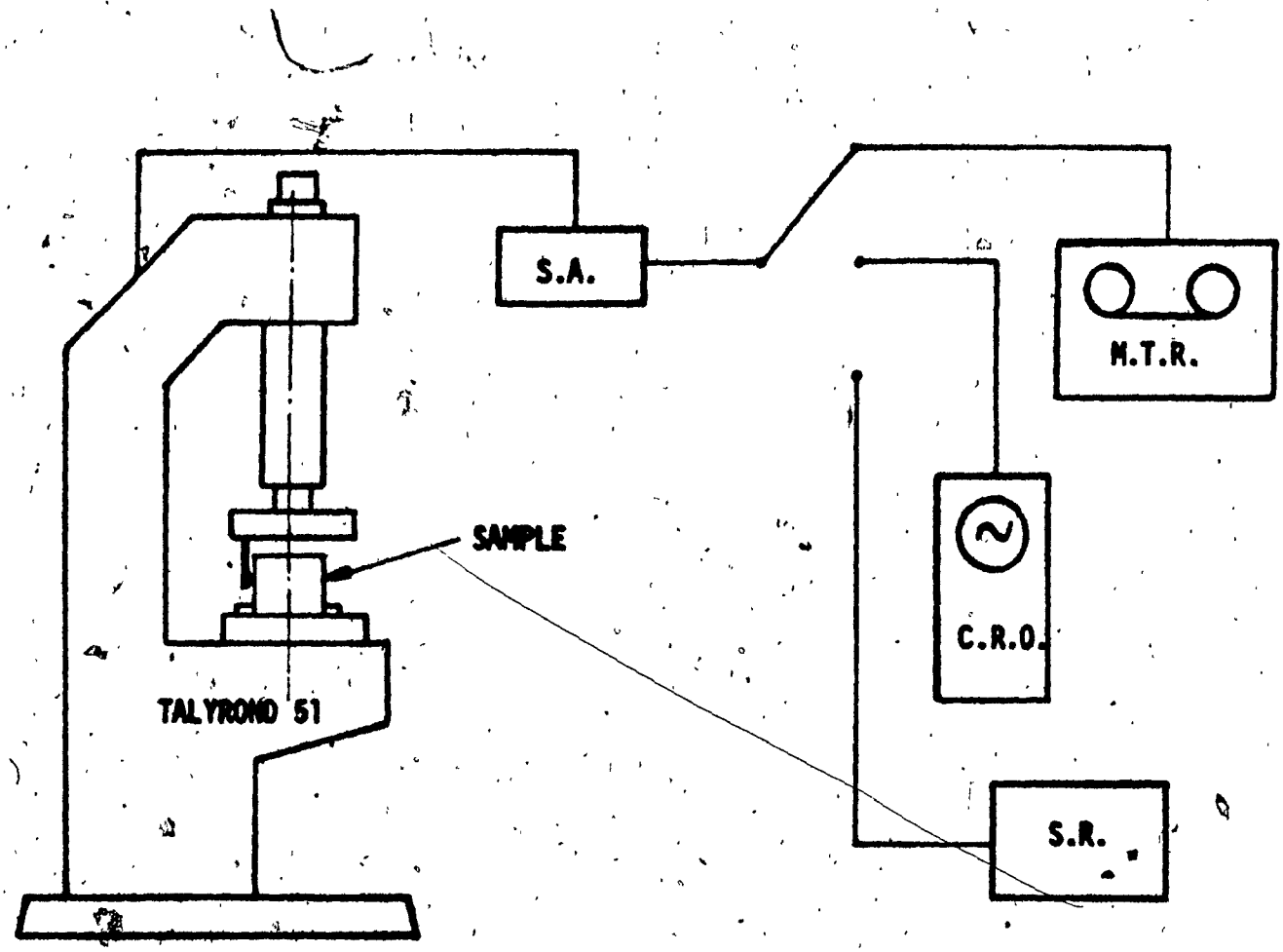

FIG. 3.1 - BLOCK DIAGRAM OF THE SET-UP FOR ROUNDNESS MEASUREMENTS.

S.A. - special amplifier

M.T.R. - magnetic tape recorder

C.R.O. - cathode ray oscilloscope

S.R. - strip-chart recorder

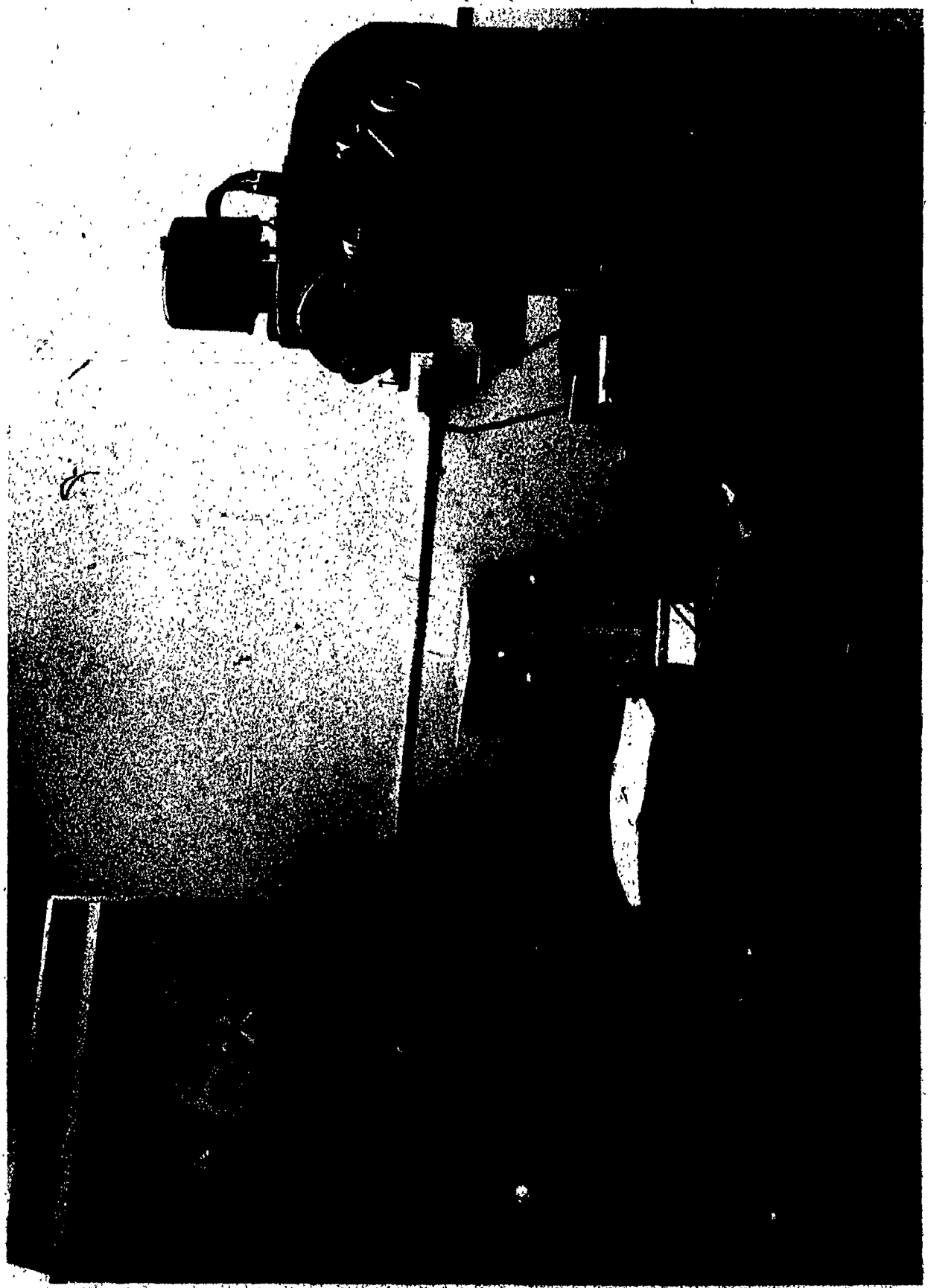

FIG. 3.2 - ACTUAL EXPERIMENTAL SET-UP

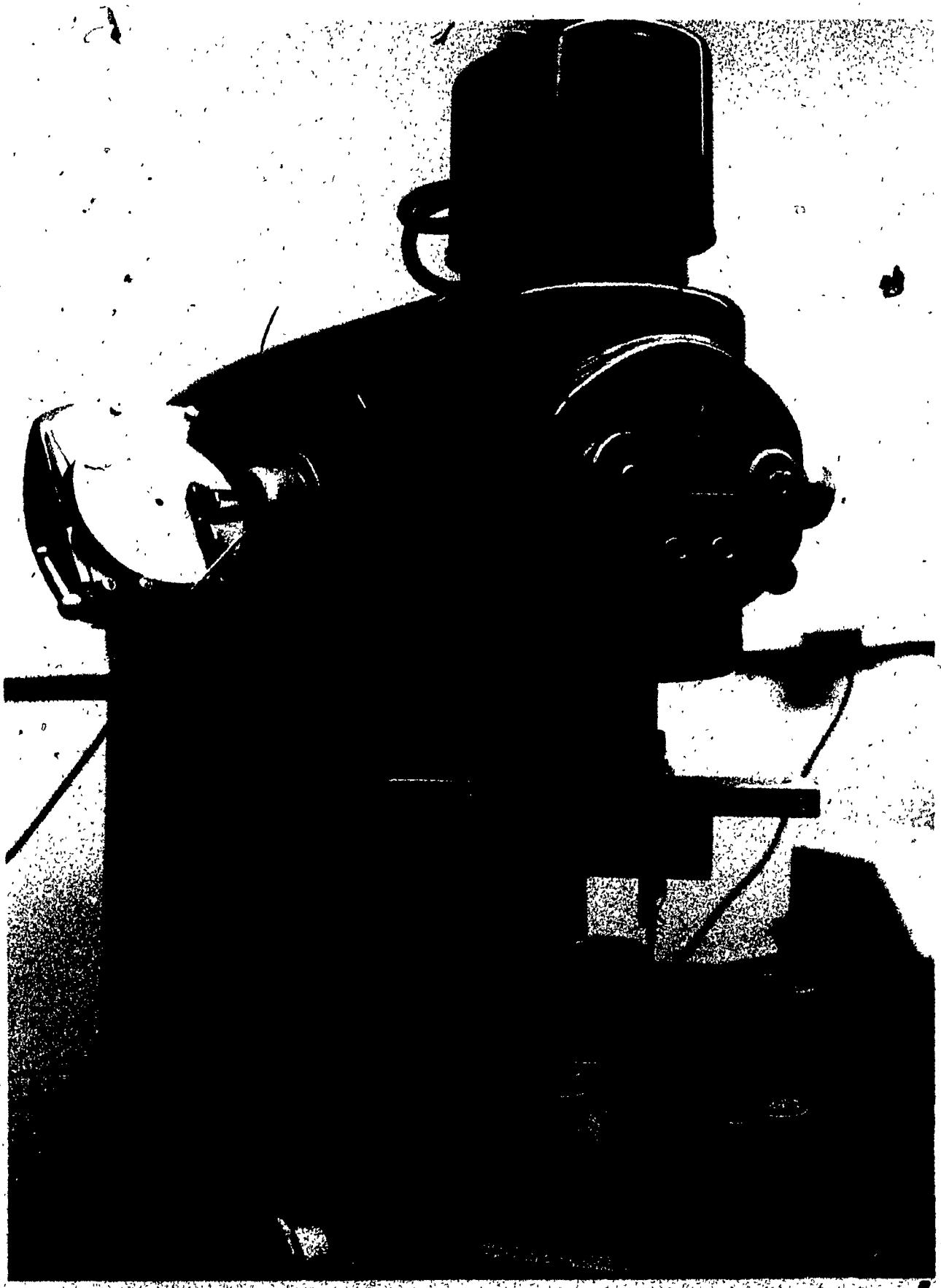

FIG. 3.3 - ACTUAL EXPERIMENTAL SET-UP

AMPLIFIER MA 741

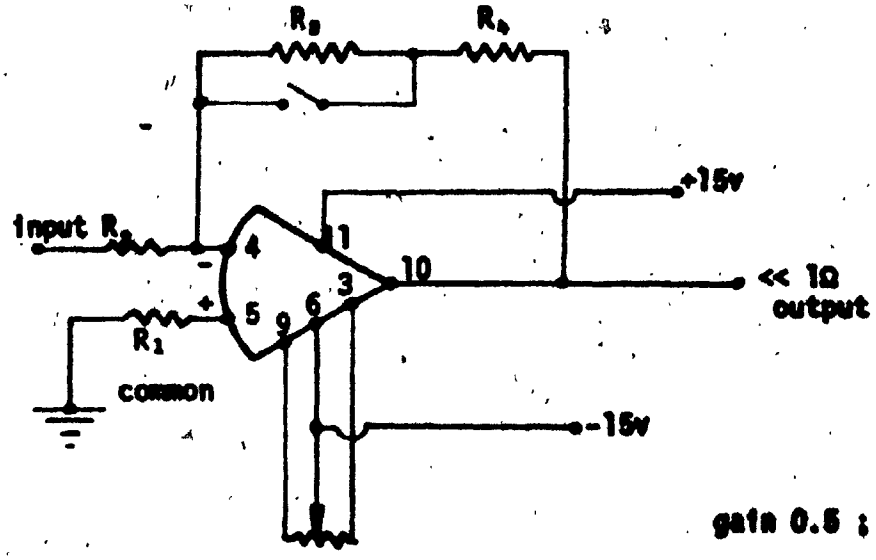

R_1 = 1 kΩ
R_2 = 100 kΩ
R_3 = 50 kΩ
R_4 = 50Ω

gain 0.5 ; 1.0

AMPLIFIER MA 1439

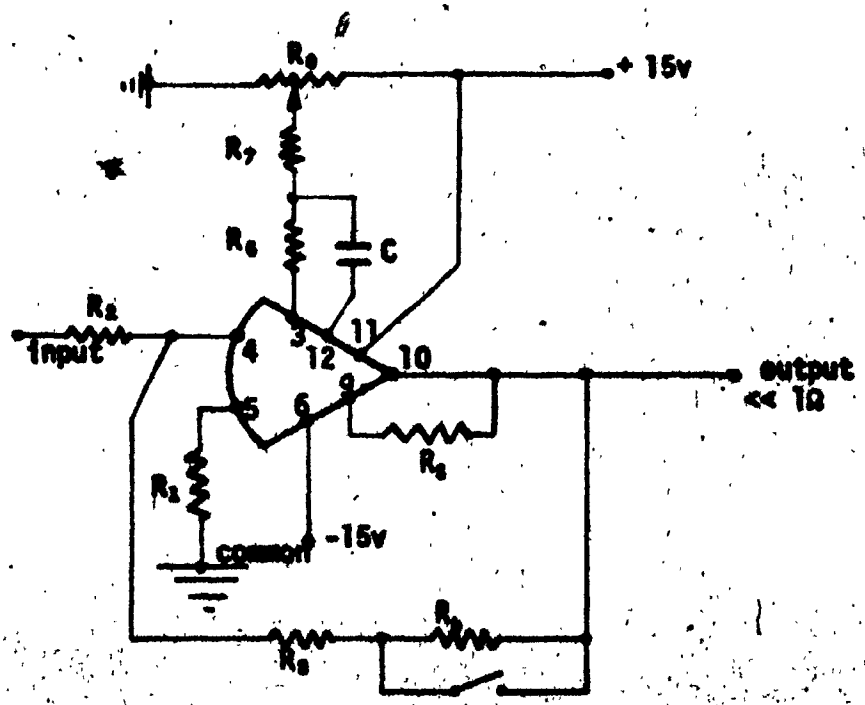

R_1 = 1 kΩ
R_2 = 100 kΩ
R_3 = 25 Ω
R_4 = 50 kΩ
R_5 = 10 kΩ
R_6 = 390 Ω
R_7 = 1 mΩ
R_8 = 20 kΩ
C = 2200 pF

gain 0.25 ; 0.75

FIG. 3.4 - SPECIAL AMPLIFIER

The magnetic tape recorder characteristics are given in the Appendix II. The analog signals of the surface roundness stored on the magnetic tape were converted to sets of discrete data points for the purpose of analysis. The conversion was made by a sequence of programs running on an Electronics Associate Incorporated 690 analog computer (EAI-690) and a Control Data Corporation 6400 digital computer (CDC-6400). The Figure 3.5 shows schematically the arrangement of data processing. Before processing a signal, the conversion program for EAI-690 is first loaded. Then the magnetic tape out-put signal line is connected to an analog-to-digital conversion channel and the magnetic is started. Digitilizing and storing of the roundness signal in the EAI-690 memory buffer is initiated by a command from the operator. The reading rate on the analog-to-digital channel is adjustable. When the memory buffer is full, the program on the EAI-690 automatically enters the out-put phase. In this phase, the contents of the buffer are converted to a form which can be transmitted over telephone lines. Then the transmission is made and the digitized signal is stored on a disc file of the CDC-6400 computer. The data are transmitted in logical records of eighteen data points at a rate of thirty characters per second. Based on the theory described in the previous chapter, the required parameters were calcualted.

3.3 Specimens Investigated

There were six samples used in the present investigation. Three samples were produced in the machine shop of Concordia University and the other three were standard bearings. The characteristics of these samples are given in the tables 3.1 and 3.2. The table 3.3 gives the file names

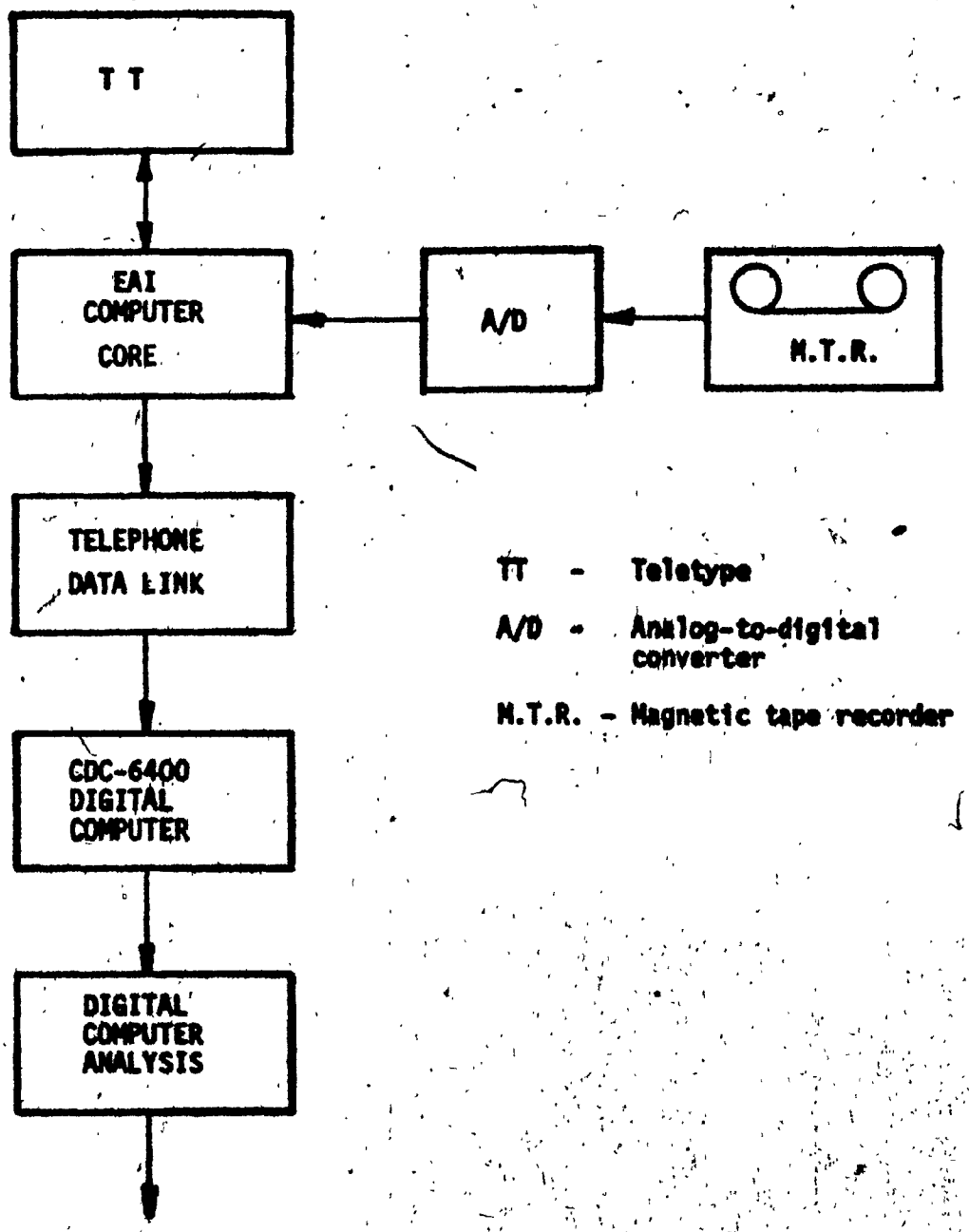

FIG. 3.5 - SCHEMATIC ARRANGEMENT FOR DATA PROCESSING

	Sample produced on	Internal diameter	External diameter
1	12" SWING HARRISON LATHE	1.5" Speed 289 r.p.m. Feed 0.0017 in/rev. Depth of cut 0.01 in.	2.2" Speed 289 r.p.m. Feed 0.0034 in/rev. Depth of cut 0.01 in.
2	DEMOOR LATHE	1.5" Speed 300 r.p.m. Feed 0.0017 in/rev. Depth of cut 0.01 in.	2.2" Speed 300 r.p.m. Feed 0.0034 in/rev. Depth of cut 0.01 in.
3	MEUSER & CO. Radial Drill	1.5" Speed 60 r.p.m. Feed → by handing Depth of cut 0.01 in.	2.2" by grinding

TABLE 3.1 - CHARACTERISTICS OF SPECIMENS MADE AT THE WORKSHOP OF CONCORDIA UNIVERSITY

	MATERIAL	DIMENSIONS
	Oil-impregnated bronze bearing B2432-20	I.D. 1.5" O.D. 2"
	Solid bronze bearing M2432-20	I.D. 1.5" O.D. 2"
	SKF bearing	NU 208

TABLE 3.2 - CHARACTERISTICS OF PURCHASED SPECIMENS

SAMPLE	SURFACE	FILTER	NAME
1	Ext	N	V1EN
1	Ext	B	V1EB
2	Ext	N	V2EN
2	Ext	B	V2EB
3	Ext	N	V3EN
3	Ext	B	V3EB
1	Int	N	V1IN
1	Int	B	V1IB
2	Int	N	V2IN
2	Int	B	V2IB
M2432	Ext	N	V4EN
M2432	Ext	B	V4EB
M2432	Int	N	V4IN
M2432	Int	B	V4IB
B2432	Ext	N	V5EN
B2432	Ext	B	V5EB
B2432	Int	N	V5IN
B2432	Int	B	V5IB
SKF Ext	Ext	N	V6EN
SKF Ext	Ext	B	V6EB
SKF Ext	Int	N	V6IN
SKF Ext	Int	B	V6IB
SKF Int	Ext	N	V7EN
SKF Int	Ext	B	V7EB
SKF Int	Int	N	V7IN
SKF Int	Int	B	V7IB
SKF Rol	Ext	N	V8EN
SKF Rol	Ext	B	V8EB

TABLE 3.3 - FILE NAMES -

under which the data points were entered in the computer memory.

These data points were then processed through the above program run on the CDC-6400 computer.

CHAPTER 4

EXPERIMENTAL RESULTS

CHAPTER 4

EXPERIMENTAL RESULTS

In accordance with the theory described in Chapter 2 and the experimental set-up described in Chapter 3, six specimens were investigated. The test results are given in Table 4.1. The roundness graphs along with their Cartesian conversions are shown in the Appendix III.

4.1 Amplitude Distribution Measurement

In addition to processing the surface signals through the main program amplitude distribution was measured for samples #2 and B2432. The device used was the Bruel & Kjaer amplitude distribution analyzer, model 161. Its characteristics are given in Appendix IV. The graphs of amplitude distribution along with the charts from the Talyrond 51 are shown in Figures 4.1 - 4.8.

As it was mentioned in Chapter 1, no single parameter can give a complete description of the surface. Additional parameters may include the amplitude distribution curve. Many investigations were devoted to establish these curves for different machining processes.

It has been established that on ground surfaces, the distribution is close to the Gaussian one.

As it could be seen, not all of the curves in Figures 4.1 - 4.8 approach the Gaussian curve. In our opinion it could be explained by consideration that analyzed curves represent the full surface signal and not only the roughness of the surface. It is clearly seen in Figures 4.3 and 4.4 which give the curves for the same surface but with the full

FILE NAME	CLA	COR	NP	MVE	TVE
	μ	μ	-	μ	μ x 10^3
V1EN	42.62	4.5	271	154.79	41.948
V1EB	41.98	2.75	219	192.44	42.144
V1IN	132.97	25.0	43	115.06	4.948
V1IB	131.22	20.0	14	8.96	.12544
V2EN	21.61	4.0	320	129.14	41.325
V2EB	23.89	2.5	12	8.91	10692
V2IN	86.02	6.0	11	240.53	2.646
V2IB	77.67	5.0	7	1.32	.00924
V3EN	34.79	4.0	482	88.68	42.744
V3EB	43.53	3.3	5	0.82	.0041
V4EN	57.93	3.75	114	326.38	37.207
V4EB	63.39	3.0	27	68.57	1.851
V4IN	81.24	3.75	79	186.95	14.769
V4IB	86.14	2.5	14	10.51	.14714
V5EN	41.49	7.5	91	275.22	25.045
V5EB	52.83	8.5	32	98.42	3.149
V5IN	42.61	9.5	162	176.95	28.666
V5IB	48.59	7.0	27	51.40	1.388
V6EN	46.32	2.25	24	78.97	1.895
V6EB	46.06	1.5	53	1.225	.0649
V6IN	68.92	7.5	34	151.53	5.152
V6IB	64.90	7.5	15	206.48	3.097
V7EN	14.75	1.75	375	105.53	39.574
V7EB	19.78	1.75	287	131.90	37.855
V7IN	17.88	2.25	170	178.39	30.326
V7IB	17.12	2.25	150	198.24	29.736
V8EN	17.62	.5	34	21.43	.72862
V8EB	10.94	.5	231	32.55	7.519

TABLE 4.1 - TEST RESULTS

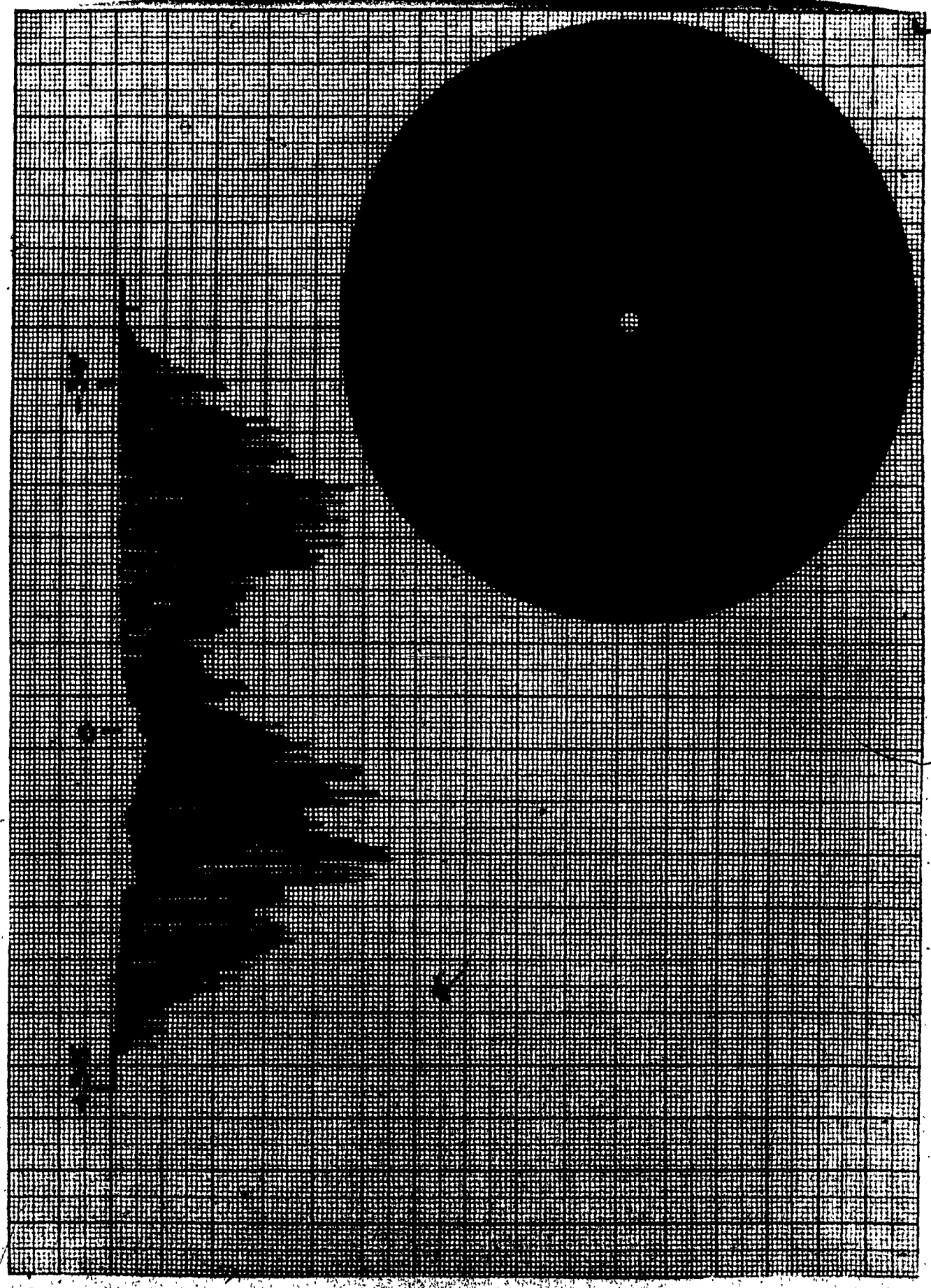

FIG. 4.1

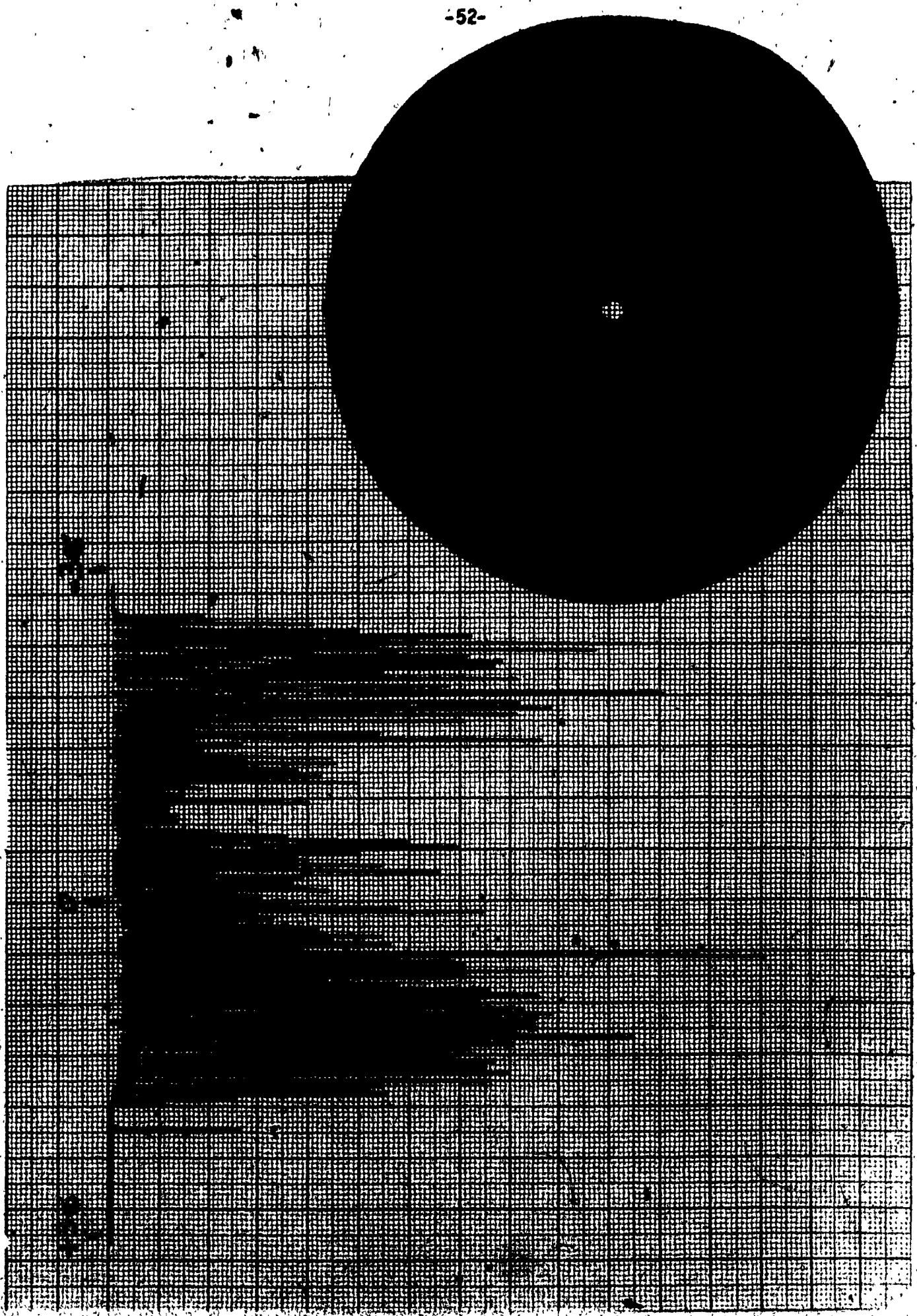

FIG. 4.2

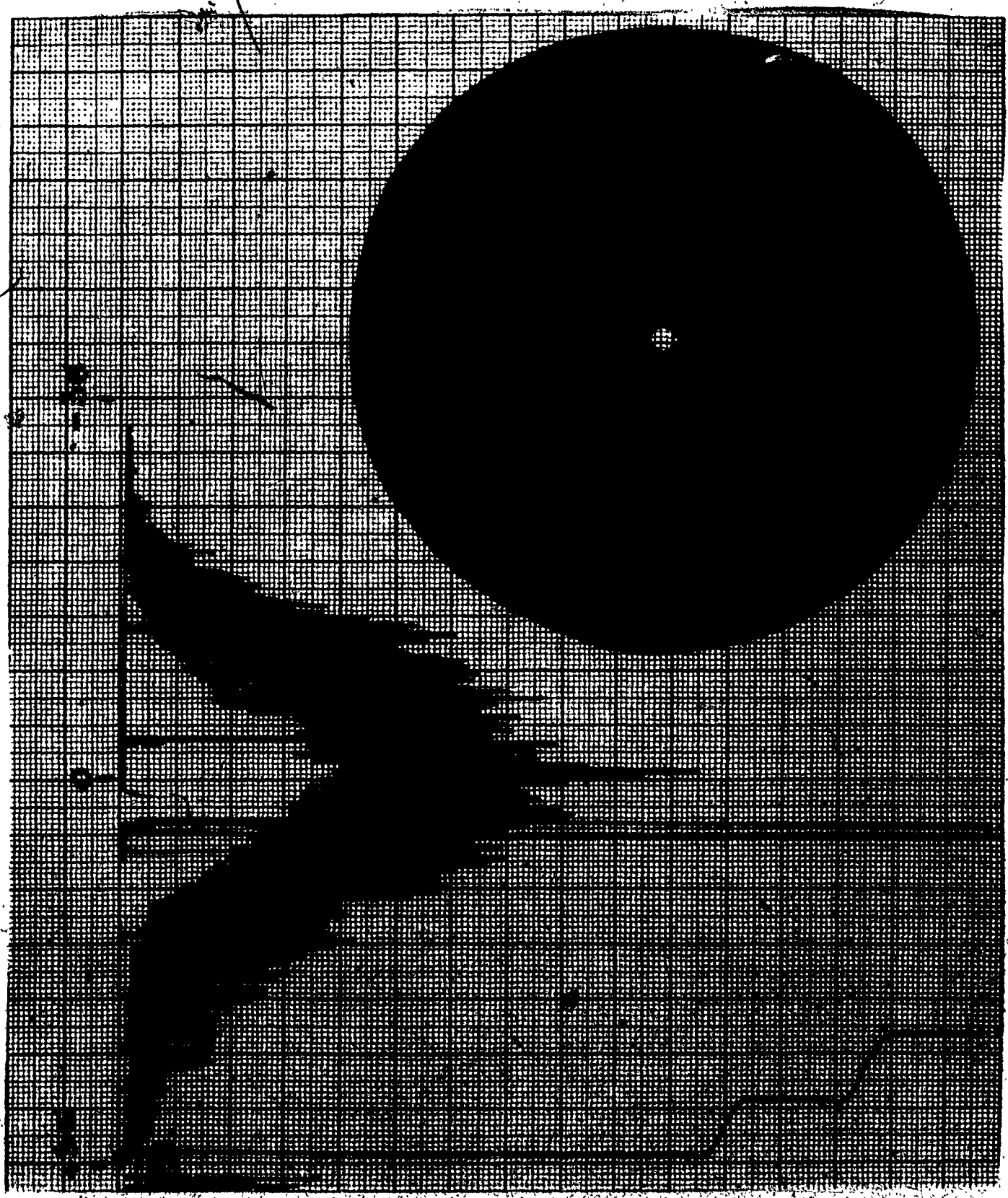

FIG. 4.3

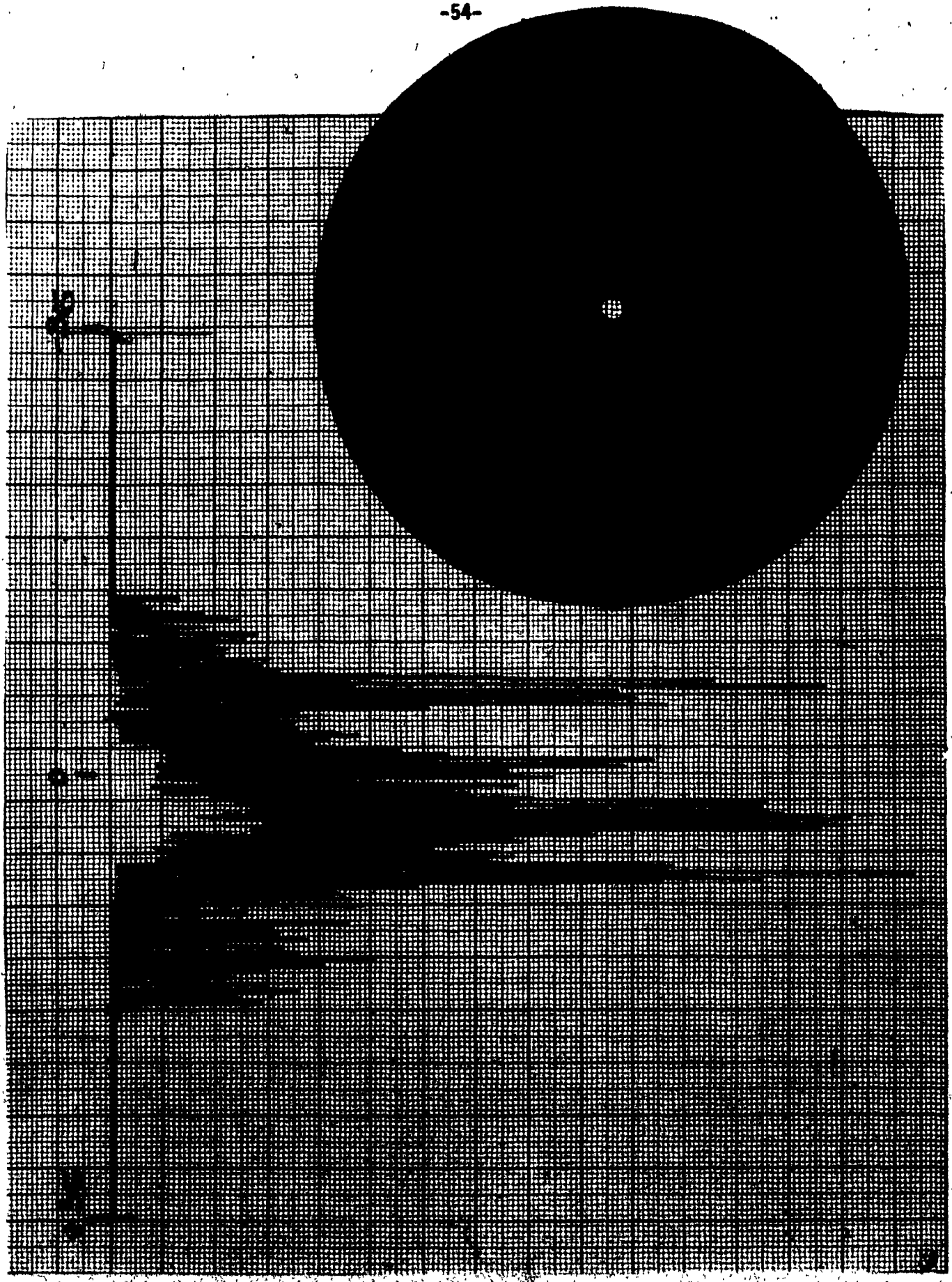

FIG. 4.4

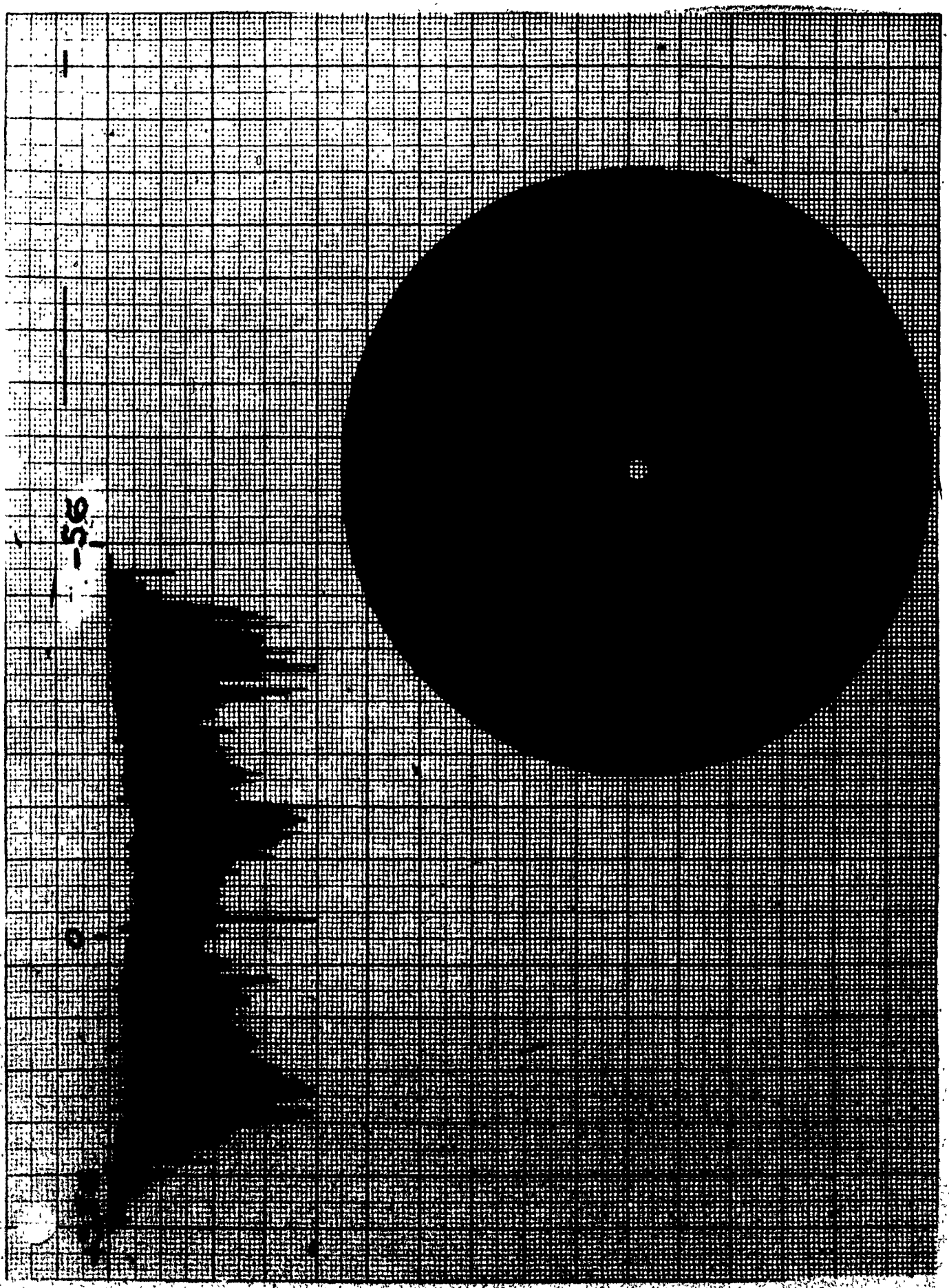

FIG. 4.5

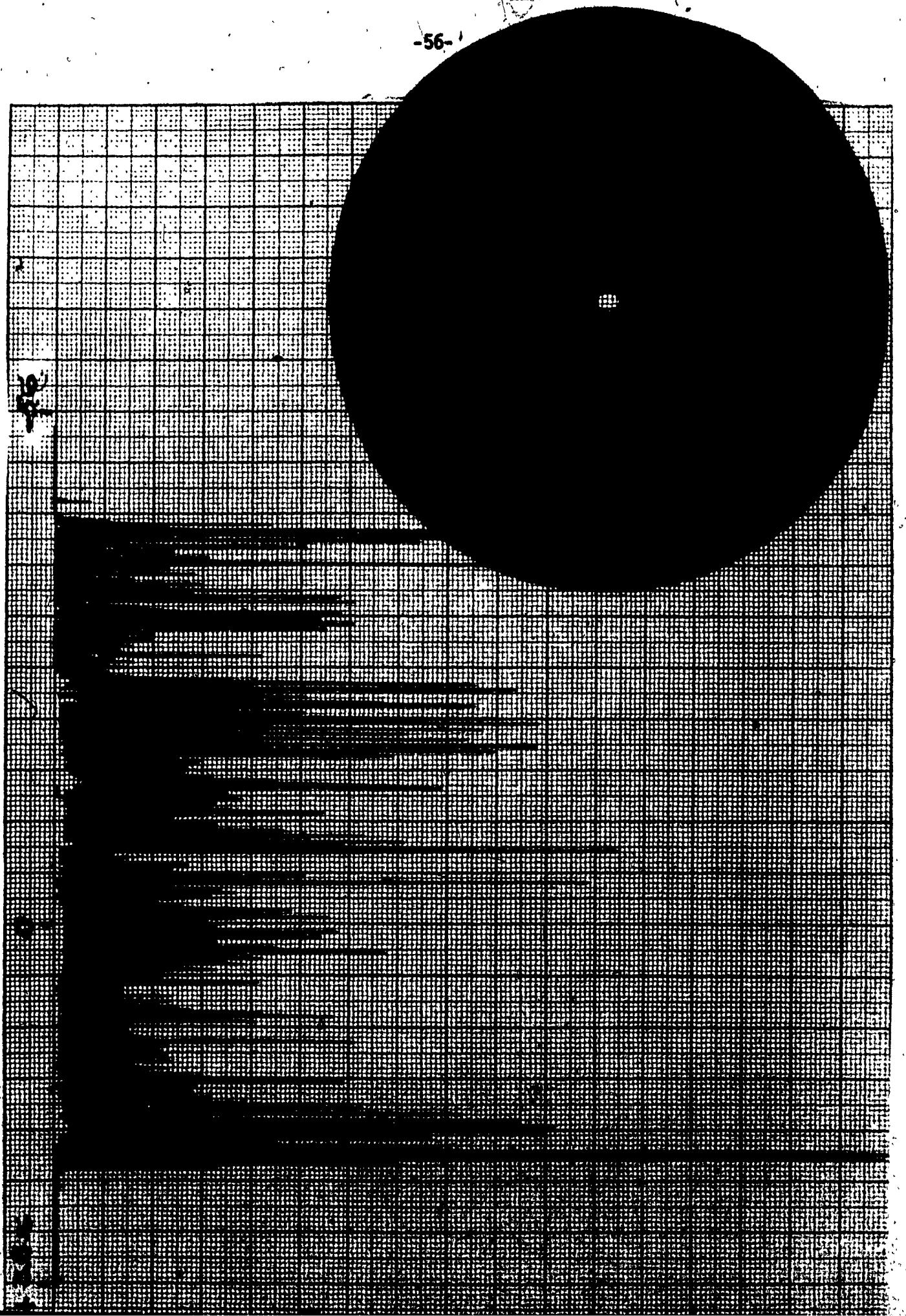

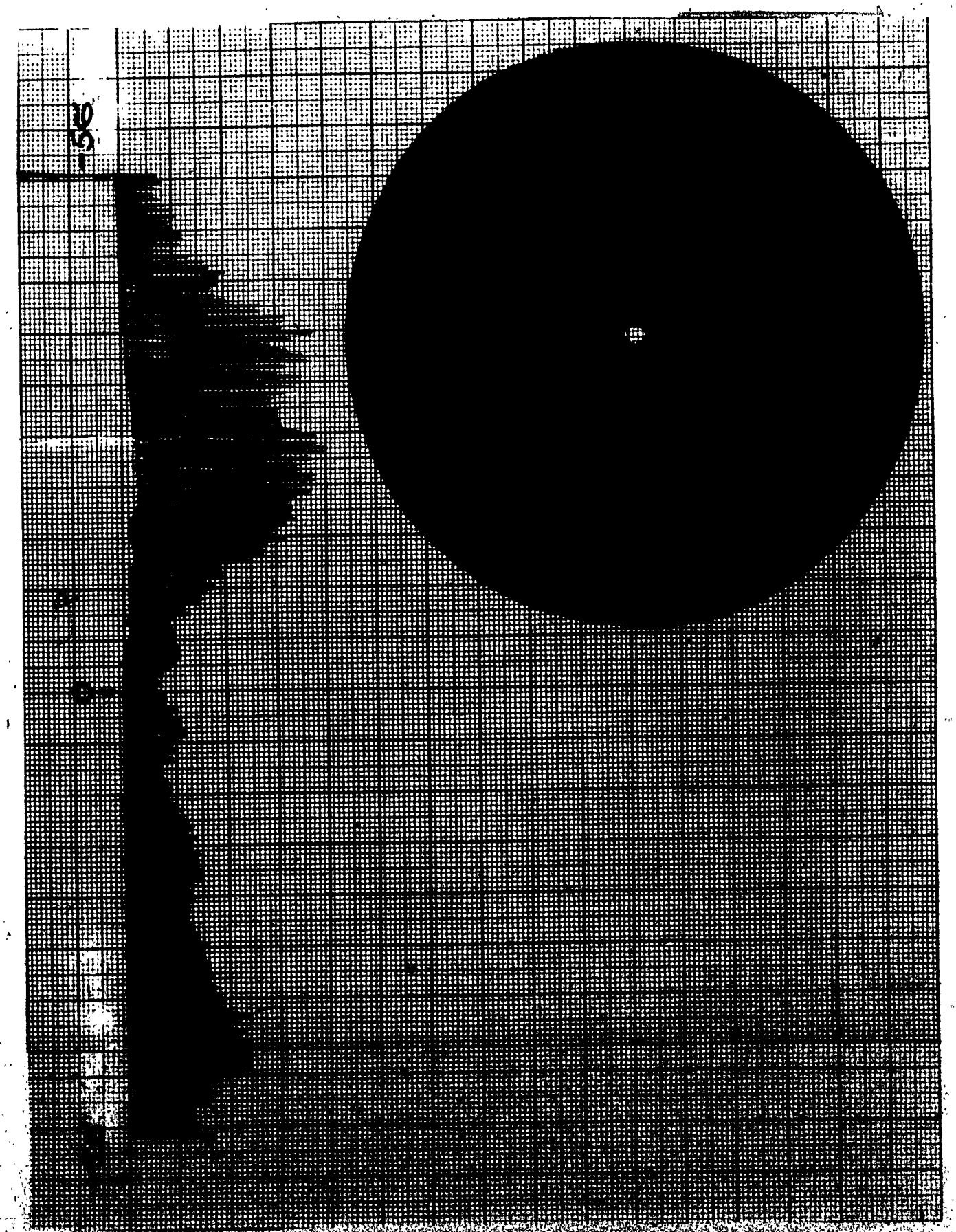

FIG. 4.7

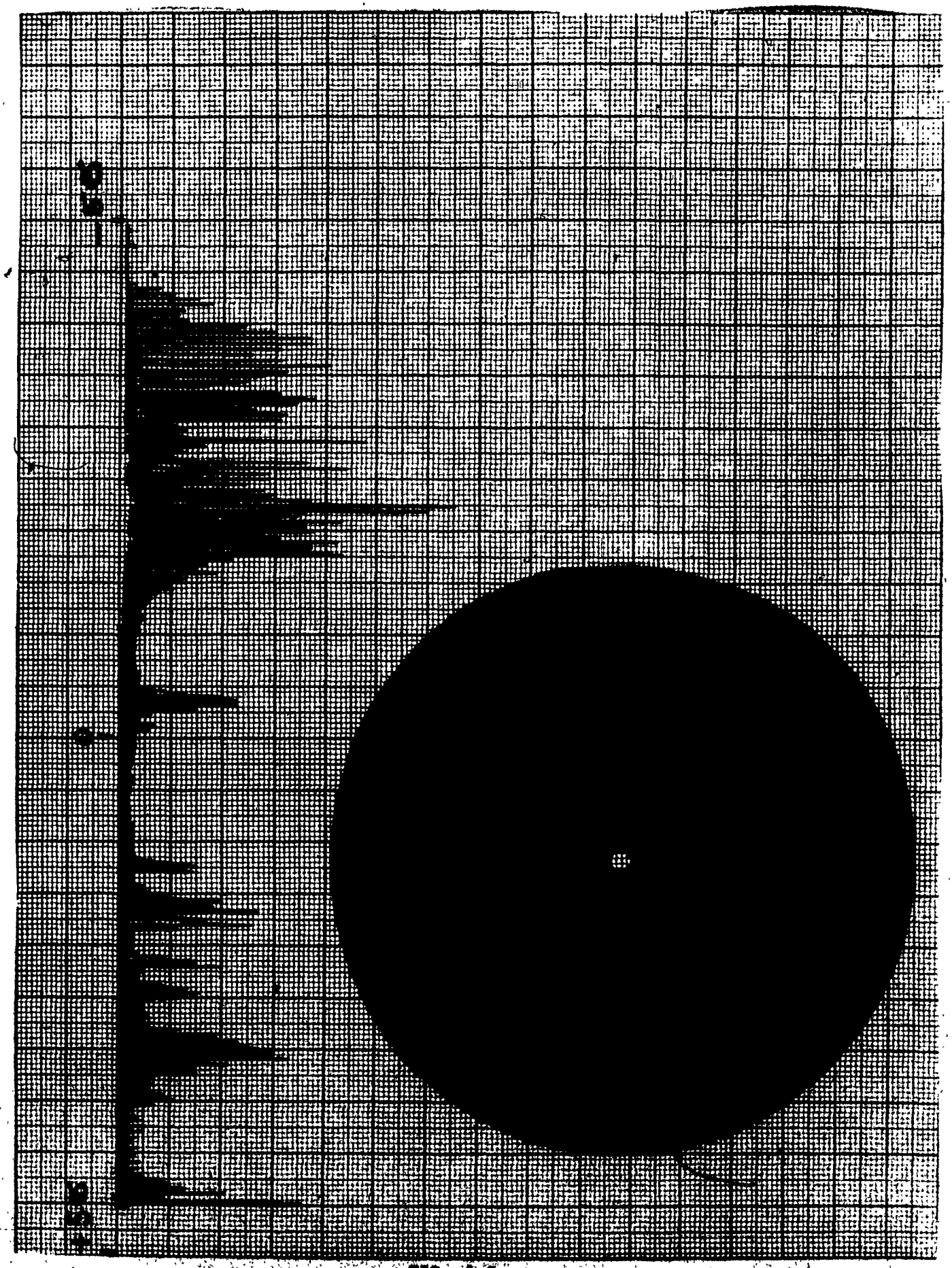

FIG. 4.8

signal (Figure 4.3) and the filtered signal (Figure 4.4) filter B.

In the filtered signal, the amplitude distribution curve is substantially distorted as compated to the full signal.

Based on the results obtained from measuring the amplitude distribution it seems to be fair to conclude that amplitude distribution of roundness error can not generally be considered as Gaussian distribution.

Since the computed parameters are based on the theory of random excursions which assumes normal signal amplitude distribution, the validity and sensitivity of the proposed parameters are to be verified theoretically and experimentally in relation to lubricant dynamics of journal bearings. This will be a subject to future investigations.

4.2 Effect of Circle Segment (Sampling Length)

It is well known that the choice of sampling length bears great influence on the value of roughness obtained from it.

Throughout the years of research in the area of surface roughness and roundness, different approaches were developed to separate roughness from errors of form and have a numerical assessment of both.

Two different systems (E-system and M-system) can be employed to establish the desired separation. The E-system uses the radius of the rolling circle for that purpose and the M-system uses the high-pass filters (cut-offs) with different characteristics. The E-system possesses a number of important advantages over the M-system, but to this day no instrument has been built that realizes the principle of the E-system.

The computer program described in Chapter 2 gives a possibility to use different sampling lengths by processing only the necessary part of

the data file. It can be stated that the use of this feature corresponds to the use of different radii of rolling circle in the E-system.

The investigation of this effect was made for samples #1, #2, #3 and M2432. The results are shown in Figures 4.9 - 4.16. As it can be seen from these figures, for the accurate assessment of the surface texture parameters the full circumference of the sample must be used. If only a part of the circumference is used, the error in the parameters will occur.

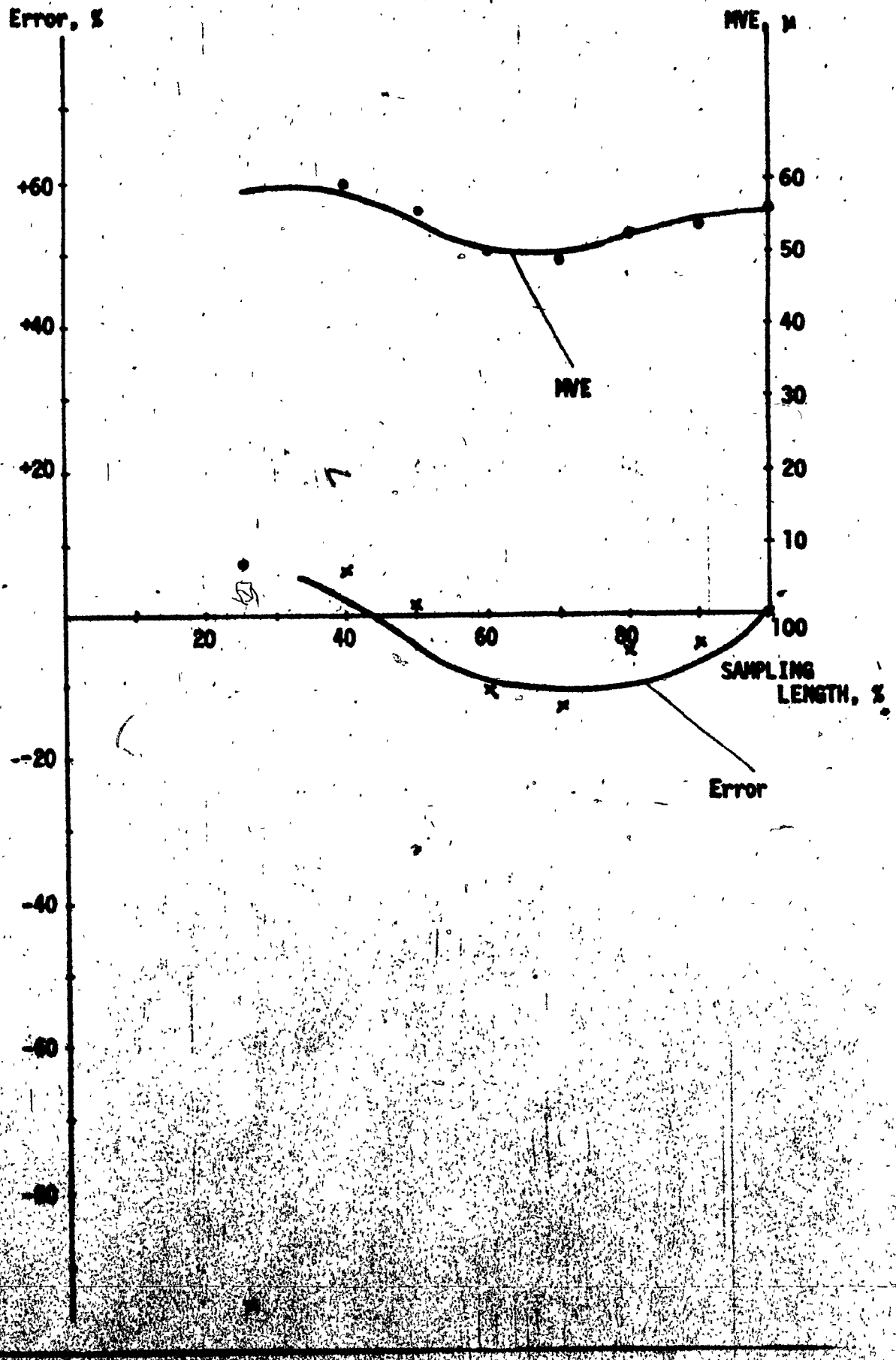

FIG. 4.8 - FILE VIEW

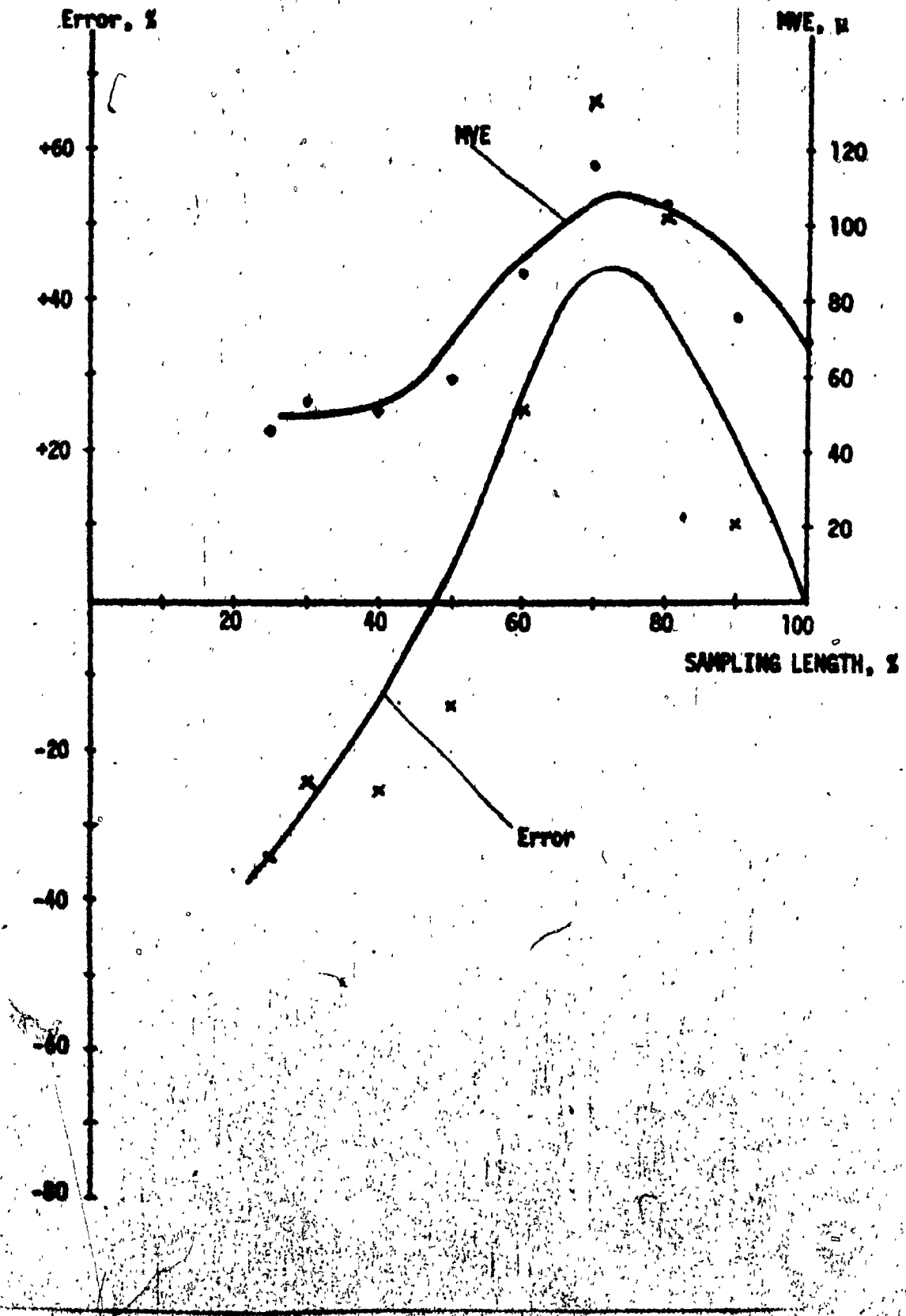

FIG. 4.10 - FILE VTEB

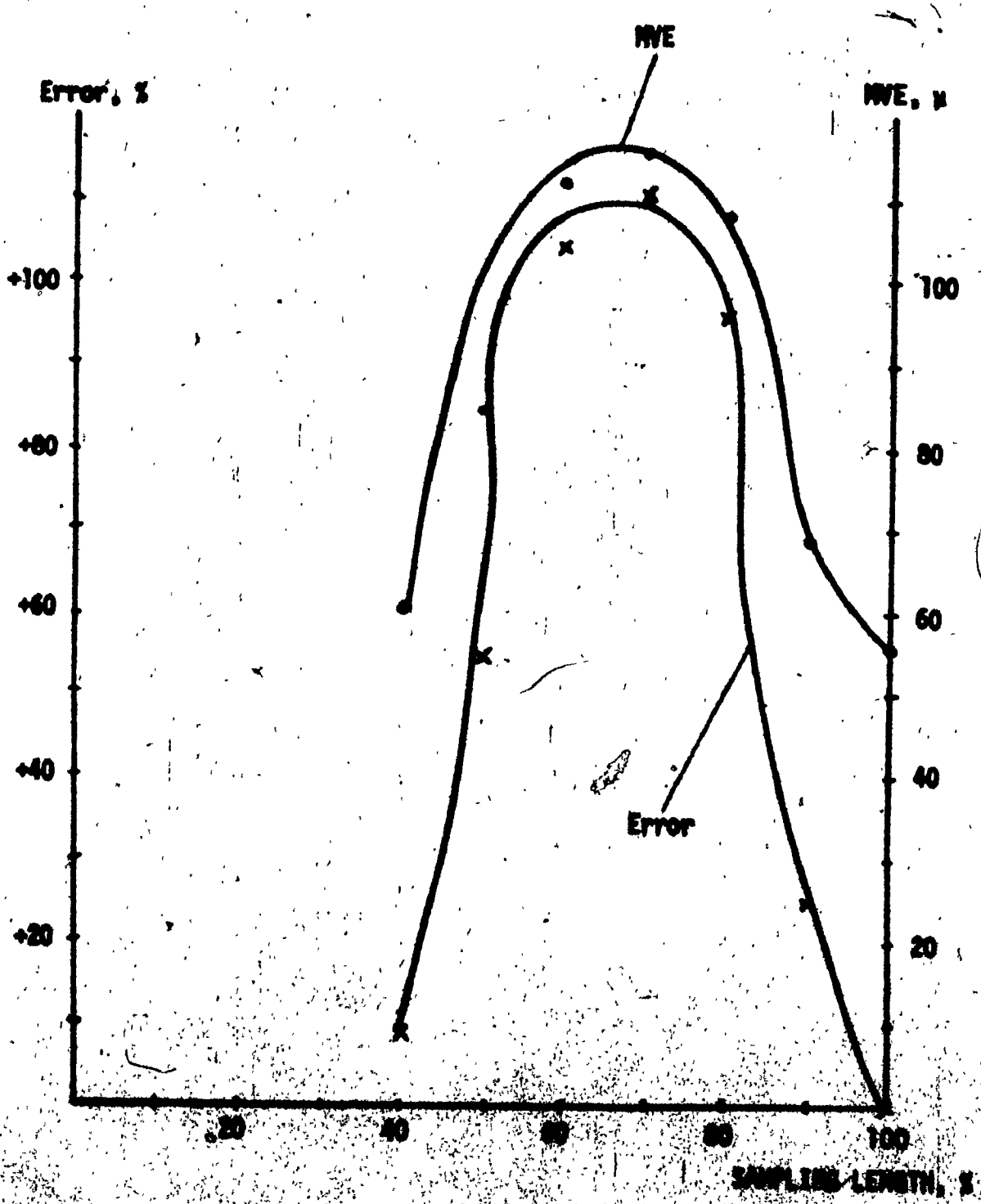

FIG. 4.11 - FILE VIEW

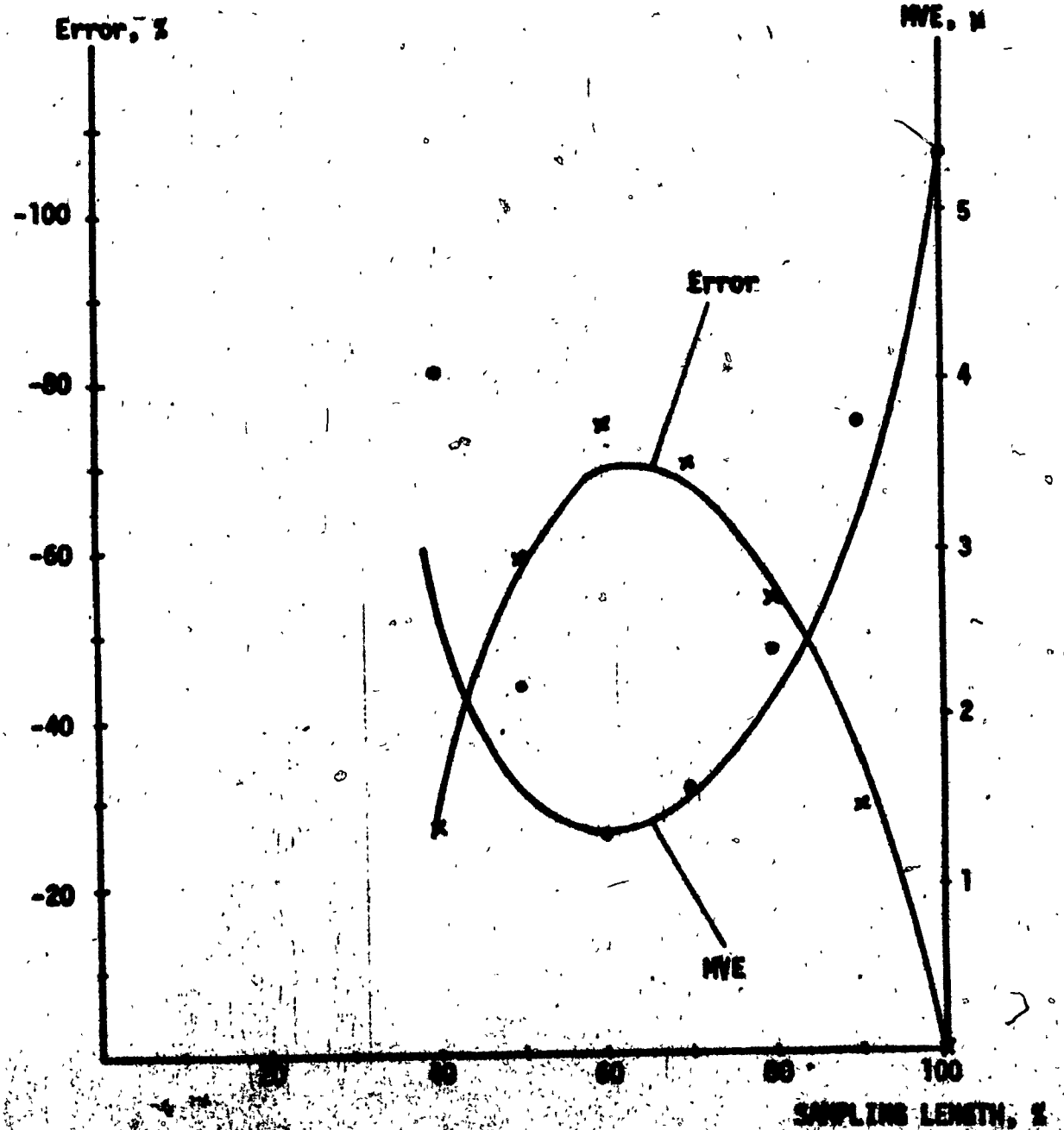

FIG. 4.12 - FILE V2B

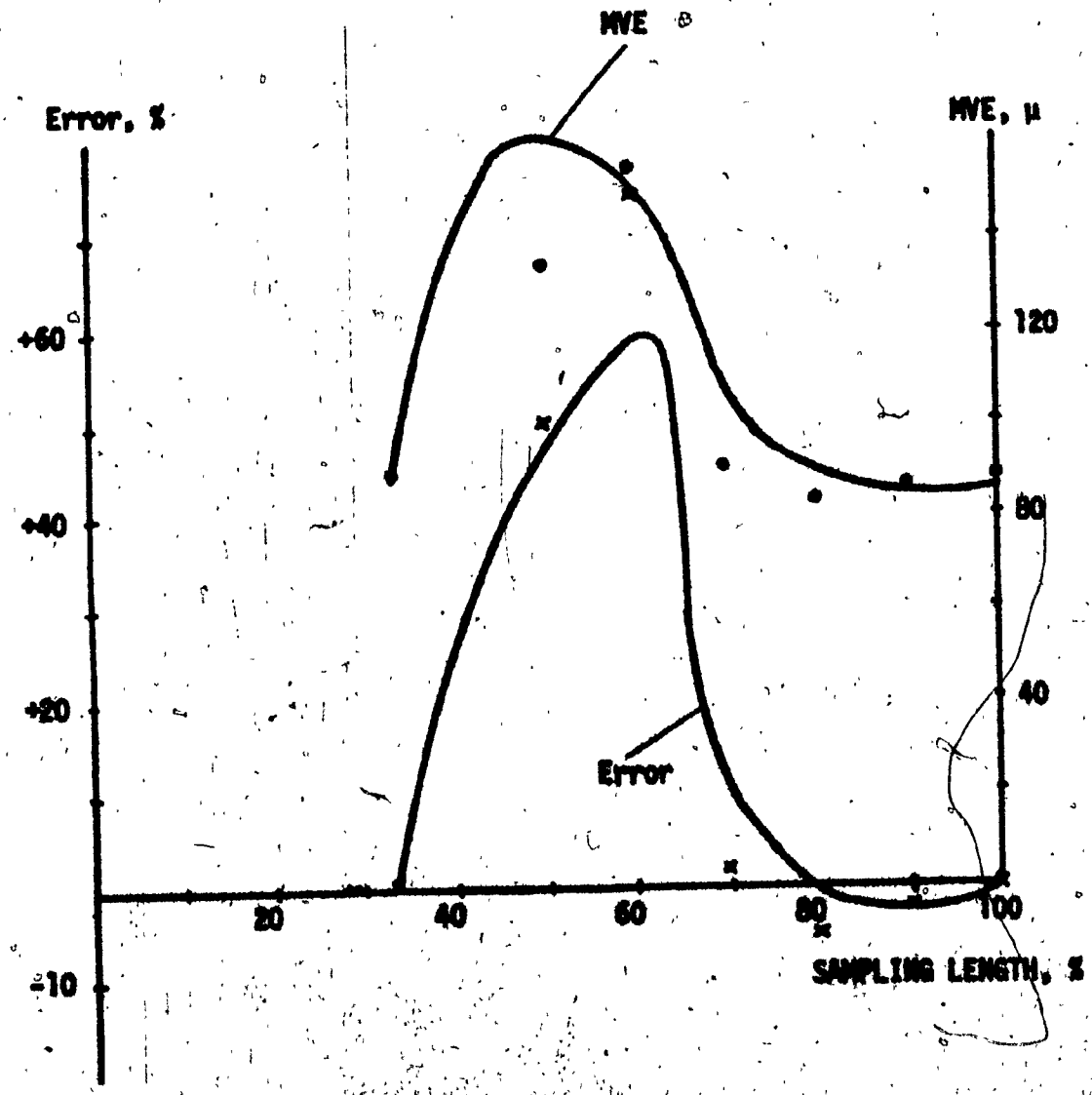

FIG. 4.33 - FILE VIEW

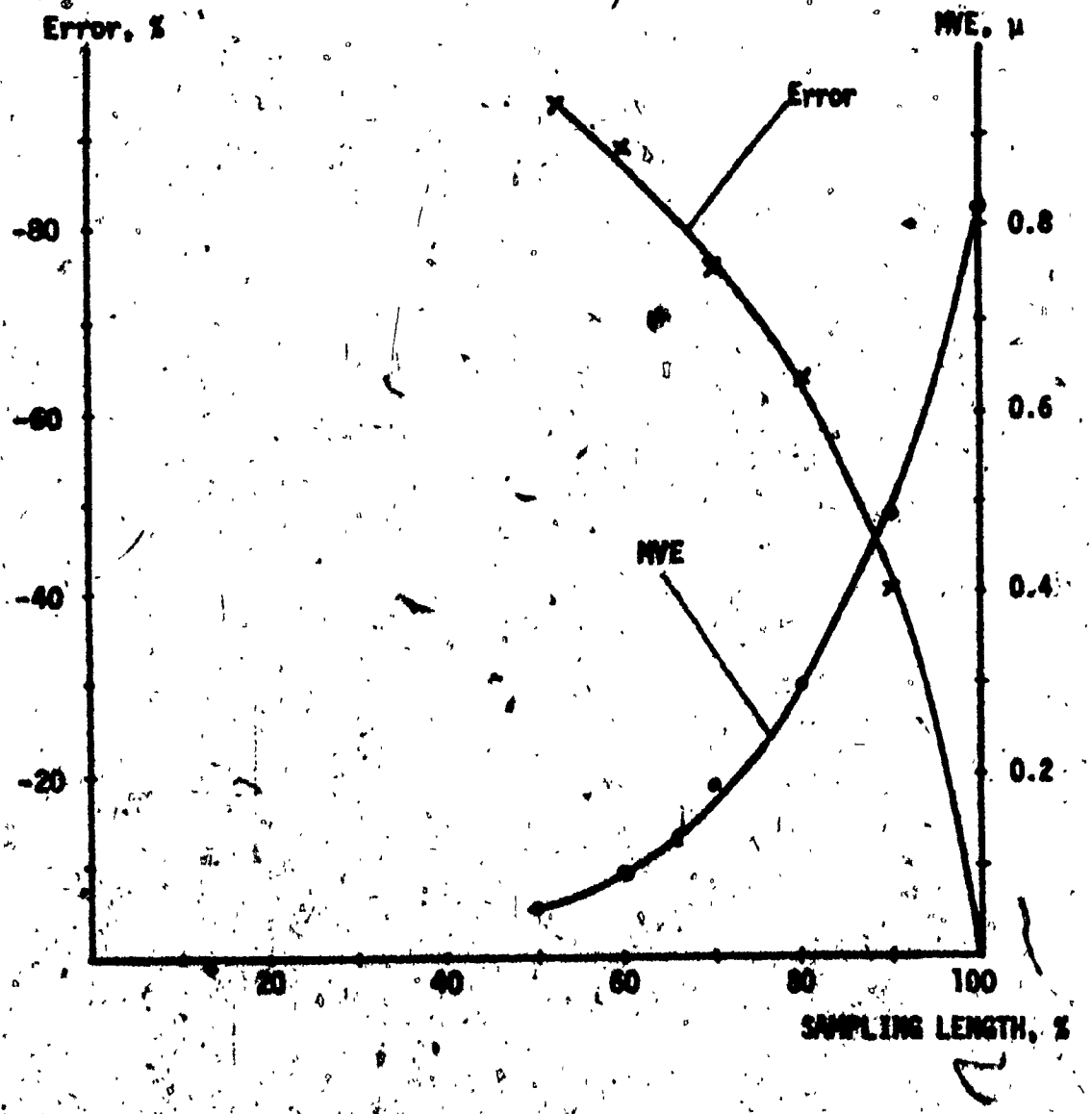

FIG. 4.14 - FILE VSEB

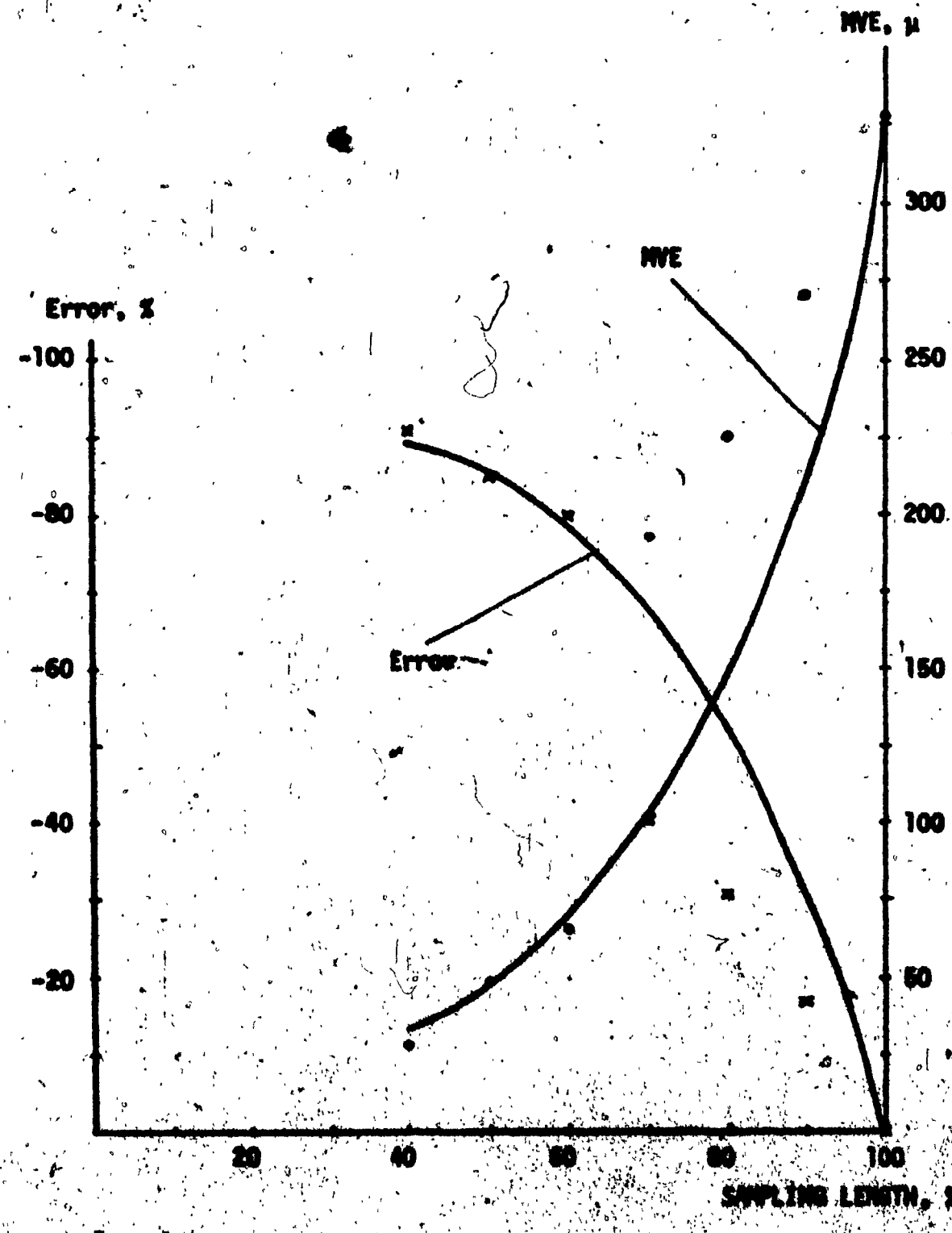

FIG. 4.15 -- FILE VIEW

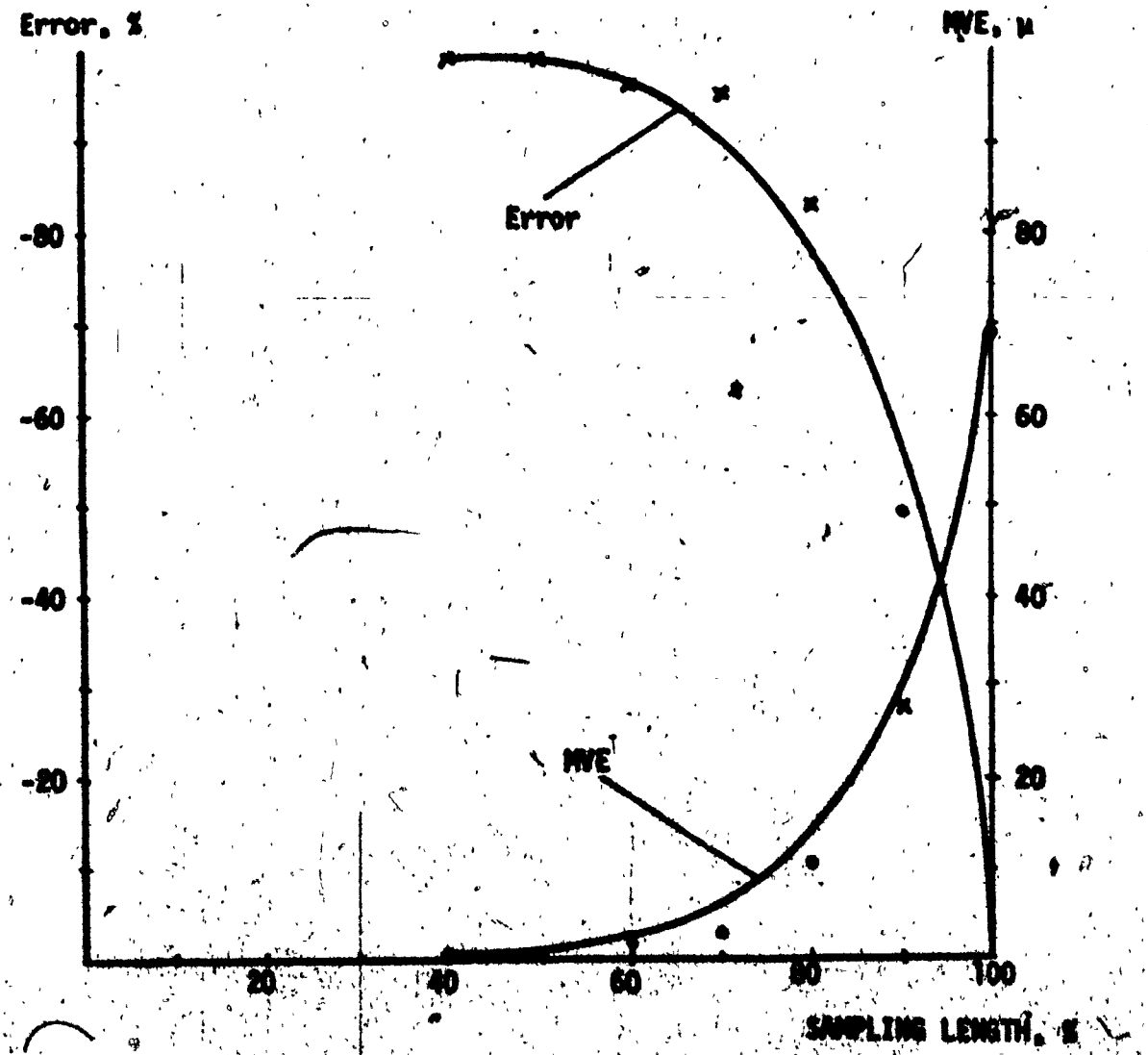

FIG. 4.16 - FILE V4EB

CHAPTER 5

PROPOSED INDICES FOR THE CHARACTERIZATION OF JOURNAL BEARING ROUNDNESS

CHAPTER 5

PROPOSED INDICES FOR THE CHARACTERIZATION OF JOURNAL BEARING ROUNDNESS

5.1 Parameters Affecting the Load Bearing Capacity and Friction Characteristics of a Bearing

In a number of investigations devoted to finding the sensitivity of different surface texture parameters and bearing performance [30, 31, 32, 33, 27], researchers have established a definite influence of surface finish and clearance upon the load bearing capacity and friction characteristics of a journal bearing.

According to [30], the bearing variables are related in the following manner:

$$\frac{P}{sN}\left(\frac{D}{V}\right)^2 = \frac{f(t)}{\left(\frac{h_m}{D}\right)^2} \qquad (5.1)$$

The experimental points approximate well the theoretical curve, and the value h_m takes account of machining process (turning, grinding, etc.) by using the Tarasov's factor [11].

The formula:

$$\frac{F/VD}{sN} = \frac{\psi(t)}{\frac{h_m}{D}} \qquad (5.2)$$

gives a relationship between friction and minimum film thickness. Again, experimental points and theoretical curve show a good correspondence.

5.2 Parameters Affecting the Stability of a Bearing

The stability of a bearing-shaft system becomes a very important

point for heavy loaded high speed bearings.

The investigations in this area [34, 35] show that there are regions of stable and unstable conditions for a bearing, depending on a number of parameters.

The analytical approach leads to two nonlinear differential equations, which can be solved by numberical methods. The solution is shown in Figure 5.1. Those curves are approximated by a set of equations, [35]:

$\gamma < \psi(u)$ - for stability

Here: $\gamma = \frac{2\pi^2 \mu N^2}{W}$ - dimensionless rotor mass

$u = \pi S (N/D)^2$

$S = (D/2u)^2 [sN/(W/VD)]$ - Somerfeld number

For $u < 0.28$ $\psi(u) = 3u^{-0.55}$

$0.28 < u < 2.9$ $\psi(u) = 6.88u^{0.094}$

$u < 2.9$ $\psi(u) = 7.65$

Now, the above equations are based on the assumption that the clearance is a constant. In the original differential equations the forcing functions are inversely proportional to the square of clearance. Therefore, the variations in clearance are important to be considered in the shape of forcing functions if the correct solution has to be obtained. The clearance varies since the diameters of the bearing and the journal are not constant. Consequently, in the assessment of surface texture a parameter should be found which can be directly related to the clearance.

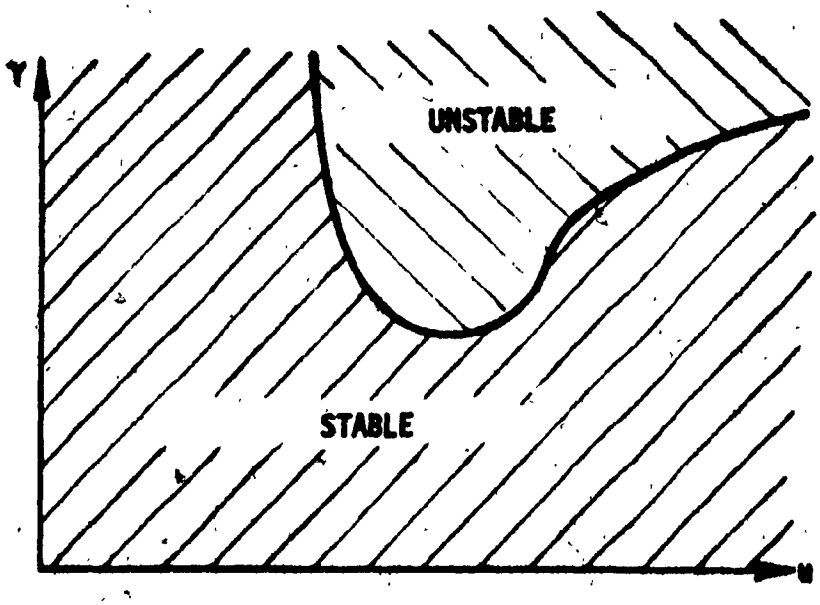

FIG. 5.1 - SOLUTION OF STABILITY EQUATIONS
(after [35])

5.3 Recommended Parameters for Characterization of Roundness

Considering all said above it is clear that there should be sufficient information given to the designer about the roundness of the bearing which will allow him to judge accurately the bearing performance. The CLA value should remain as one of the parameters. It should be obtained on conventional sampling length. The out-of-roundness (OOR) should be the other parameter and for it the total circumference of the bearing is taken. These two parameters, in our opinion, give sufficient information about the variation of clearance and minimum film thickness in the bearing.

The number of peaks is a parameter which has to be considered when stability of the bearing is important. The NP value should be related to the speed and natural frequency of the system in order to avoid excessive vibration. The NP value therefore may be used by a designer as a rejection parameter.

The lubrication and friction properties of the bearing depend to a great extent on the circumferential characteristics as well as radial ones. It is felt that MVE value can provide sufficient information about the circumferential characteristics of the bearing. To get the value which is related to the amount of fluid stored on the surface, it is proposed to use the TVE value which is a product of NP and MVE values.

It seems logical to say that the volume of fluid is also related to the product of CLA and MVE values. However, the sensitivity of these proposed parameters should be checked by further experimental work.

CHAPTER 6

CONCLUSIONS AND RECOMMENDATIONS FOR FUTURE WORK

CHAPTER 6

CONCLUSIONS AND RECOMMENDATIONS FOR FUTURE WORK

There is little doubt that characterization of roundness through one parameter (out-of-roundness) only is not at all sufficient to predict and control the behavior of a bearing under different operating conditions.

In the present investigation, a number of parameters is proposed for characterization of bearing roundness. These are:

1. OOR (out-of-roundness) value
2. CLA (center line average) value

} for radial characteristics

3. MVE (mean valley excursion) value
4. TVE (total valley excursion) value

} for circumferential characteristics

5. NP (number of peaks) value

A mathematical model is given (Chapter 2) on the basis of which the computer program is compiled to calculate the proposed parameters. An experiment was conducted the set-up of which is given in Chapter 3 and the results are discussed in Chapter 4. The amplitude distribution measurements (see Chapter 4) show that in general the roundness signal can not be considered to have normal amplitude distribution. Since the compiled computer program does assume the signal to have Gaussian amplitude distribution, the experiments must be conducted to establish the sensitivity of the proposed parameters to the bearing performance. Also, in order for the proposed parameters to be of practical value to the industry, the experiments should be made to provide the designer

with precise correlation of the proposed parameters and bearing properties. This will be the subect of future work.

The surface roughness in the axial direction of the bearing should probably be taken into account also. However, this would not complicate the problem considerably since there exists a definite correlation between the axial and radial roughness. This relationship depends primarily on the cutting conditions of the machining process.

The future investigations should also consider the question of the number of samples which gives a representative picture of the particular set of cutting conditions.

REFERENCES

REFERENCES

1. Reason, R.E., "1966 Report on the Measurement of Roundness", Rank Precision Industries Ltd., Leicester, England, 1966.

2. Avdulov, A.N. Polunov, Y.L. Tabenkin, A.N. Faradjev, I.A. and Shuster, V.G., "Some Aspects of Measurement of Roundness", Proceedings of Institution of Mechanical Engineers, Vol. 182, Pt 3K, 1968, pp. 425-429.

3. Canadian Standard CSA B95-1962, "Surface Texture (Roughness, Waviness, and Lay)".

4. British Standard BSI 1134-1961, "Centre-Line Average Height Method for Assessment of Surface Texture".

5. American Standard ASA B46.1-1962, "Surface Texture (Roughness, Waviness, and Lay)".

6. Soviet Standard GOST 2789-59, "Surface Roughness".

7. International Standard ISO R.468-1966, "Recommendation for Surface Roughness (Ten Point Height R_z)".

8. Dunin-Barkovski, I.V. and Karthasheva, A.N., "To the Application of the Surface Roughness Standard", Standardization, No. 9, 1959, pp. 10-13, (in Russian).

9. Dyachenko, P.E. and Vainstein, V.A., "Some Aspects of the Surface Roughness Standard", Standardization, No. 4, 1960, pp. 25-28, (in Russian).

10. Chestnov, A.L., "Standardization of Surface Roughness", Standardization, No. 5, 1958, pp. 55-58, (in Russian).

11. Tarasov, L.P., "Relation of Surface-Roughness Readings to Actual Surface Profile", Transactions of ASME, Vol. 67, 1945, pp. 189-196.

12. Burgvits, A.G. Ilsums, M.Z. and Rudzit, Y.A., "Method of Calculating Maximum Height of Roughness Profile", Izvestiia Vysshikh Uchebnykh Zavadenii, No. 8, 1970, pp. 40-43, (in Russian).

13. Moore, D.F., "A History of Research on Surface Texture Effects", Wear, 13, 1969, pp. 381-412.

14. Nydell, R.R., "Surface Textures: The Proposed New Standard", Machinery, July 1967, pp. 143, 145.

15. Hydell, R.R., "Today's Need - Functional Surface Roughness Control", Proceedings of Institution of Mechanical Engineers, Vol. 182, Pt 3K, 1968, pp. 127-134.

16. Butler, R.D. and Pope, R.J., "Surface Roughness and Lubrication in Sheet Metal Working", Proceedings of Institution of Mechanical Engineers, Vol. 182, Pt 3K, 1968, pp. 162-170.

17. Sharman, H.B., "Influence of Sample Size and the Relationship Between the Common Surface Texture Parameters", Proceedings of Institution of Mechanical Engineers, Vol. 182, Pt 3K, 1968, pp. 416-424.

18. Vitenberg, Yu.R., "Evaluation of Surface Finish by Co-variance Functions", Russian Engineering Journal, Vol. XLIX, No. 1, pp. 58-60.

19. Peklenik, J. and Kwiatkowski, A.W., "New Concepts in Investigating the Manufacturing Systems by Means of Random Process Analysis", Proceedings of the I.M.T.D.R. Conference, September 1966, pp. 683-700.

20. Peklenik, J., "Contribution to the Theory of Surface Characterization", Annals of the C.I.R.P., Vol. XIII, No. 3, 1964, pp. 173-178.

21. Peklenik, J., "Investigation of the Surface Typology", Annals of the C.I.R.P., Vol. XV, 1967, pp. 381-385.

22. Shain, T.S., "Stochastic Modelling of the Microgeometrical State of a Manufacturing Surface", Master Dissertation at Sir George Williams University, 1972.

23. Pesante, M., "Determination of Surface Roughness Typology by Means of Amplitude Density Curves", C.I.R.P. Annals, Vol. XII, No. 2, pp. 61-68.

24. Spragg, R.C. and Whitehouse, D.J., "A New Unified Approach to Surface Metrology", Proceedings of Institution of Mechanical Engineers, Vol. 185, 47/71, 1971, pp. 697-707.

25. Sankar, T.S. and Osman, M.O.M., "Profile Characterization of Manufactured Surfaces using Random Function Excursion Technique", Part I, Transactions of ASME, Journal of Engineering for Industry, Vol. 97, Series B, No. 1, pp. 190-195.

26. Osman, M.O.M. and Sankar, T.S., "Profile Characterization of Manufactured Surfaces using Random Function Excursion Technique", Part II, Transactions of ASME, Journal of Engineering for Industry, Vol. 97, Series B, No. 1, pp. 196-202.

27. Huffington, J.D., "The Relation Between Friction and Surface Microtopography", Research for Industry, Vol. 34, 1961, pp. 193-195.

28. Gupta, P.K. and Cook, N.H., "Statistical Analysis of Mechanical Interaction of Rough Surfaces", Transactions of ASME, Journal of Lubrication Technology, January 1972, pp. 19-26.

29. Tikhonov, V.I., "The Distribution of the Duration of Excursions of Normal Fluctuations", from "Non-Linear Transformations in Stochastics Processes", Pergamon Press, 1965, pp. 354-367.

30. Ocvirk, F.W. and DuBois, G.B., "Surface Finish and Clearance Effects on Journal-Bearing Load Capacity and Friction", Transactions of ASME, Vol. 81(2), 1959, pp. 245-253.

31. Garside, D.W. and Hother-Lushington, S., "The Influence of Clearance and Journal Surface Finish on the Load Capacity of Water-Lubricated Plain Bearings", Proceedings of Institution of Mechanical Engineers, Vol. 180, Pt 3K, 1966, pp. 235-242.

32. Dowson, D. and Whomes, T.L., "Effect of Surface Quality Upon the Traction Characteristics of Lubricated Cylindrical Contacts", Proceedings of Institution of Mechanical Engineers, Vol. 182, Pt 1, No. 14, 1968, pp. 292-299.

33. Christensen, H., "Some Aspects of the Functional Influence of Surface Roughness in Lubrication", Wear, Vol. 17, No. 2, 1971, pp. 149-162.

34. Lund, J.W. and Saibel, E., "Oil Whip Whirl Orbits of a Rotor in Sleave Bearings", Transactions of ASME, Vol. 89, Series B, 1967.

35. Sairey, A. and Ezzat, H., "Optimum Design of Hydrodynamic Journal Bearings", ASME-Paper 60-WA/Luc. 3, 1960.

APPENDIX I

MODEL 51 TALYROND

APPENDIX I

The Model 51 'Talyrond' is a robust and compact instrument, precision built and equally suitable for use in the standards room or the production workshop. This instrument, the smallest in the series of Talyronds, has been developed primarily for the inspection of the smaller type of component, such as balls and rollers, ball and roller races, pistons, cylinders, etc.

For large capacity work such as crankshafts and cylinder blocks, the Model 2 Talyrond is available.

The accuracy of measurement is within the accuracy of the spindle (see specification) but the overall degree of instrument stability likely to be experienced during a series of recordings will of course be affected to some extenet by the environmental conditions. For this reason the site for installation should be chosen carefully with draughts and excessive vibration in particular to be avoided.

Principle

The principle of the Talyrond is shown in skeleton form in Figure A.I.1 which will be largely self-explanatory.

The part W to be measured is mounted, with its axis vertical, on the table C. It remains stationary during the measurement.

Above the part is a precision spindle F carried with its axis vertical in a head S mounted on the top of the column D. Adjustments are provided for bringing the axis of the spindle accurately into line with the nominal axis of the part.

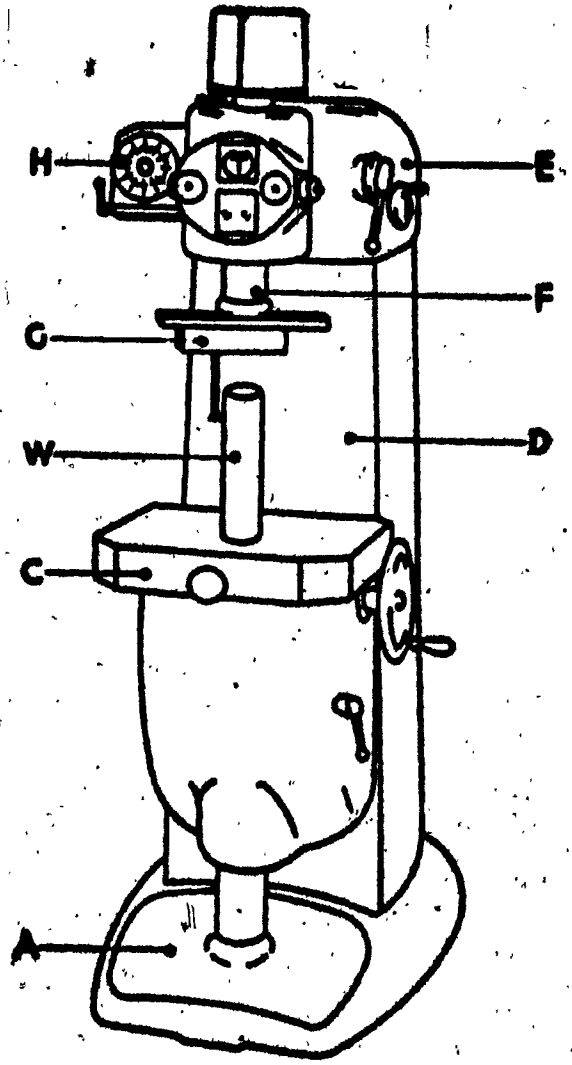

FIG. A.I.1 - PRINCIPLE OF TALYROND 51

The lower end of the spindle carries an electric gauge head G (known as the Pick-up) which is radially adjustable so that its stylus can be brought into contact with the surface of the part.

The spindle is slowly rotated by a geared motor in the head so that the stylus can trace the variations in the radius of the part.

The Pick-up is connected via the Amplifier to an indicating meter and also to the Recorder H, a pen with radial movement marking on a circular chart. The chart is geared to run in synchronism with the spindle.

In use, the part is first centered to the axis of the spindle as well as possible by movement of the table C by lateral and transverse controls.

The output from the Amplifier is then switched to the Recorder and a graphic representation of the variations in the radius of the part is obtained.

Geometrically, the graph shown, on a greatly enlarged scale the variations in the radius of a cross section of the part measured from the point where the axis of the spindle intersects the cross section.

In the instrument itself, the center of the imaginary gauge is the axis of the spindle, and the surface of the gauge is represented by the circular path that would be traced by the stylus if it were clamped relative to the body of the Pick-up. The process of centering the part represents the imaginary operation of positioning the gauge so that it surrounds the part as evenly as possible.

If the work is truly round and is perfectly centered on the axis of the spindle, there will be no radial change in the position of the stylus as it rotates [illegible] and the graph will plot as a circle

concentric with the hole in the paper.

The radial ordinates are printed on the chart, and the 1/10 in. (metric paper 2 mm) divisions along them will often provide a convenient radial scale; but to allow for slight residual imperfections of centering, the circular ordinates are printed on a separate transparent template under which graph can be floated about until a best fit is obtained.

It is possible by use of the Reference Computer to superpose on the profile graph a reference line based on the principle of 'least squares' - a principle often used in statistical work to provide a mean line for a fluctuating quantity. This has the advantage of saving time and uncertainty.

Diametrically opposite points on the specimen are represented by diametrically opposite points on the graph, taking the hole as center, regardless of the eccentricity of the graph to the hole.

All Talyrond roundness graphs, whether of holes or shafts, are plotted so that an increase in the radius of the part results in an increase in the radius of the graph. Metal is therefore represented on the outside of the graph of a hole and on the inside of the graph of a shaft.

The enormous scale of enlargement often used needs to be appreciated. For example, a change of 0.0001 in. (2.5μm) in the radius of the part may be represented by a change of 1 in. (25 mm) in that of the graph (10,000 magnification).

Specification

Spindle Accuracy

The spindle is tested at a uniform temperature between 66° and 70°F., in a situation free from draughts. Its accuracy is such that in 95 per cent of the tests made of a truly round test specimen, the maximum departure of the trace from a true mean circle does not exceed one millionth of an inch (0.025μm).

Measuring Capacity

The range of components capable of being measured on this instrument is as follows:

External diameters	Up to 14 in.(350 mm)
Internal diameters	Up to 14 in.(350 mm)
Maximum height	16 in.(406 mm)
Maximum recommended load on work table	150 lb.(68 kg)

Basic Dimensions--Instruments

Overall height	64 in.(1625 mm)
Overall width	19 in.(482 mm)
Depth	37 in.(940 mm)
Dimensions of work table	14¾ wide x 15¼ in. deep (375 mm x 400 mm)
Distance from face of guide rail to axis of spindle	8 in.(203 mm)
Horizontal movement of work table in any direction relative to spindle	0.1 in.(2.54 mm)
Vertical movement of work table	16 in.(406 mm)
Height of work table surface from floor level	26 in. to 39 in. (660 mm to 978 mm)
Weight of instrument	Approx. 1¼ cwt (254 kg)

Basic Dimensions-'Masterform' Instrument Desk

Overall width	46 in.(1170 mm)
Overall height	30 in.(760 mm)
Overall depth	30 in.(760 mm)
Weight	200 lb.(90 kg)

Table of Magnifications

'Magnification' is a one-word term for the scale of enlargement of the errors considered in the radial direction, and is the ratio of the movement of the recording pen to that of the stylus.

The magnification varies according to the length of the stylus arm and the setting of the magnification switch. Magnifications for the three lengths of stylus arm supplied are given in the Table A.I.1.

Metric Graph Paper

	Magnification Switch Position					
	1	2	3	4	5	6
6.2 cm. Arm 1 DIV.	200 10μm	400 5μm	1,000 2μm	2,000 1μm	4,500 0.5μm	10,000 0.2μm
12.5 cm. Arm 1 DIV.	100 20μm	200 10μm	500 4μm	1,000 2μm	2,000 1μm	5,000 0.4μm
25 cm. Arm 1 DIV.	50 40μm	100 20μm	250 8μm	500 4μm	1,000 2μm	2,500 0.8μm

Three different filters are provided, selected by the switch. Their effect is best described in terms of the range of undulations (in terms of number per revolution) on which the filter has little or no effect, as shown in the table below. Undulations lying outside the range will tend to be suppressed. The transition, however, is not abrupt but occurs gradually. The filter characteristics are shown in the Table A.I.2.

	Normal	A	B	C
3 r.p.m.	1-450	1-45	1-15	15-450

TABLE A.I.2. - TABLE OF FILTER TRANSMISSIONS
(undulations per revolution)

APPENDIX II

HEWLETT-PACKARD MAGNETIC DATA RECORDING SYSTEM

MODEL 3917-B : SPECIFICATIONS

APPENDIX II

NUMBER OF TRACKS:
7

TRACK WIDTH:
0.08 in. (1.27 mm)

TRACK SPACING:
0.07 in. (1.78 mm) center-to-center

INTERCHANNEL TIME DISPLACEMENT ERROR:
Maximum ± 1μ sec at 60 ips (1524 mms) and ± 4μ sec at 15 ips (381), measuring between 2 adjacent tracks on same head.

TAPE SPEED:
60, 30, 15, 7-1/2, 3-3/4, 1-7/8 inches per second. Push-button controlled from front panel.

TAPE WIDTH:
1/2 in. (12.7 mm)

TAPE THICKNESS:
.65, 1.0, and 1.5 mil (1.0 mil recommended).

TAPE LENGTH:
2400 ft (731.5 m), 1.5 mil tape; 3600 ft (1097.3 m), 1.0 mil tape; 4800 ft (1463 m), .65 mil tape.

REEL SIZE:
10-1/2 in. (266.7 mm) Phenolic Hub either 1/2 in. (12.7) or 1 in. (25.4) wide (7 or 14 track systems).

START TIME:
4 seconds maximum, at 60 ips machine meets flutter specifications within 8 seconds.

STOP TIME:
2 seconds maximum.

REWIND TIME:
Approximately 1-1/2 minutes for 2400 ft (731.5 m) and 2 minutes for 3600 ft (1097.3 m) of tape, maximum.

CONTROLS:
Operating controls - LOAD (Power), STOP, PLAY, REVERSE, FORWARD (Fast), RETURN (unloaded) and supervised relays.

DRIVE SPEED ACCURACY:
± 0.25% of nominal capstan speed which is directly proportional to line frequency.

WEIGHT:
Total system weight is approximately 310 lbs.(139.5 kg) net.

DIMENSIONS:
Total system is 72-1/8 in. high, 22-1/16 in. wide, 30 in. deep (1654 x 559 x 762 mm).

POWER REQUIREMENTS:
Total system is 105 to 125 volts rms, 60 c/s (Hz). Approximately 500 watts.

TAPE SPEED	EQUALIZATION PLUG-IN	MID-FREQUENCY (R2)	HIGH FREQUENCY (L2)	BANDWIDTH
1-7/8 ips	3900-22A	1.2 kc	7.0 kc	50 cps - 7 kc
3-3/4 ips	3900-23A	2.0 kc	15.6 kc	50 cps - 15.6 kc
7-1/2 ips	3900-24A	5.0 kc	31.25 kc	50 cps - 31.25 kc
15 ips	3900-25A	10.0 kc	62.5 kc	100 cps - 62.5 kc
30 ips	3900-26A	18.0 kc	125.0 kc	150 cps - 125 kc
60 ips	3900-26B	40.0 kc	250.0 kc	300 cps - 250 kc

TABLE A.II.1. - DIRECT EQUALIZATION OF PLUG-IN ALIGNMENT

TAPE SPEED	FM FREQUENCY PLUG-IN	BANDWIDTH
1-7/8 ips	2000-1300-C3	0- 625 cps
3-3/4 ips	2000-1300-C4	0- 1,250 cps
7-1/2 ips	2000-1300-C5	0- 2,500 cps
15 ips	2000-1300-C6	0- 5,000 cps
30 ips	2000-1300-C7	0-10,000 cps
60 ips	2000-1300-C11	0-20,000 cps

TABLE A.II.2. - FM FREQUENCY PLUG-INS.

APPENDIX XXI

BOREHOLE GRAPH

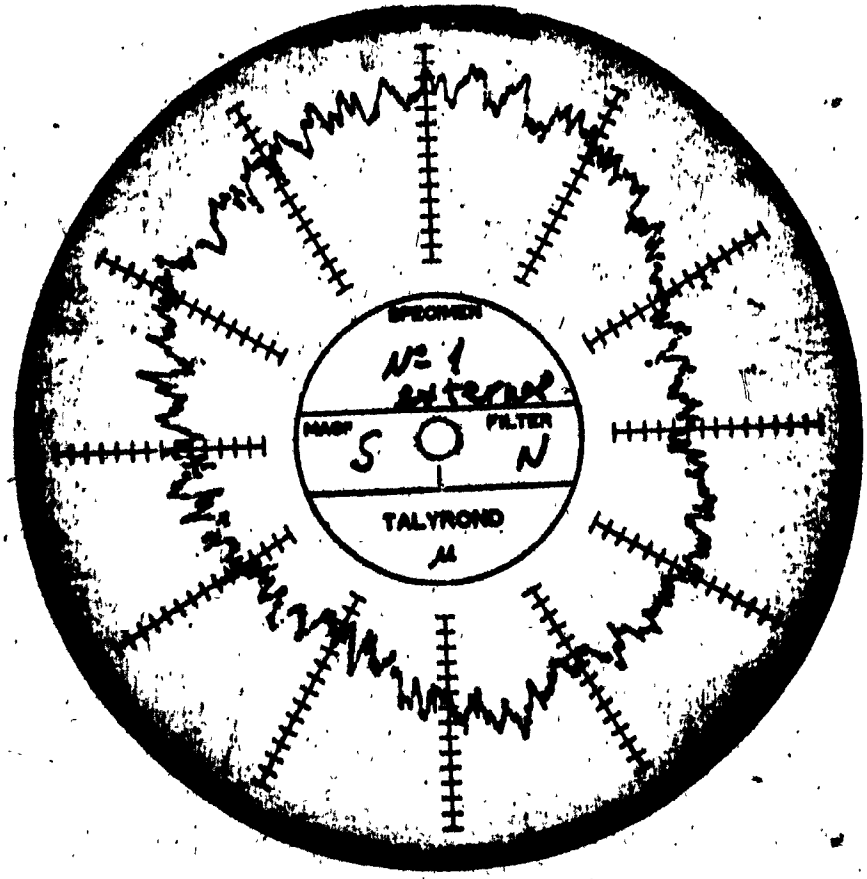
SPECIMEN
N° 1
extérieur
MAGN
S
FILTER
N
TALYROND

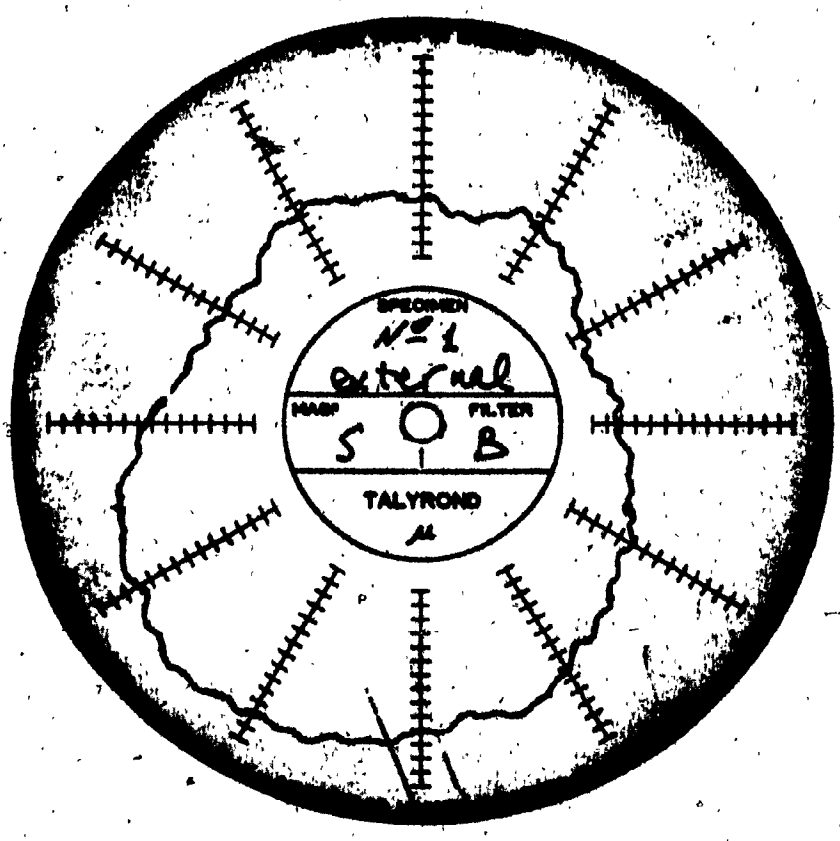

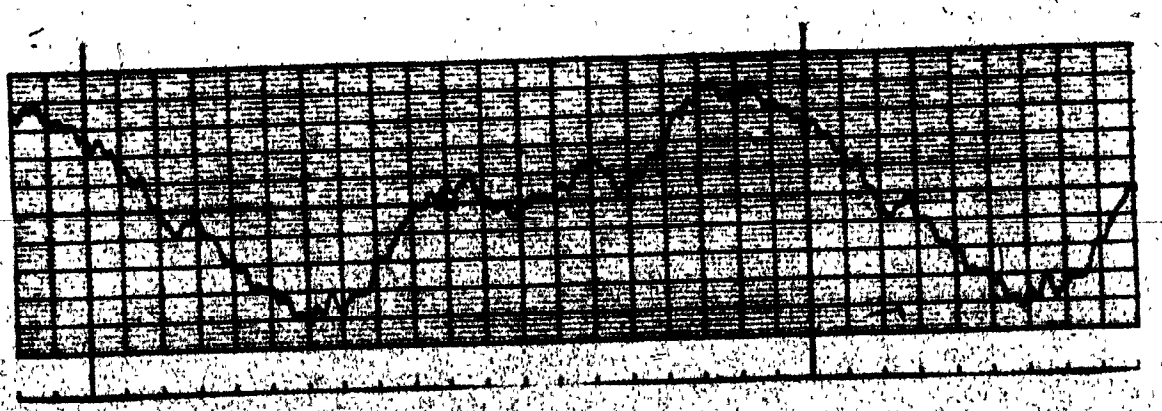

Fig. A.III.3

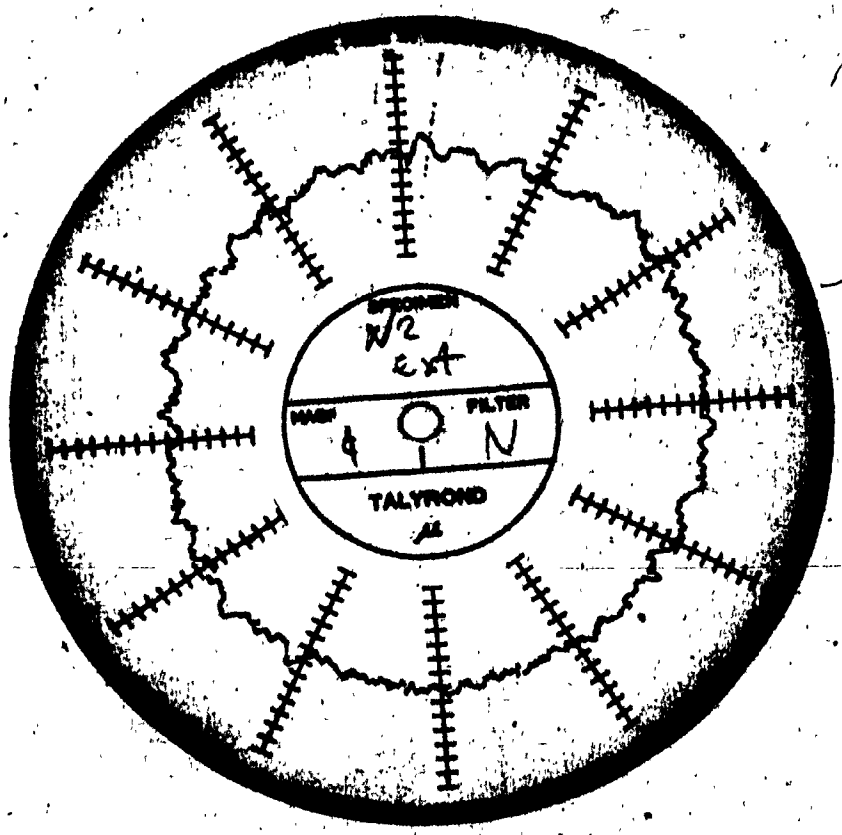

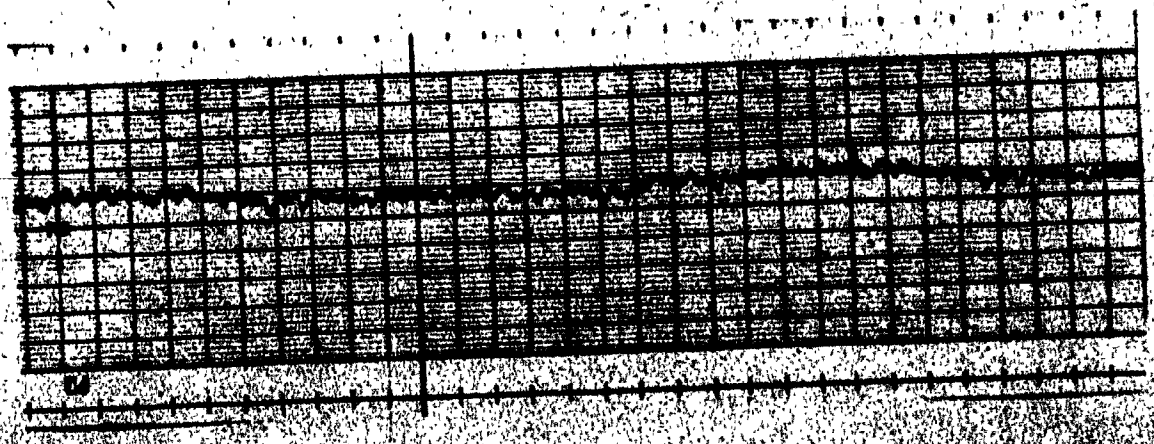

FIG. A.III.3

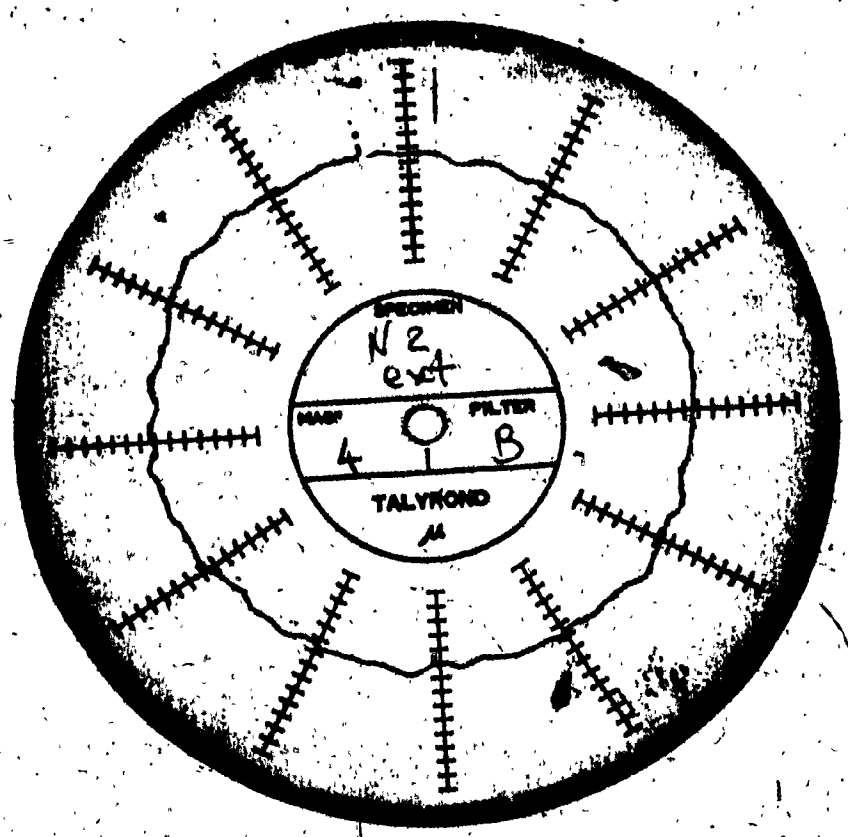
SPECIMEN
N 2
ext
HAUT
FILTER
4
B
TALYROND
M

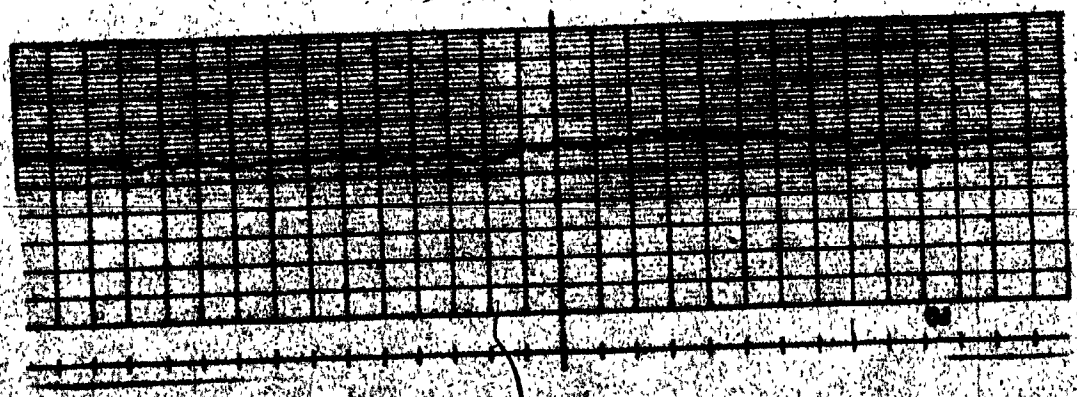

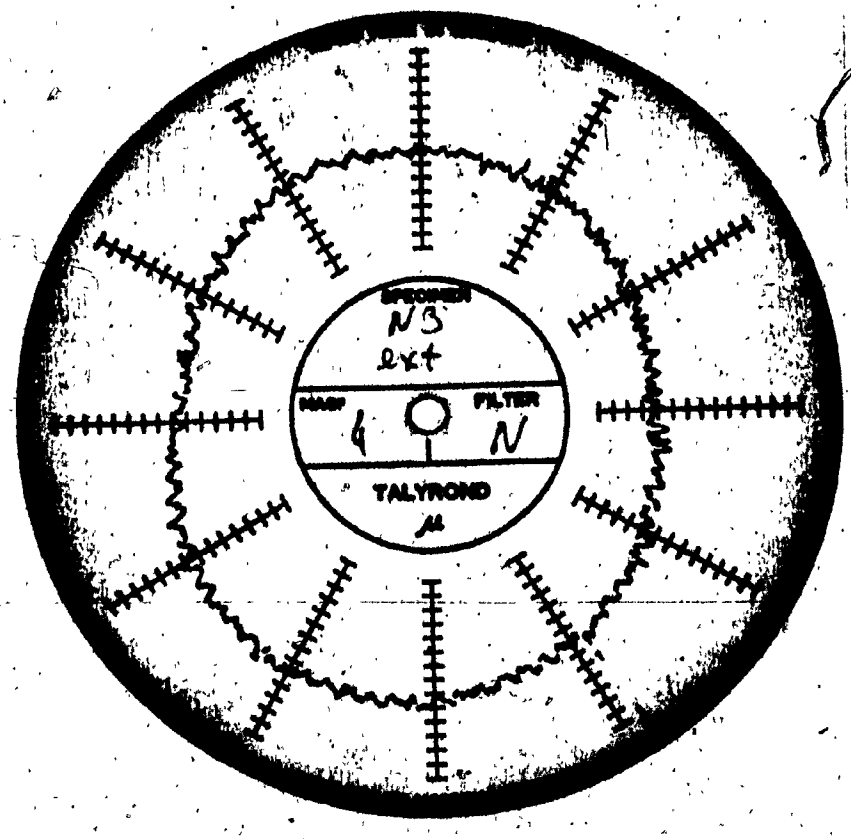
SPECIMEN
N3
ext
MAG
4
FILTER
N
TALYROND
M

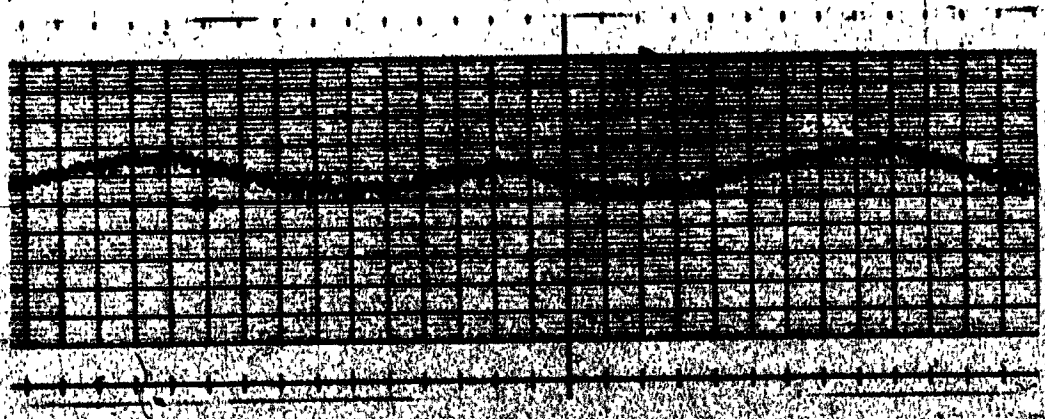

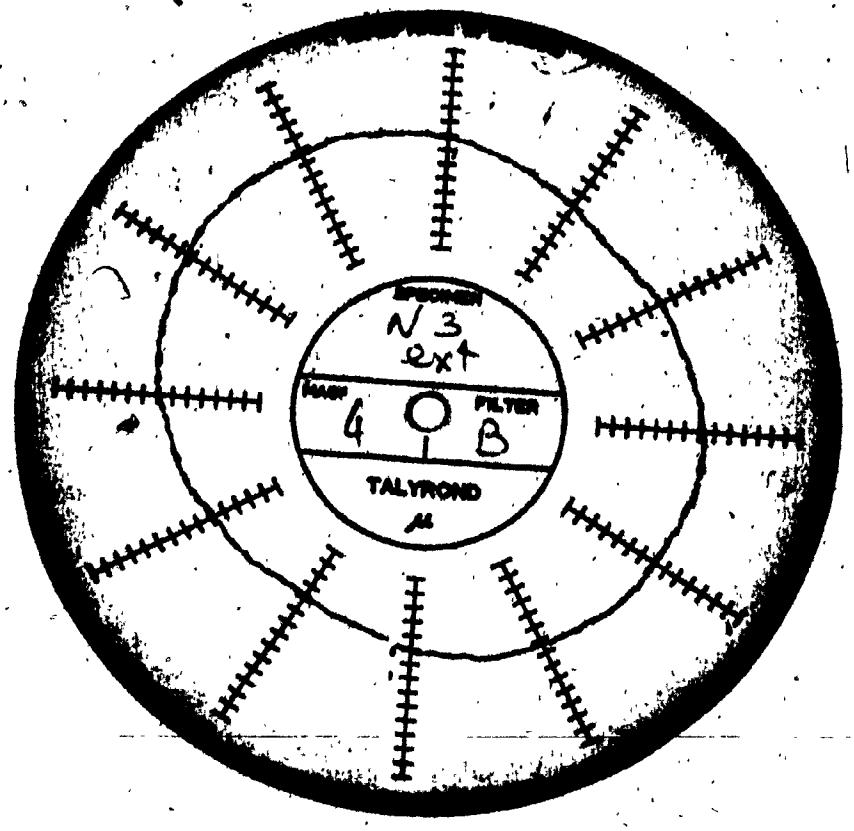

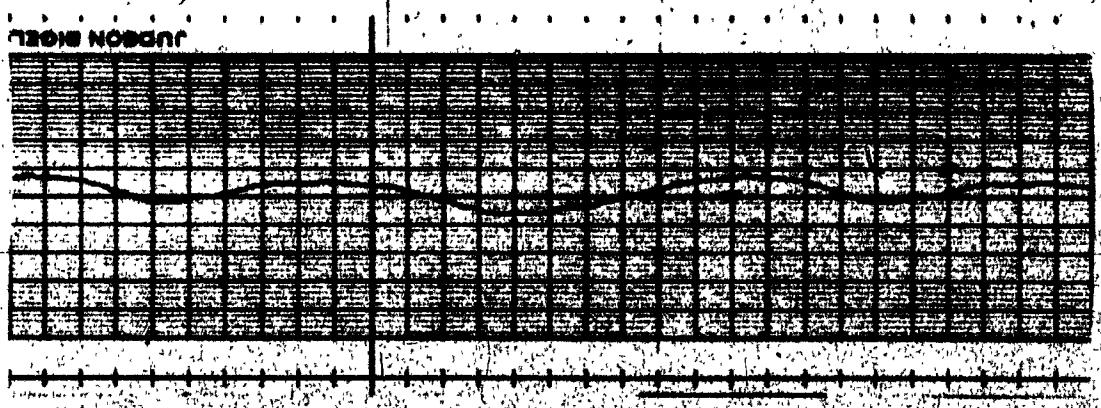

FIG. A.III.6

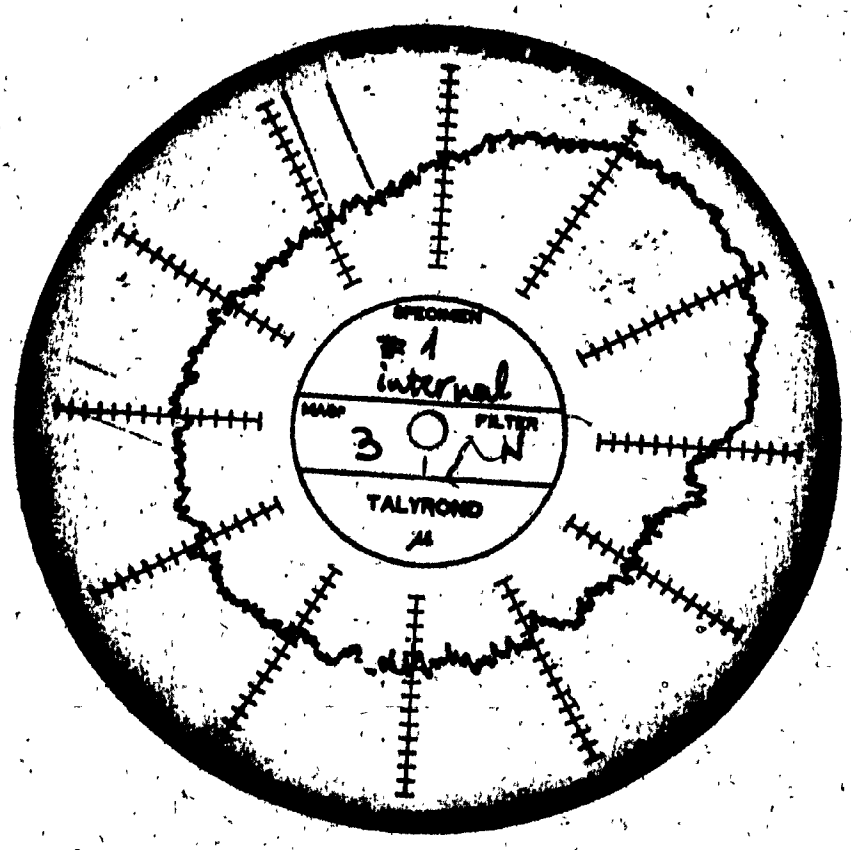
SPECIMEN
1
interval
MAG
FILTER
3
TALYROND

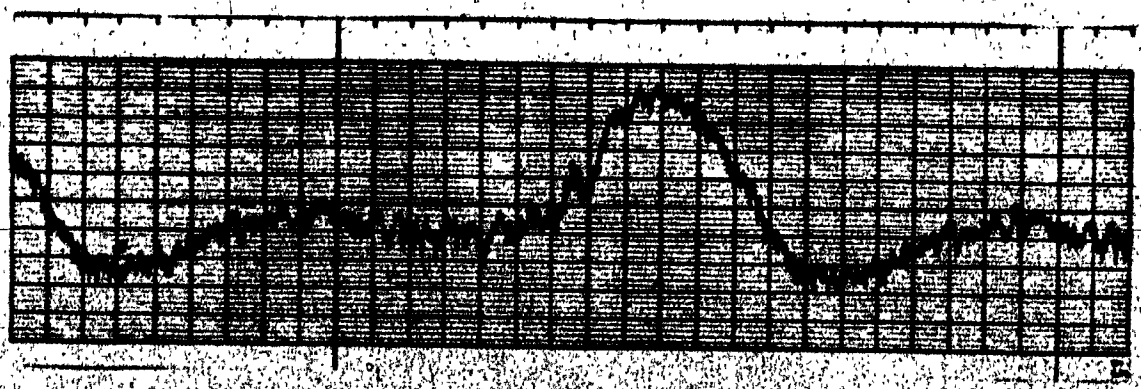

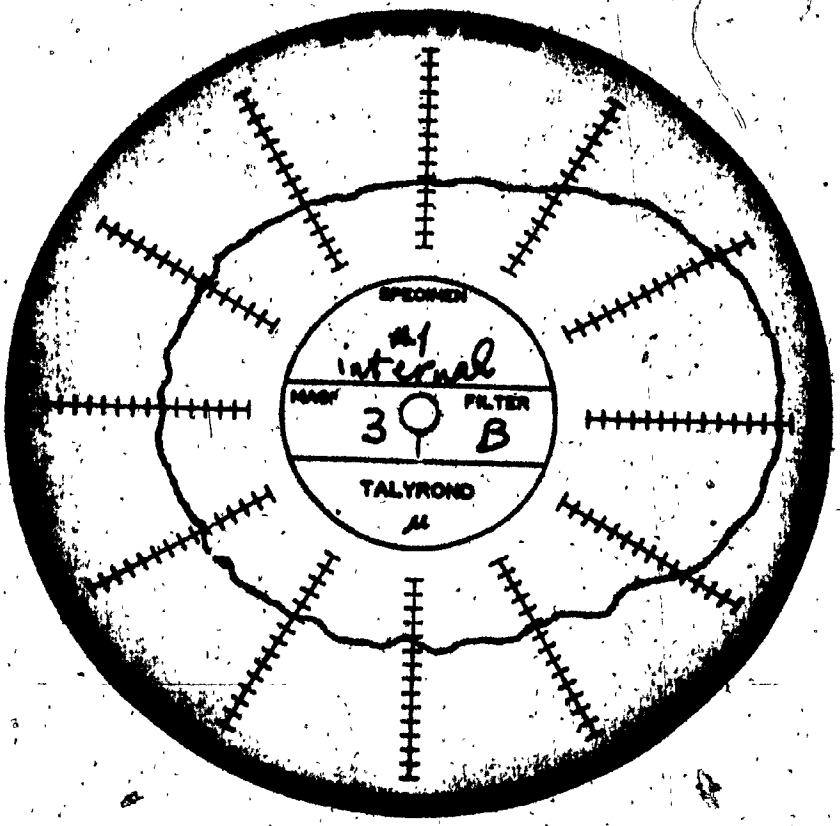
SPECIMEN
No 1
interval
NAME
3
FILTER
B
TALYROND
μ

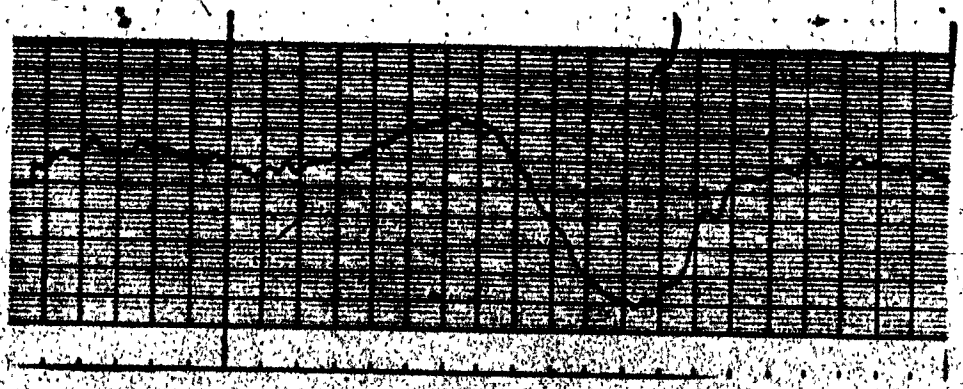

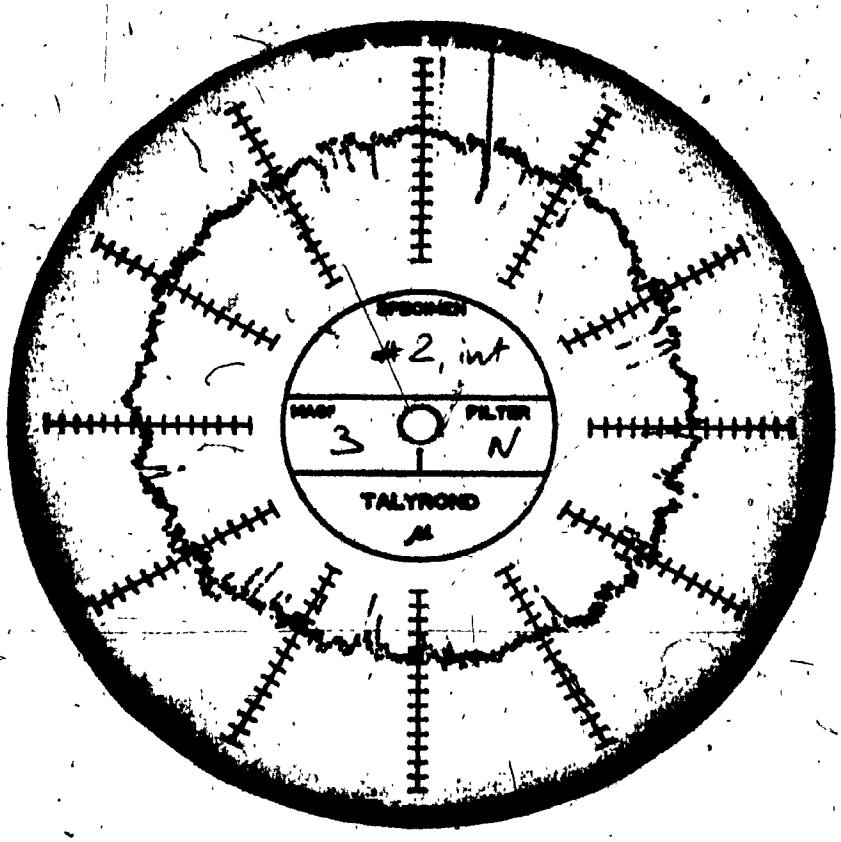

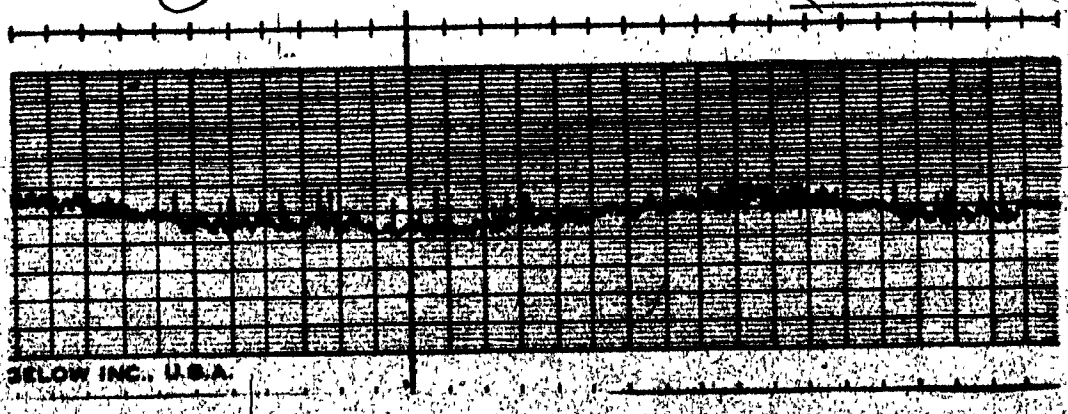

FIG. A.III.9

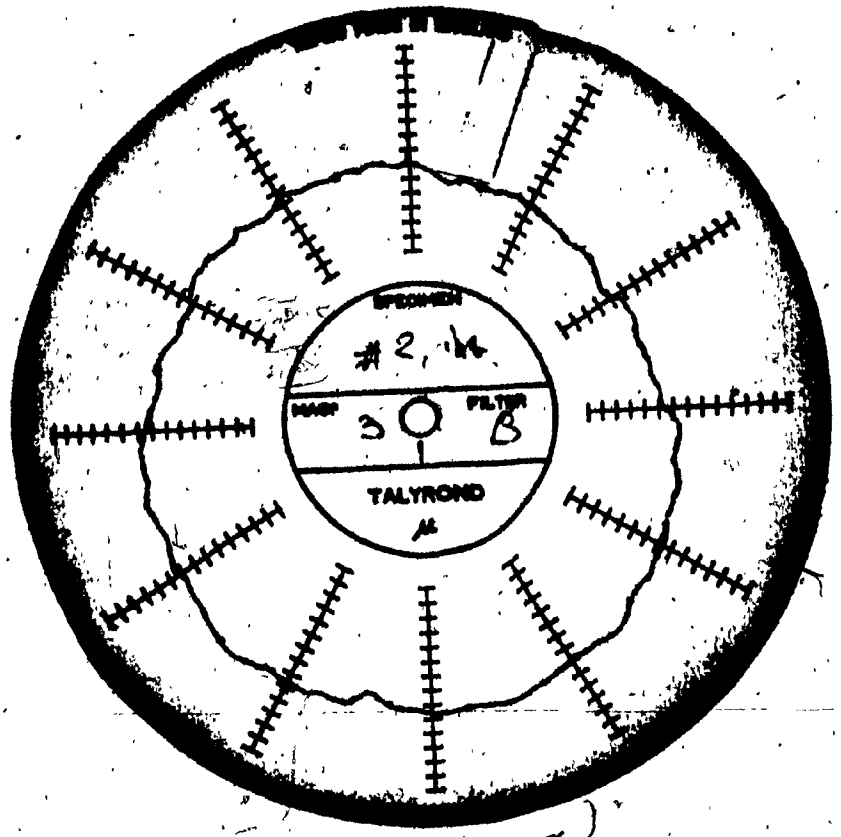

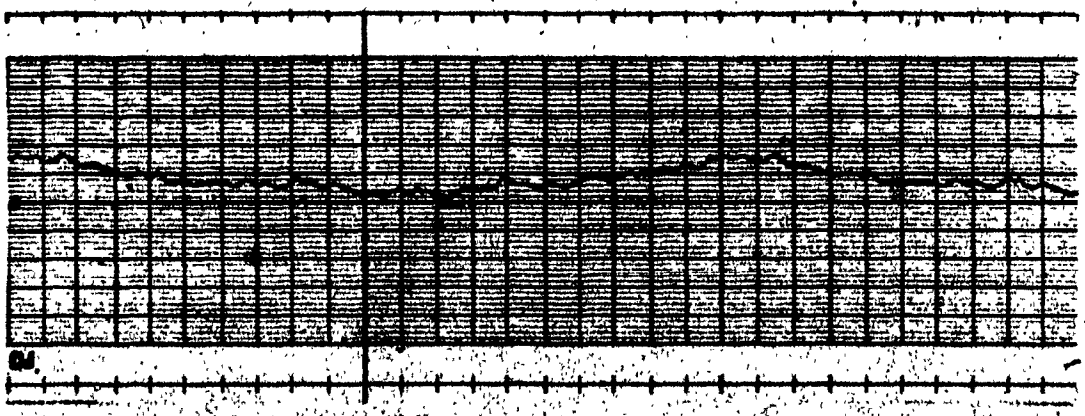

FIG. A.III.19

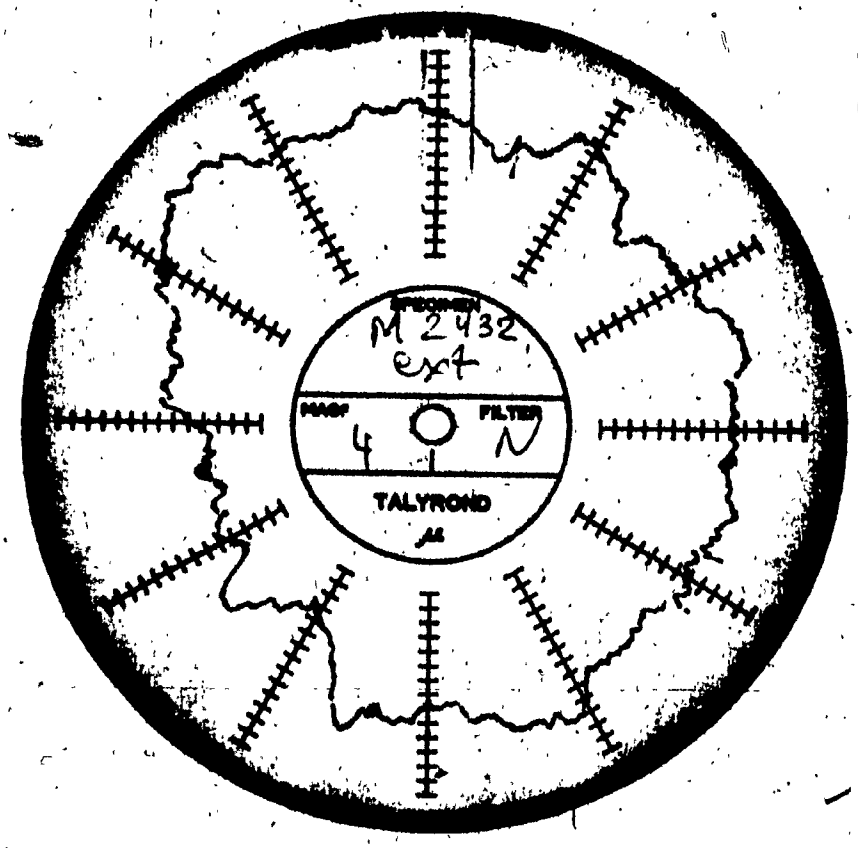

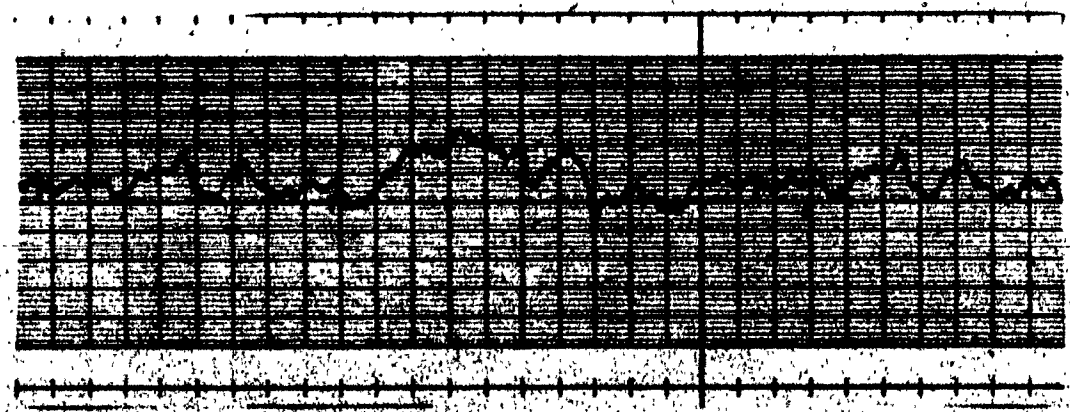

Fig. A.III.11

A.III.23

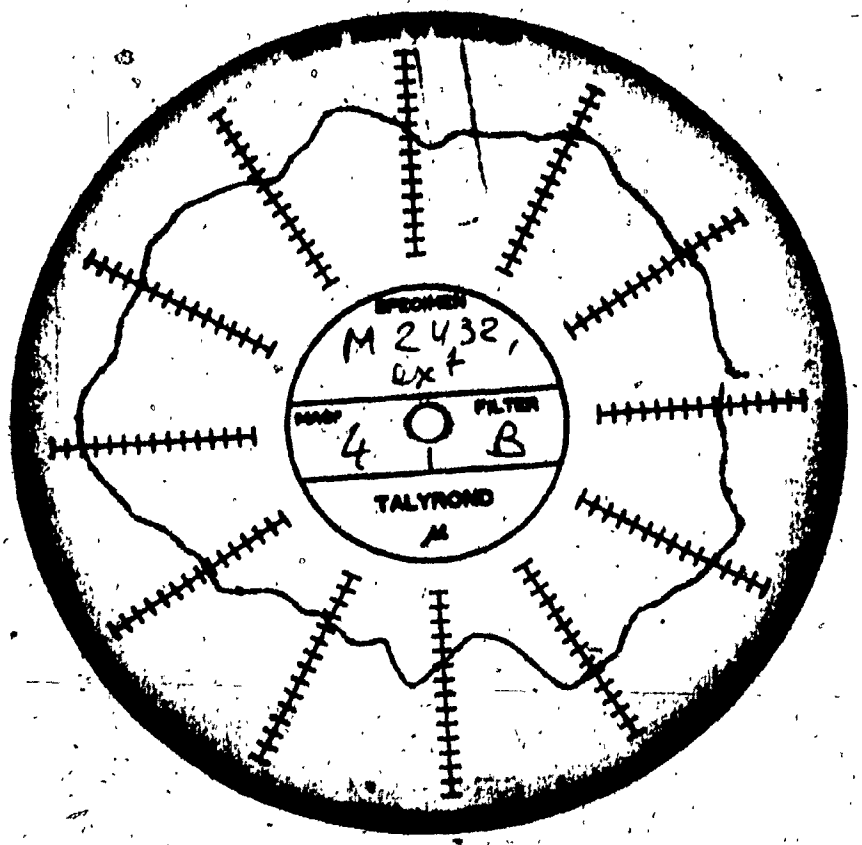

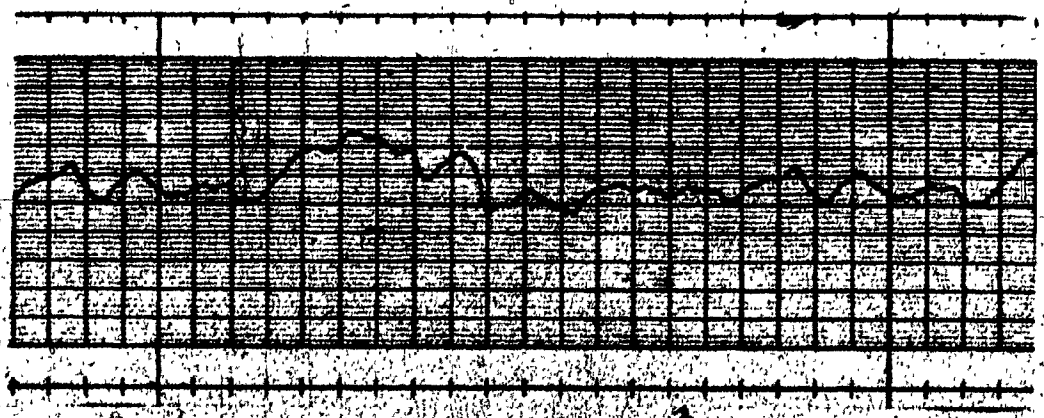

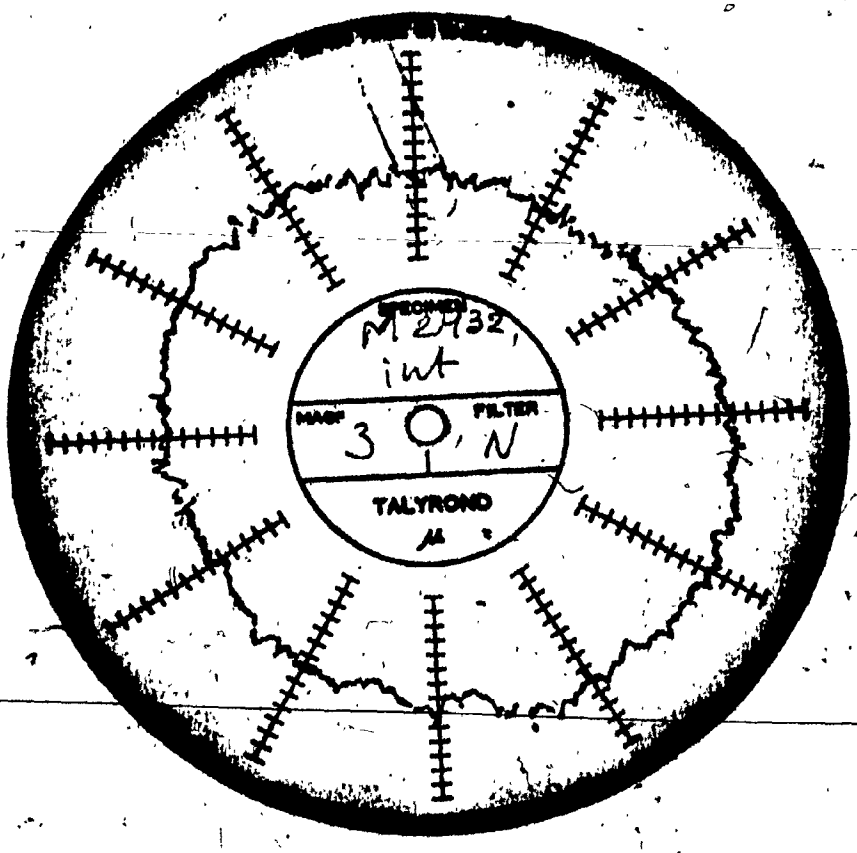

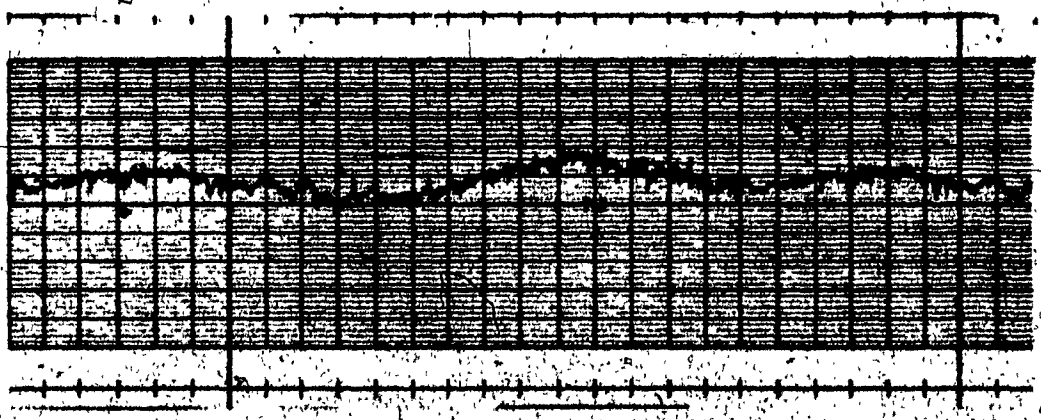

FIG. A.III.19

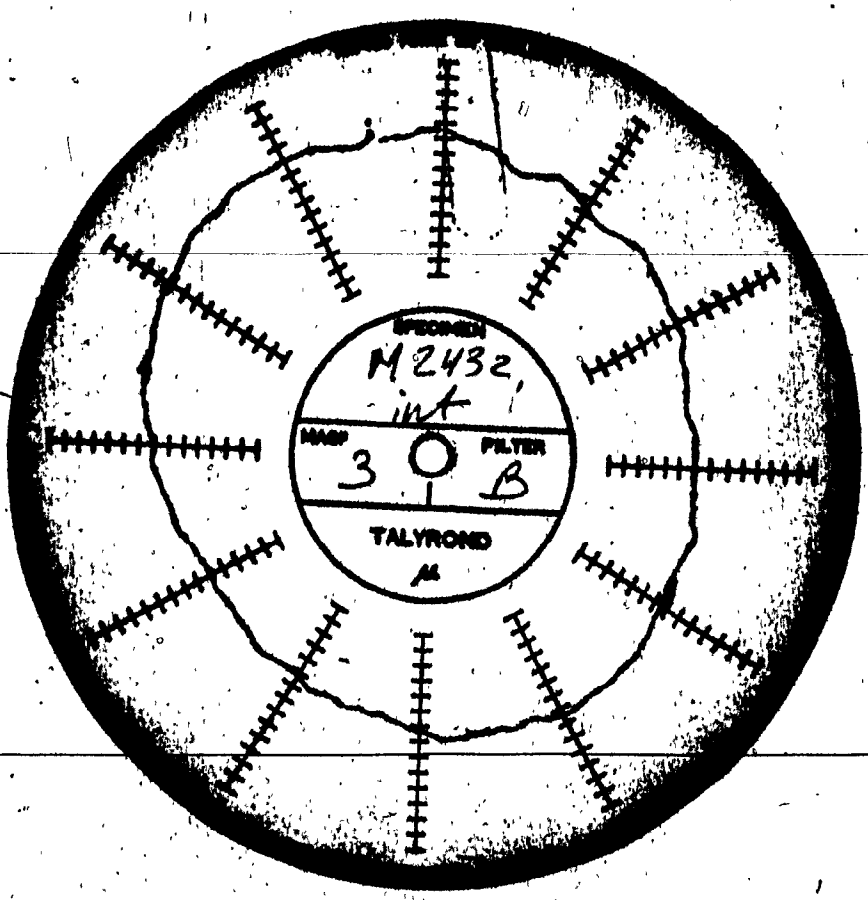
M2432,
int
MAG
3
FILTER
B
TALYROND

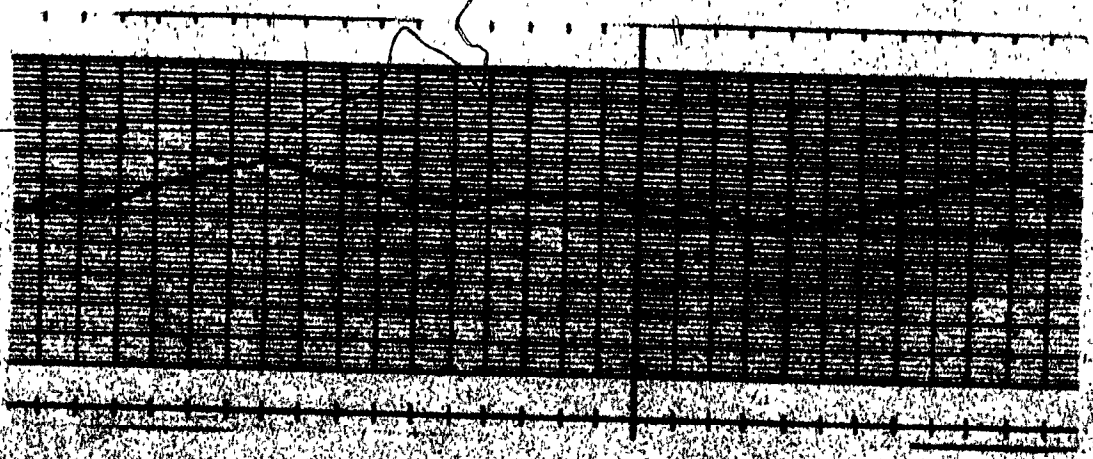

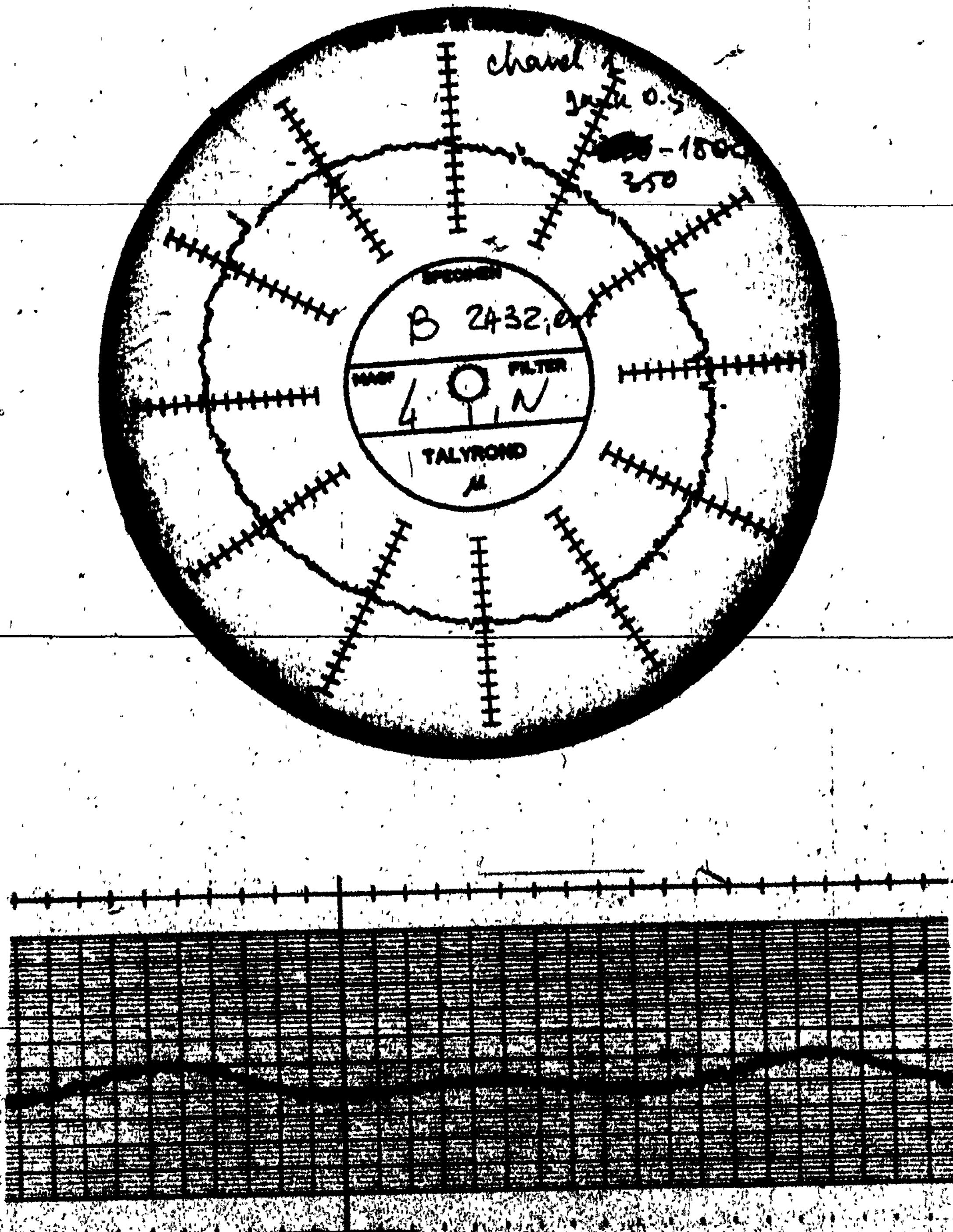
SPECIMEN
MAGN
FILTER
TALYROND
μ

[illegible]

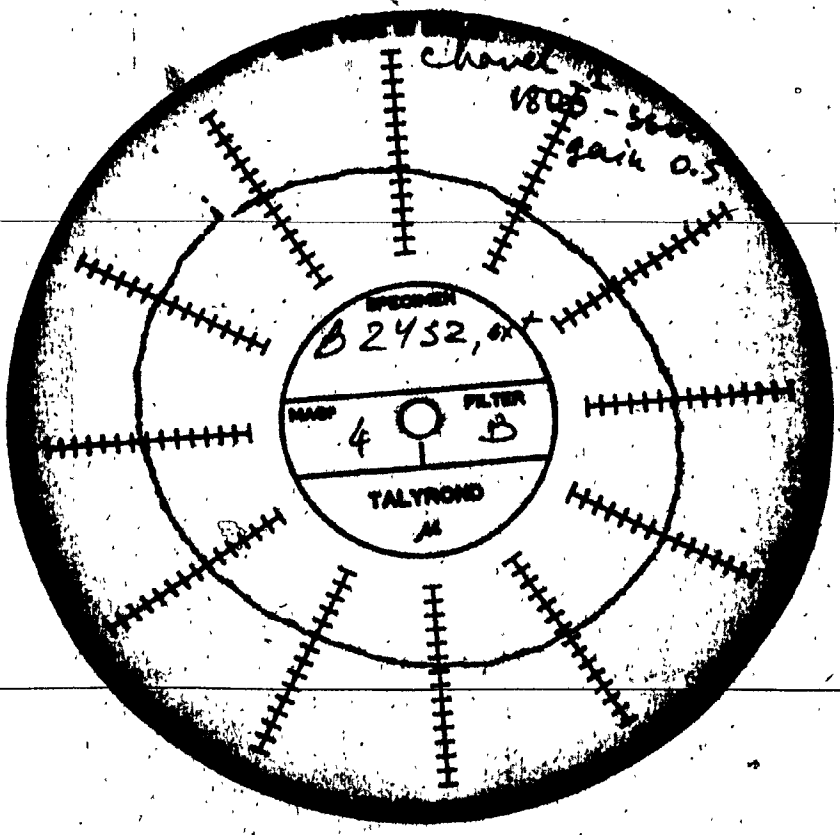
Chevet
gain 0.5
SPECIMEN
B 2452, 01
MAG
4
FILTER
B
TALYROND

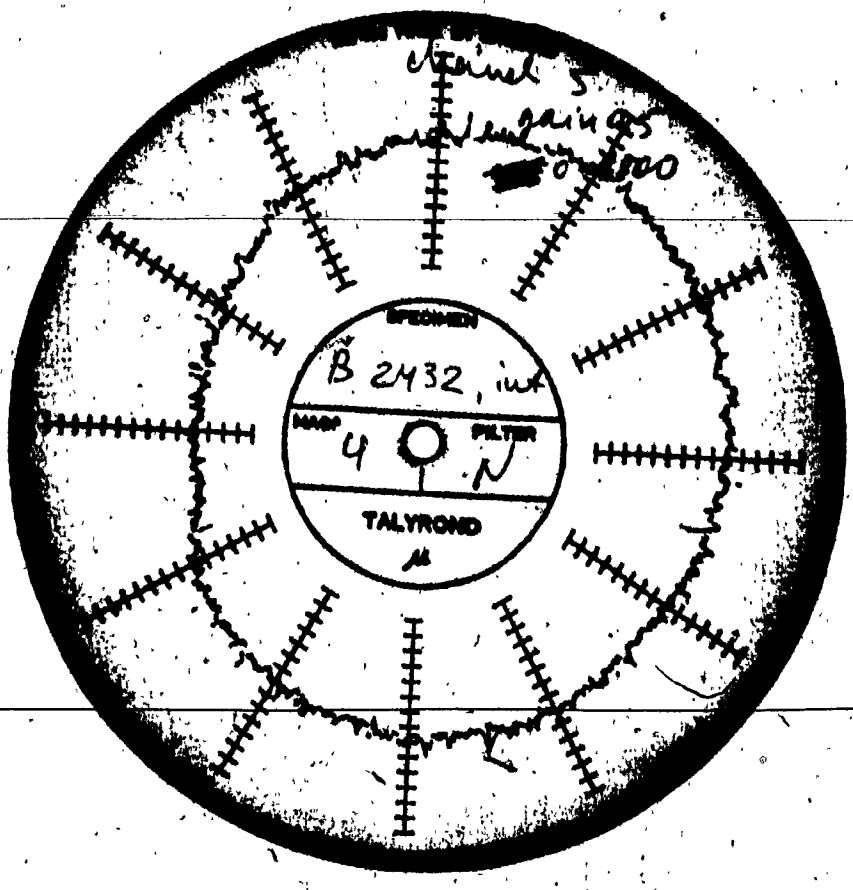

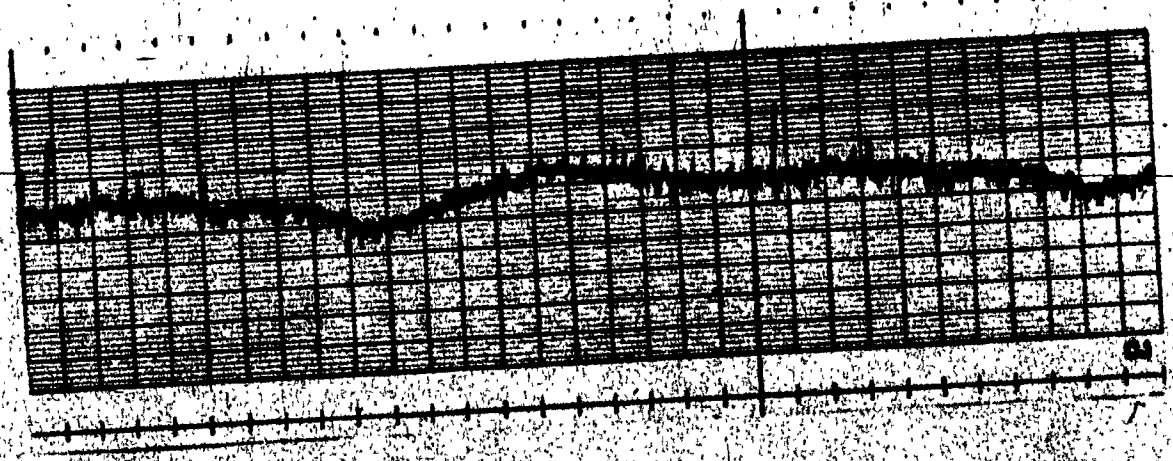

FIG. A.III.27

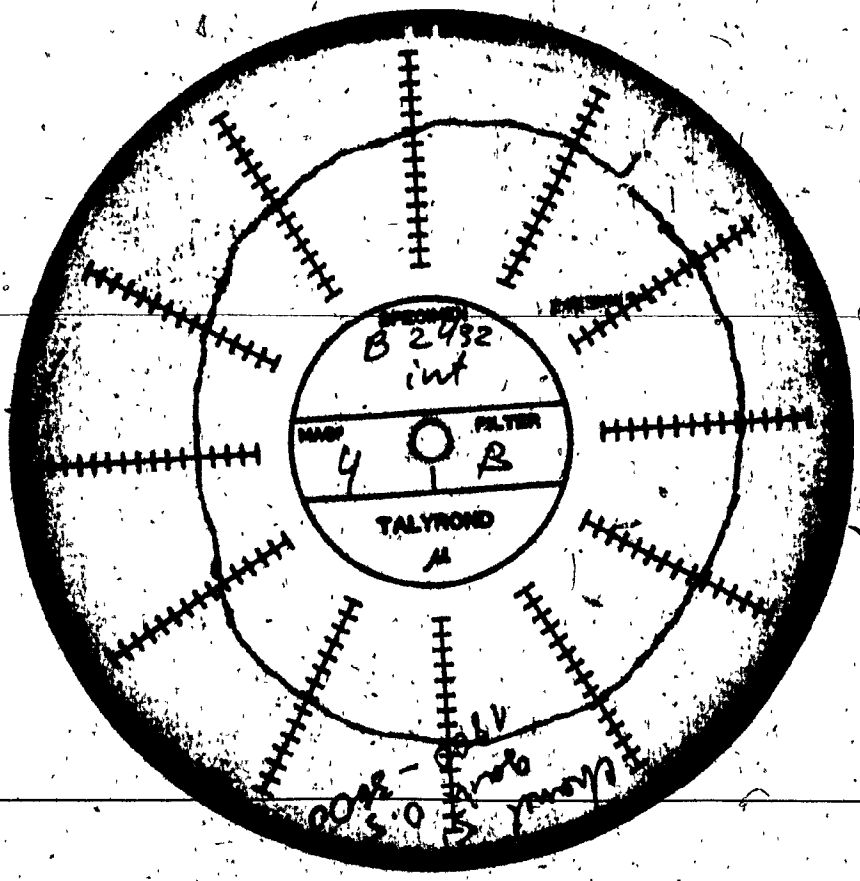
B 2432
int
FILTER
B
TALYROND

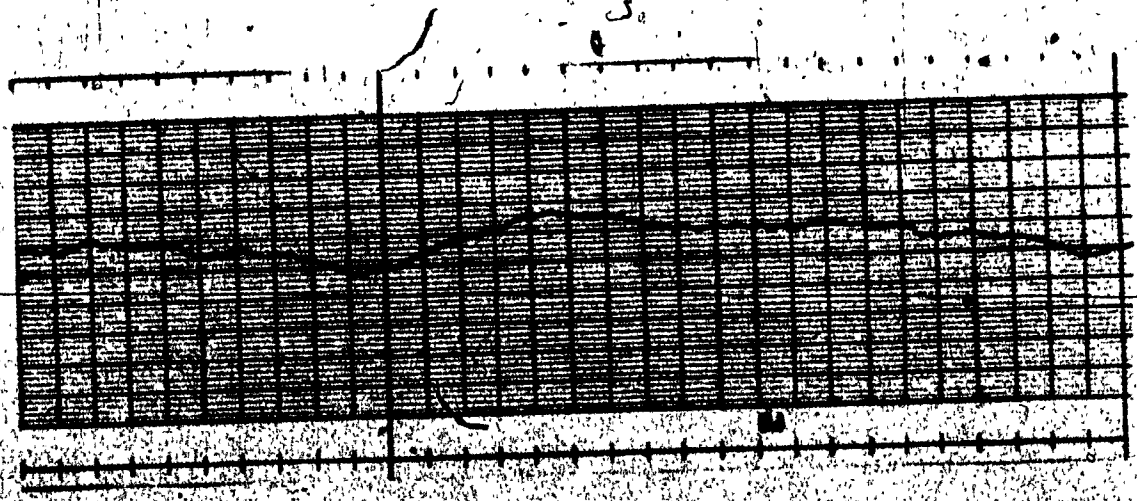

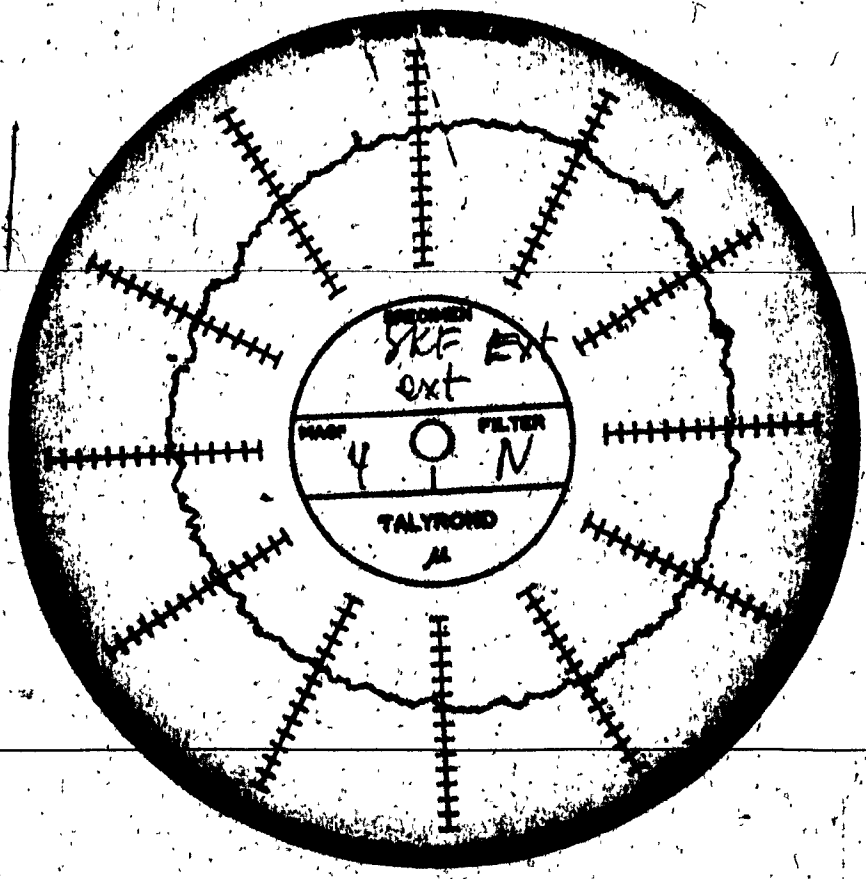
SKF ex
ext
MAKE
FILTER
4
N
TALYROND
μ

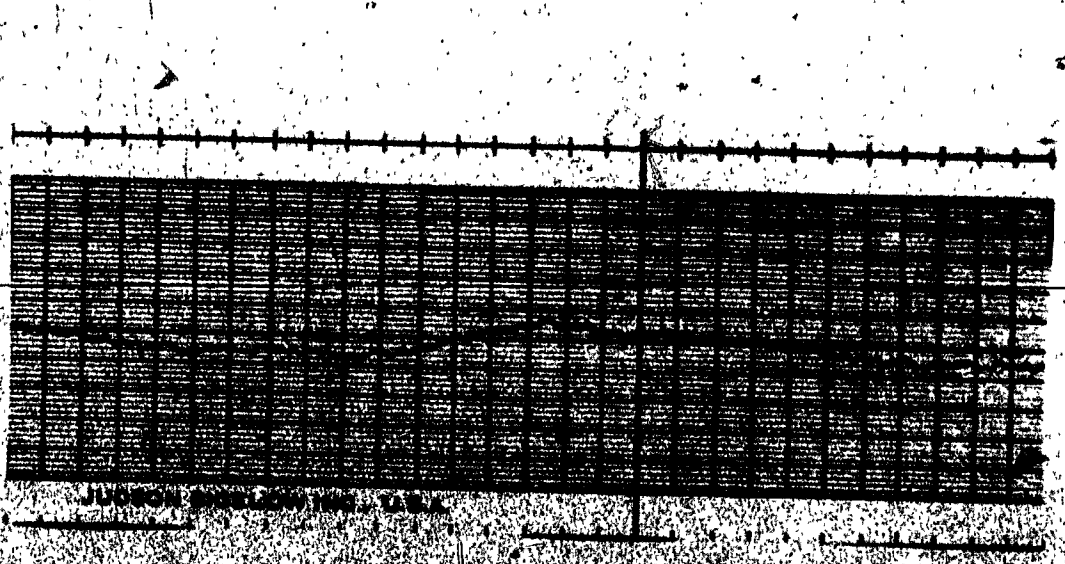
JUDSON PIGELOW INC. U.S.A.

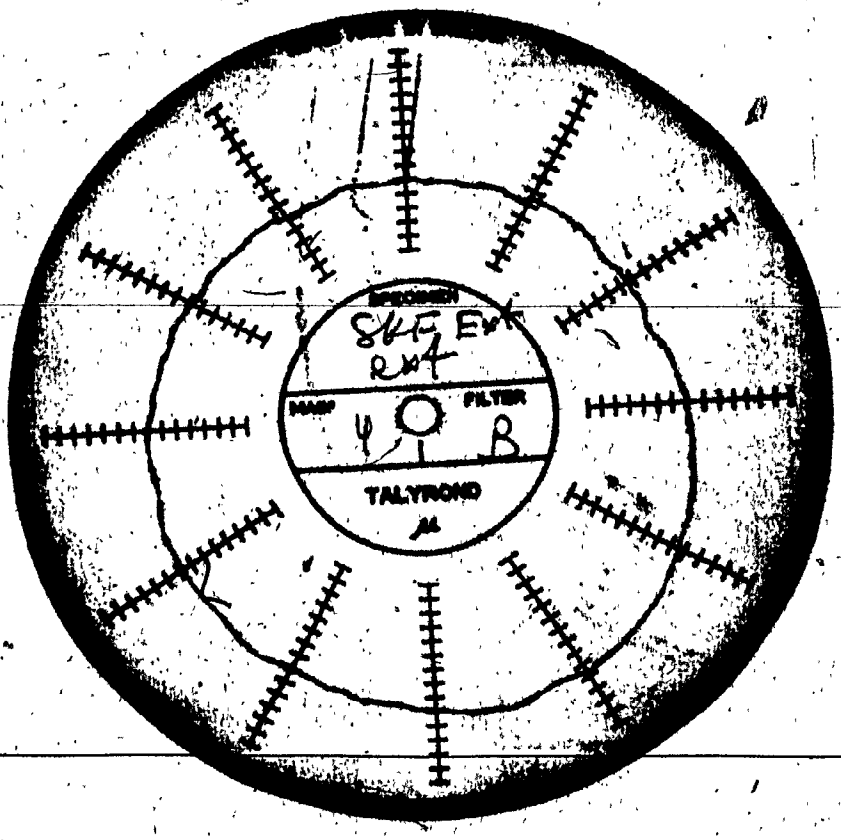
SKF EM
RM
FILTER
B
TALYROND

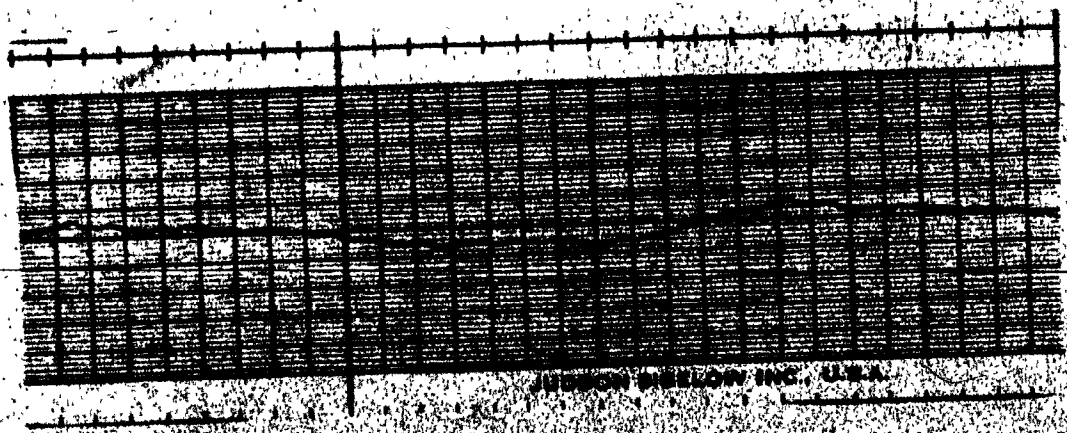
JUDSON BEELOW INC., U.S.A.

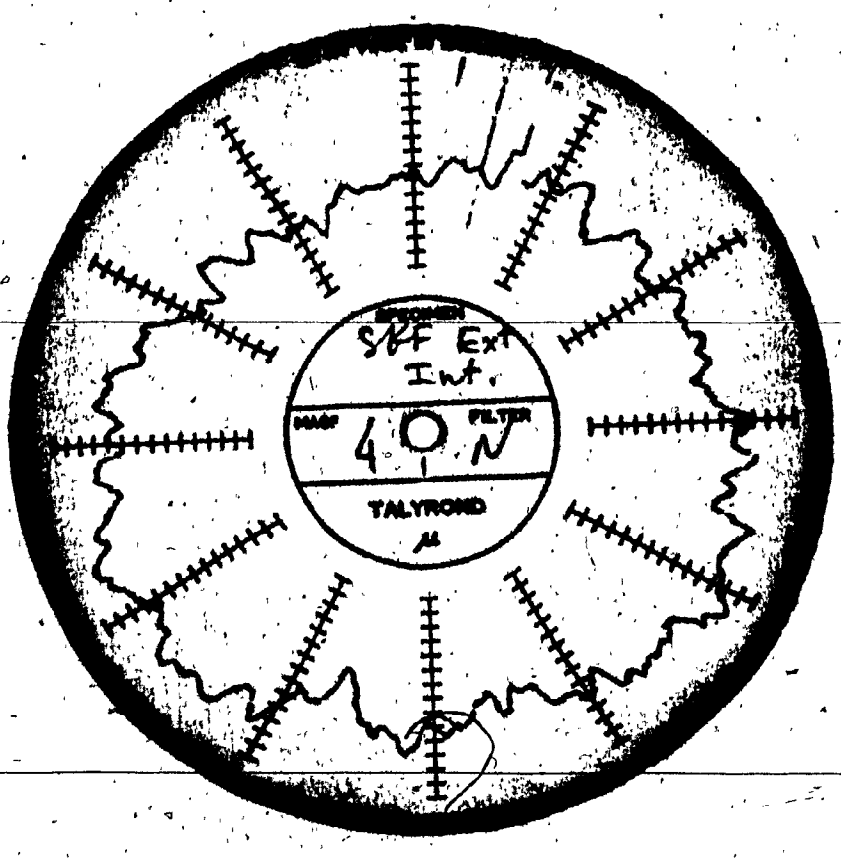
SPECIMEN
SRF Ext
Int.
MAG
4.0
FILTER
N
TALYROND
M

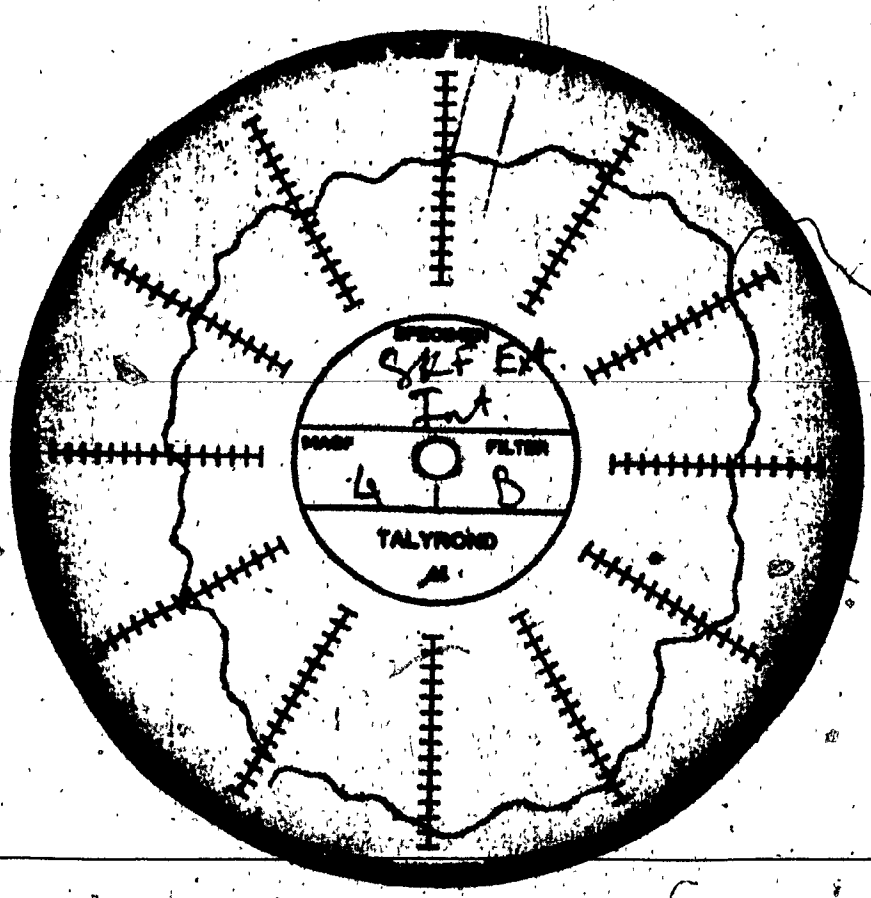
SELF EX
Ext
FILTER
TALYROND

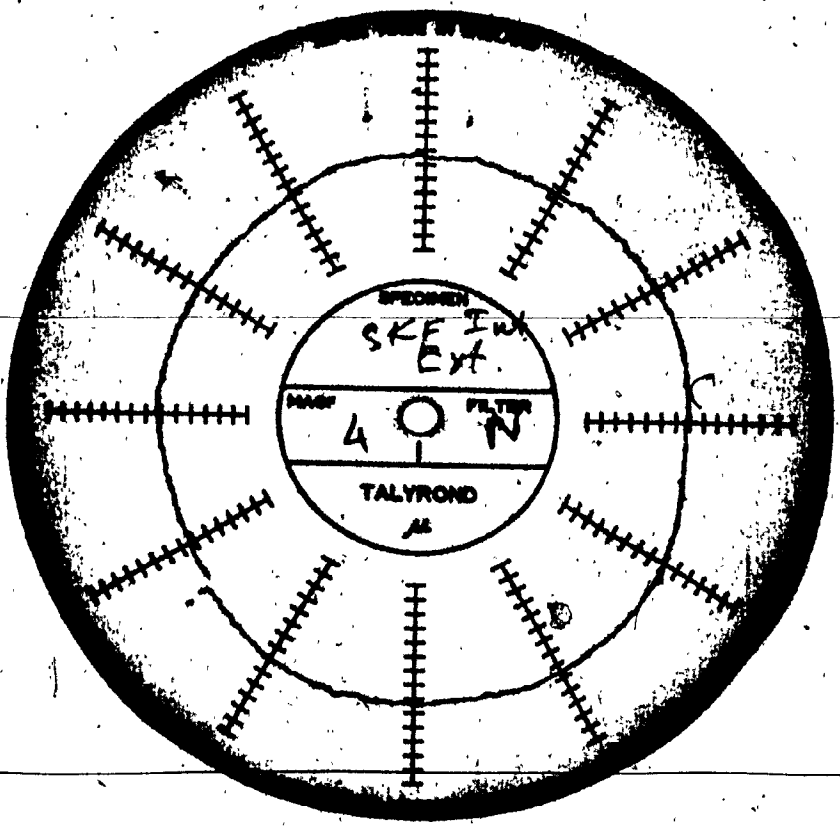

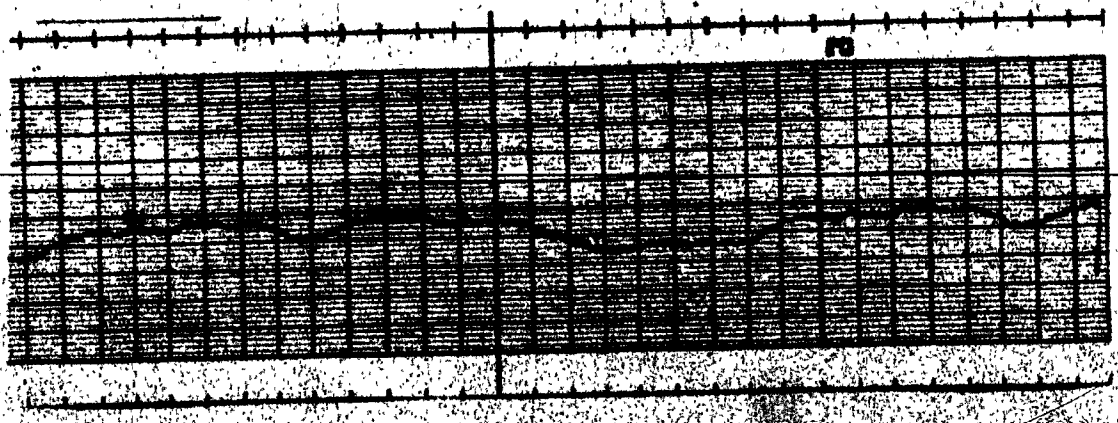

FIG. A.III.23

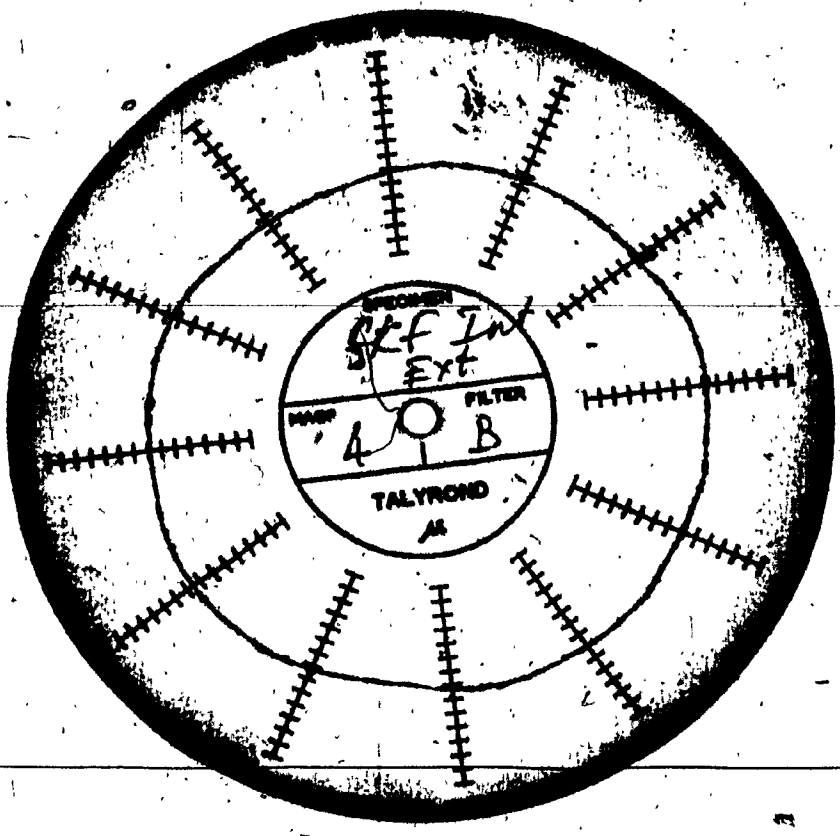

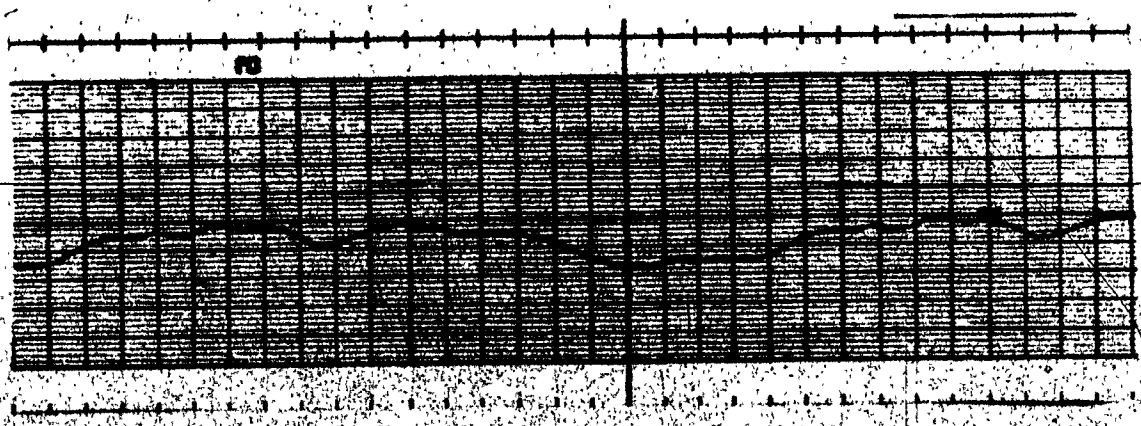

FIG. A.III.35

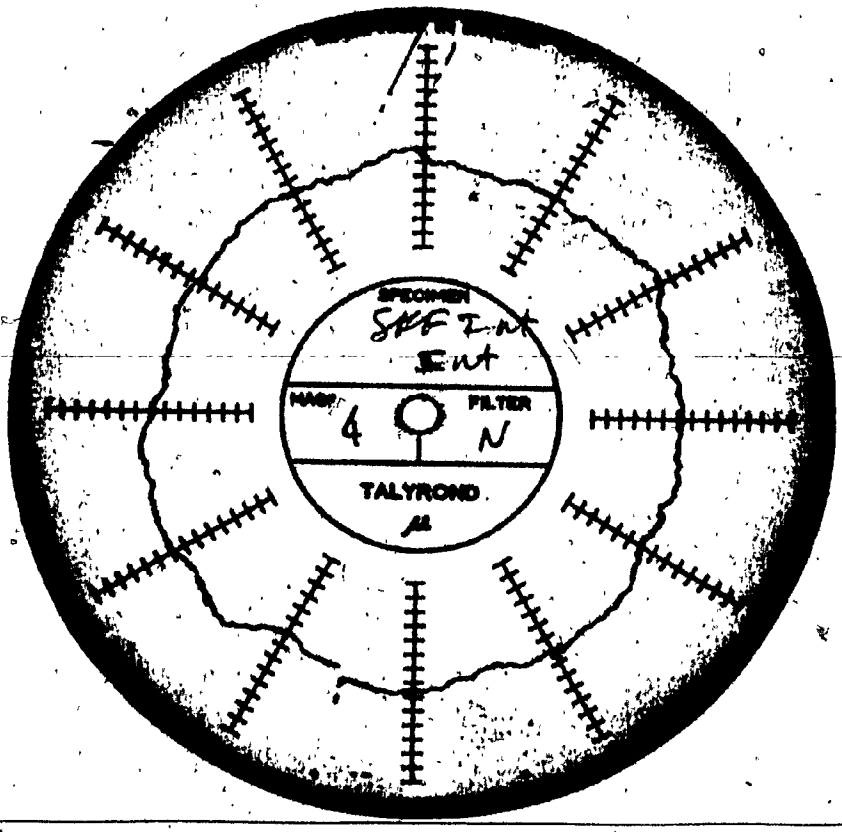

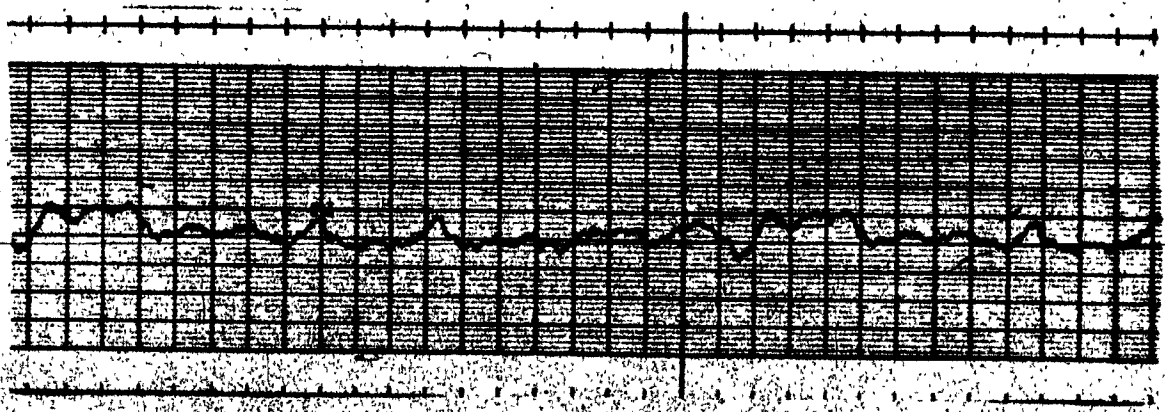

FIG. A.III.36

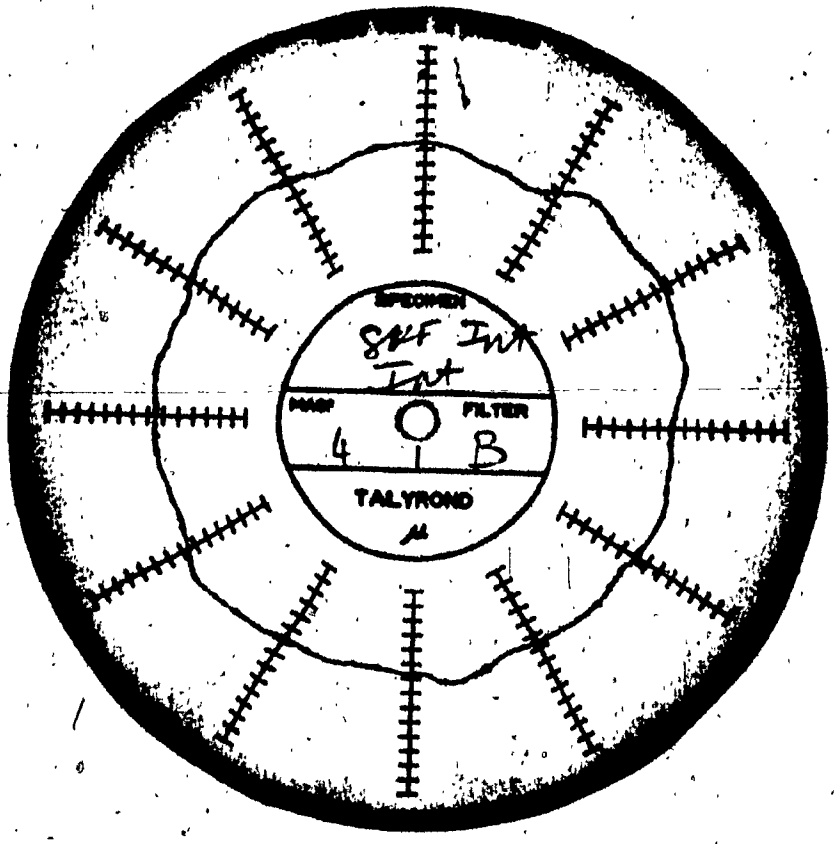

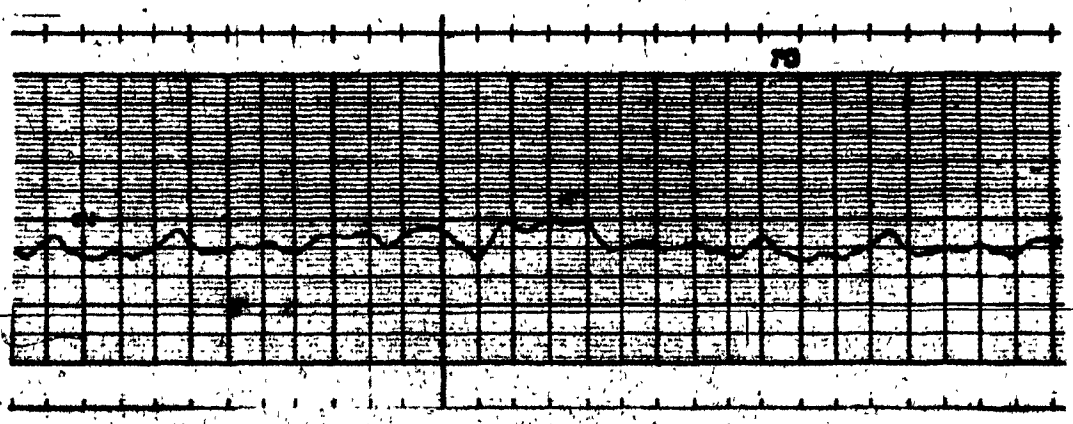

FIG. A.III.26

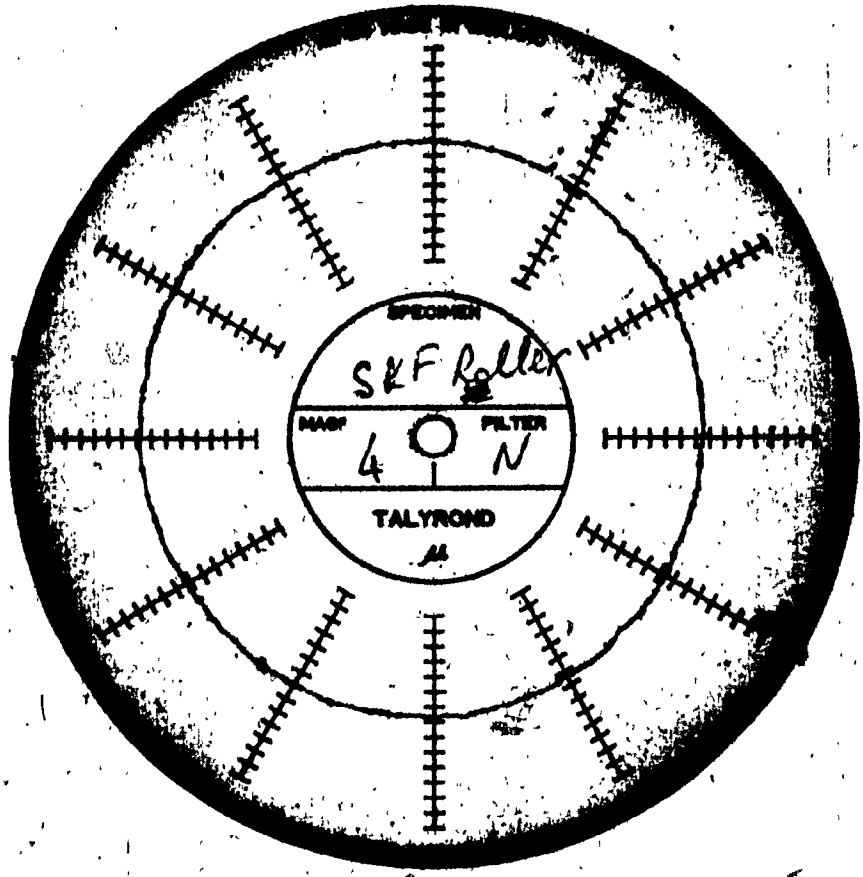

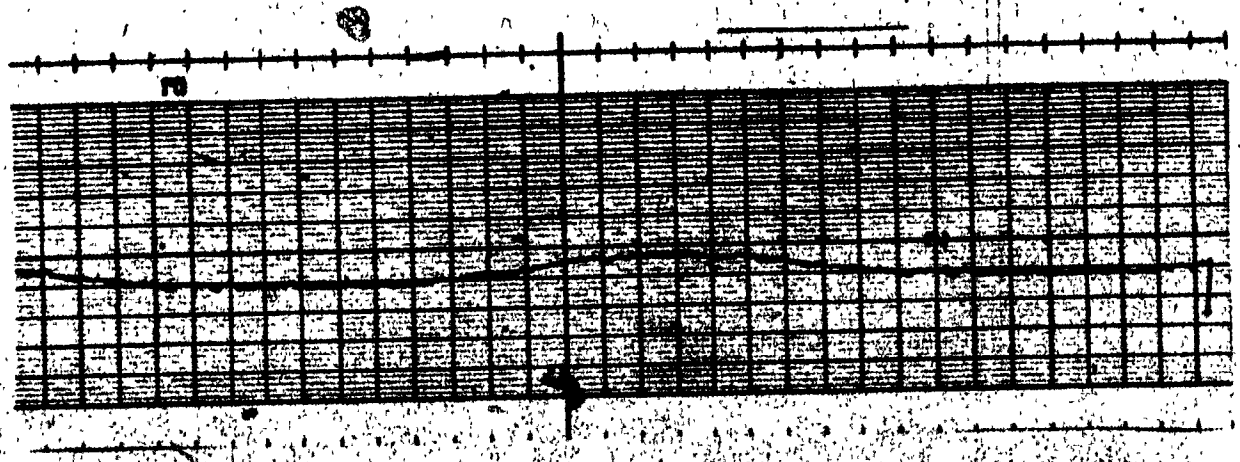

FIG. A.III.37

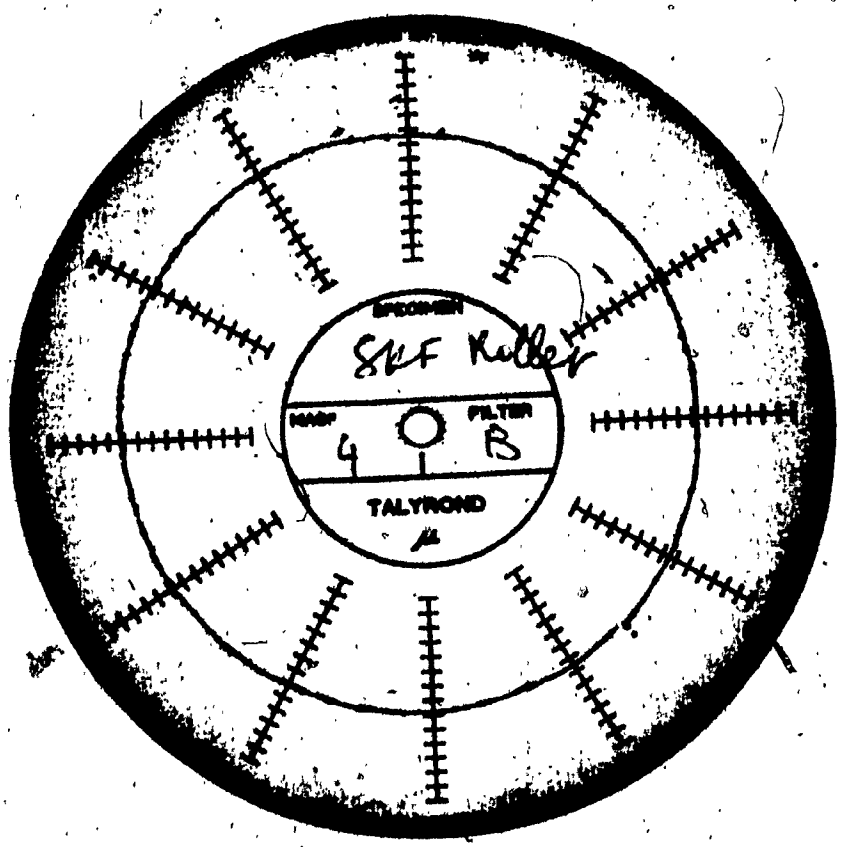

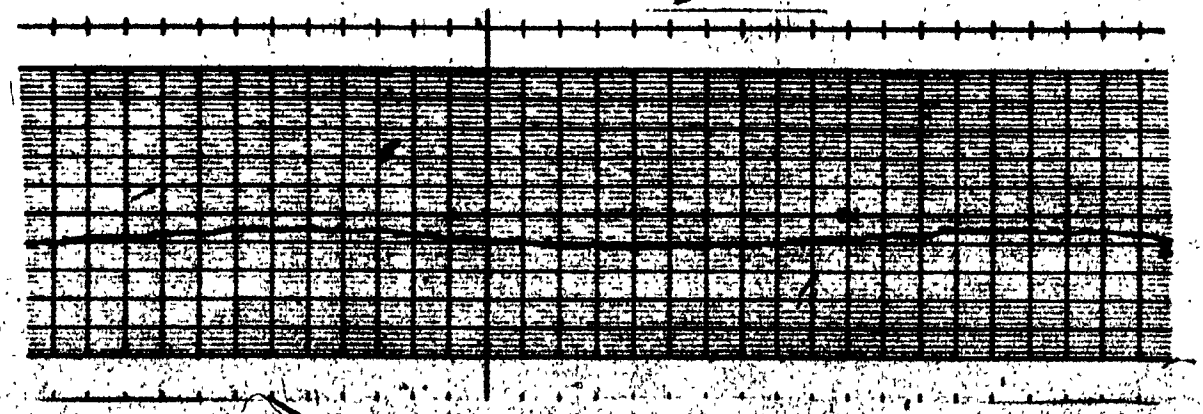

FIG. A.III.39

APPENDIX IV.

AMPLITUDE DISTRIBUTION ANALYZER

B & K INSTRUMENTS INC., MODEL 161

APPENDIX IV

The B & K Model 161 Amplitude Distribution Analyzer permits direct study of the amplitude characteristics of random and complex signals. It provides a more powerful technique for the study of random signals than the standard frequency analysis methods.

Probability Density Analysis

The Probability Density Plot shows the scatter of instantaneous amplitude values of a signal. The plot can be interpreted as:

X amplitude - in units of sigma (σ).
where σ = the RMS signal level

VERSUS.

Y probability-the probability that the instantaneous signal value can be seen at the X amplitude

Figure A.IV.1 shows how the Model 161 derives the probability density plot. The instrument looks at an input signal through a narrow amplitude window which can scan the signal between the values of -5σ and $+5\sigma$. The window is adjusted to a width of 0.1σ. The Model 161 computes the relative time during which the signal appears in this window and produces a voltage proportional to that time. With this analog voltage fed to the Y-input of a plotter and the X-axis synchronized to the window scanning mechanism, the plotter will draw the probability density function.

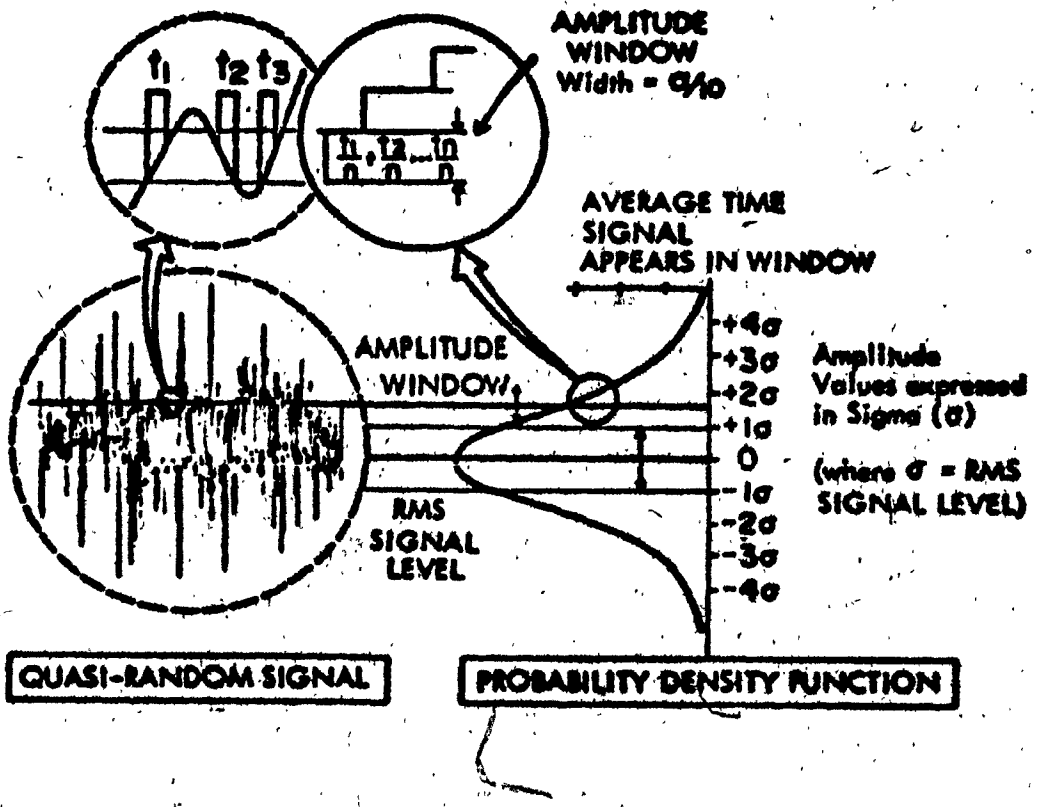

FIG. A.IV.1 - DERIVATIONS OF THE PROBABILITY DENSITY PLOT

MODEL 161 SPECIFICATIONS

1.- Data Input

1.1. Impedance: 10,000 ohms

1.2 Voltage Range: 1 volt to 50 volts RMS

1.3 Peak Factor: ± 5:1

1.4 Frequency Range: DC to 20,000 Hz (DC), 20 Hz to 20,000 Hz (AC)

1.5 Input Metering: true RMS circuit

2.- X Axis

2.1 Window width: .1 sigma

2.2 Output: obtained from internal X-axis potentiometer ± 5 volts = ∓ 5 sigma

2.3 Output impedance of external load should be 100K ohms or greater

2.4 Alternate X-axis output: 10K ohms potentiometer coupled to X-axis sweep potentiometer

2.5 Marker: microswitch provides momentary contact closure at 1 sigma intervals

2.6 X-pot sweep time: 2, 4, 8, 16, 32, 64 minutes ± 5% for complete traverse from + 5 to - 5 sigma

2.7 External sweep: jack provided for external sweep

3.- Output: Y (Probability Axis)

3.1 Impedance: approximately 100 ohms (not less than 10K load)

3.2 Voltage: ±1.5 volts for probability density of 1

3.3 Time constants: 0.2, 0.42, 0.75, 1.4, 3.4, 6.4 seconds for sweep speed settings of 2, 4, 8, 16, 32 and 64 minutes respectively.

3.4 Meter Scale #1: 0 to 0.4 probability density (±2% F.S.)

3.4.1 Meter Scale #2: 0 to 1 probability density (±2% F.S.)

4.- Digital Outputs: Y Axis

4.1 Impedance: approximately 100 ohms

4.2 Voltage: 1 volt peak

4.3 Frequency: 1 or 10 megacycles, switch selectable

5.- Pulse Output

5.1 Impedance: 1000 ohms

5.2 Amplitude: 1 volt

5.3 Connector: BNC

6.- Joint Probability Density

6.1 Provision for driving X-pots of 2 separate 161's synchronously, while reading out joint probability density on one unit

6.2 Connector: BNC

7.- Probability Distribution

7.1 Impedance: approximately 100 ohms (not less than 10K load)

7.2 Voltage: -6 volts full scale

7.3 Connector: BNC

8.- Negative Probability Distribution

8.1 Meter display only

9.- Crossing Rates: Analog and Pulse Outputs, 2 to 20,000 Hz

9.1 Axis or zero crossing rate

9.2 Set-in level crossing rate

9.3 Positive slope level crossing rate

9.4 Negative slope level crossing rate

9.5 Connectors: BNC

9.6 Rate circuit slewing time constant, 0.05 seconds

10.- Distribution of Peaks: Analog and Pulse Outputs, 2 to 20,000 Hz

10.1 Reads average frequency of peaks lying within window

10.2 Pulse output: 1.5 microsecond pulse to 1.5 milli-second pulse depending on rate multiplier setting

10.3 DC output: -0.5 volts corresponds to full scale meter reading

Dimensions: 7" high, 16¼" wide, 14" deep; brackets available for standard 19" rack mounting.

Weight: 21 pounds

Power Required: 30 watts, 105-125 volts; 50 to 400 Hz; plug-in transformer available for 220 volts operation